The Abdus Salam
International Centre for Theoretical Physics

United Nations
Educational, Scientific
and Cultural Organization

International Atomic
Energy Agency

Workshop on "Physics for Renewable Energy"
October 17 - 29, 2005

301/1679-11

"Computer Modeling of Amorphous & Mircocrystalline Silicon-based Solar Cells"

F. A. Rubinelli
INTEC
Argentina

Computer Modeling of Amorphous and Microcrystalline Silicon based Solar Cells

F.A. Rubinelli

INTEC, Universidad Nacional del Litoral, Güemes 3450, 3000, Santa Fe, Argentina


Laguna Setubal
Santa Fe
Santa Fe, Argentina
Laguna La Cuarentena
Laguna del Recreo
Parana
Image © 2005 EarthSat
Image © 2005 DigitalGlobe

Solar Cell Modeling Computer Codes

- **True computer modeling solves:**

- Poisson's Equation.
- Continuity Equation for Electrons
- Continuity Equations for Holes.

} → **free electricity.**

- **First comprehensive computer modeling:**
- G.A.Swartz, RCA (1982), I.Chen and S.Lee (1982).
- T.Ikegaki et all (1985), **M.Hack and M.Shur (1985).**

.

- **Commercial computer codes:**
- **Medici** – TMA company; **Atlas** – SILVACO company.

  Broad range of crystalline semiconductor devices: poly-Si, a-Si TFT and solar cells; 1-D and 2-D codes.

  Models describing a-Si are relatively simple.

Academic Computer Codes

- **AMPS** - PennState University – USA (S.Fonash, P.McElheny, J.Arch) (**D-AMPS**)
- **ASPIN** - Ljubljana University – Slovenia (Smole, Furlan, Topic, Vukadinovik)
- **ASA** – Delft University of Technology – Netherlands (Zeeman, Tao, Willeman)
- **SCAPS** – University of Gen – Belgium, (Burgelman et al.)
- **P1CD** – Sandia Labs.- UNSW, Australia
- **ADEPT** - Purdue University, USA, (Jeff Gray et al.)
- Forschungzentrum Jülich (Germany) – Germany, (Stiebig at al.)
- Others: **ASCA** (New UnIv. Lisbon), Chaterjee (INDIA), Misiakos (Florida USA), Mittiga (La Sapienza, ROMA), Bruns (BERLIN)

Differences in the academic computer codes

- Choice of independent variables: Ψ, E_{FN}, E_{FP} or Ψ, n, p.
- Numerical solution techniques: Newton-Raphson, Gummel.
- Description of the DOS distribution: Tails and Gaussians.
- R-G statistics of localized states; SRH, amphoteric DB.
- Contact treatment: generic, ohmic.
- Special features: defect pool model, tunnel-recombination junctions, etc.
- Optical models: Interference, scattering.
- Friendly interface: AMPS, ASA, ASPIN (no D-AMPS).
- 1-D modeling is well suited for a-Si solar cells on flat substrates.
- 2-D modeling might be needed on: textured substrates in high efficient a-Si solar cells (spatial variations in device structure) or in spatially non-homogenous μc-Si devices.

D-AMPS

AMPS core (Penn State Univ. USA)
+ New Developments (INTEC, Argentina)

3 unknown or independent state variables:
1 - the electrostatic potential $\Psi(x)$
2 - the electron quasi-Fermi level $E_{FN}(x)$
3 - the hole quasi-Fermi level $E_{FP}(x)$

Numerical technique:

Finite difference discretization
Newton Raphson formalism
Trial functions of Scharletter Gummel (J at i-1/2 i+1/2)

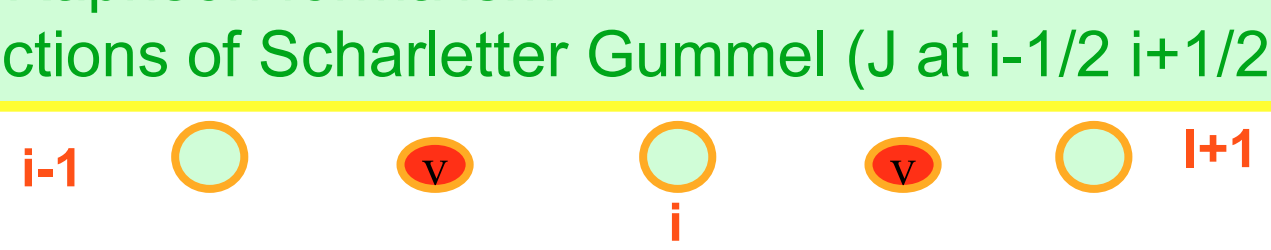

Tasks in device modeling:

- Development of new models to accurately describe material properties, interfaces and device operation → **up-dating.**
- Constant testing of existing and new computer modeling in increasingly complex structures of solar cells.
- Accurate calibration of input parameters (electrical and optical) in order to reproduce a broad range of experimental results:

  (a) - Dark and illuminated current – voltage (J-V) curves.

  (b) - Spectral response (SR) characteristic curves.

  → **reliable inputs**. Some are unknown.
- Use of the computer code as predicted tool.

  → Design of solar cells to reach the best performance.
- Alternative modeling of steady state: small signal, transients.

Advantages of computer modeling

- Examine the influence of internal parameters that can not be experimentally determined.
- Ponder the impact on the solar cell performance of small changes in device configuration.
- Optimal design of the solar cell structure.
- Understanding the physic controlling the electrical transport of interesting experimental results.
- It is becoming increasingly cheaper.

Drawbacks of computer modeling

- *Too many input parameters?? → to be discussed.*
- *Analytical modeling → some parameters are ignored or results are assumed to be independent of these input values.*
- *Some input parameters are not well known (cross sections, mobilities). We have to work within the range published in the literature.*
- *Very time consuming task:*

  programming + fitting
- *Difficulties found in matching output curves of some devices.*

  example: SR under forward bias.
- *Structures of solar cells are becoming increasingly complex.*

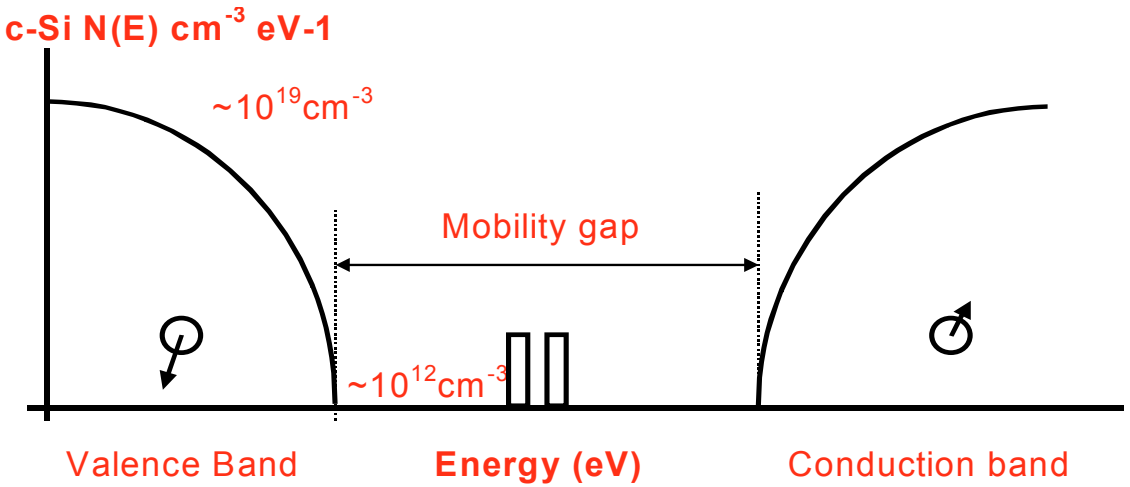

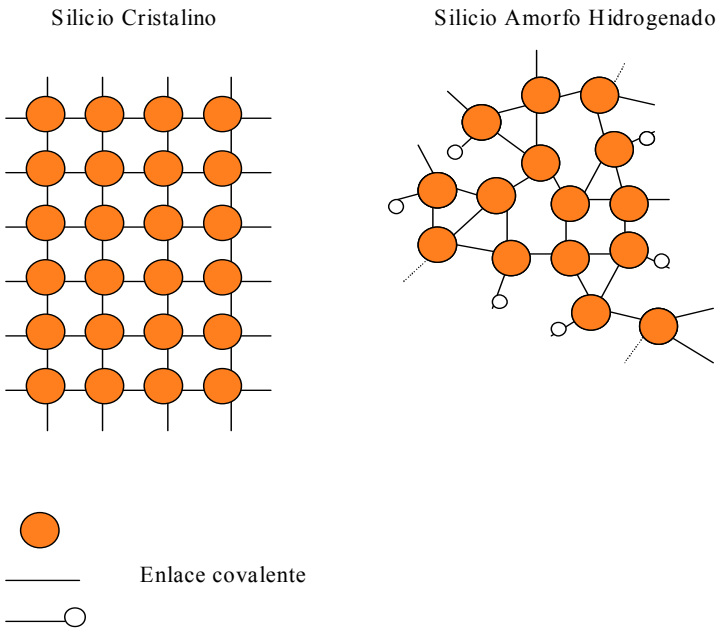

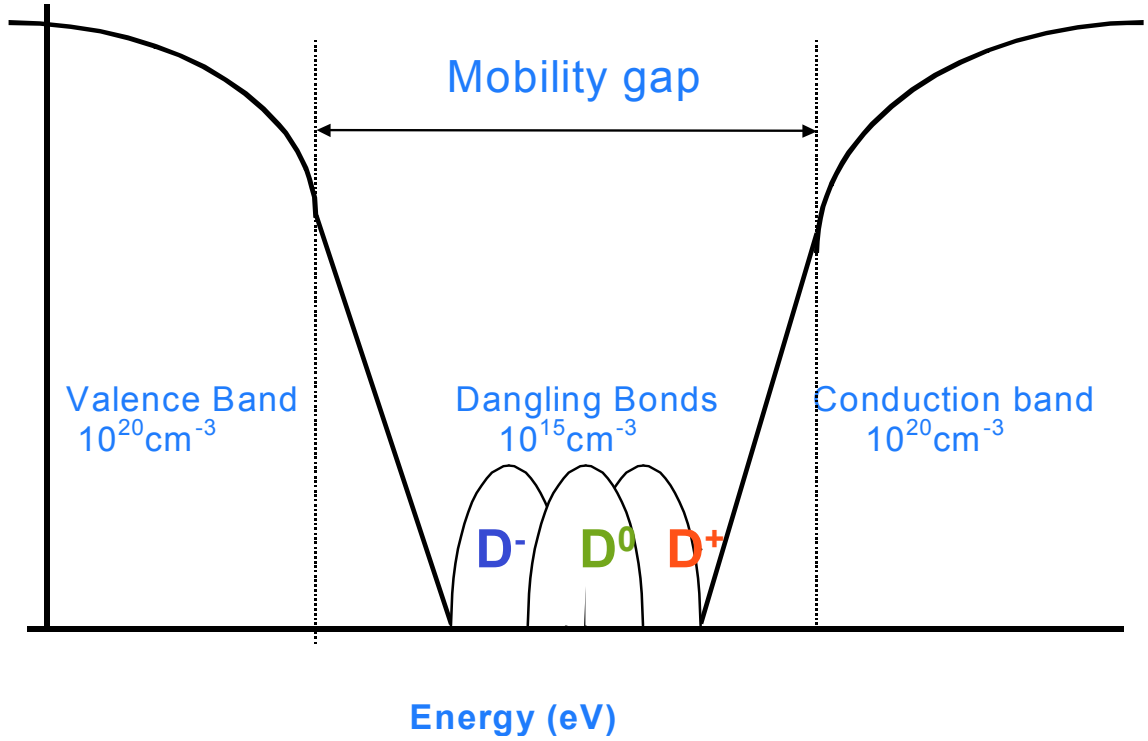

a-Si:H and c-Si

DB density:

10^{15} - 10^{16} / 10^{12} cm^{-3}.

Mobilities:

2-20/

480-1500 $cm^2eV^{-1}sec^{-1}$

Gap: 1.80-1.72eV / 1.12eV

Absorption coefficient:

one order higher in a-Si:H

in the visible range.

Density of States

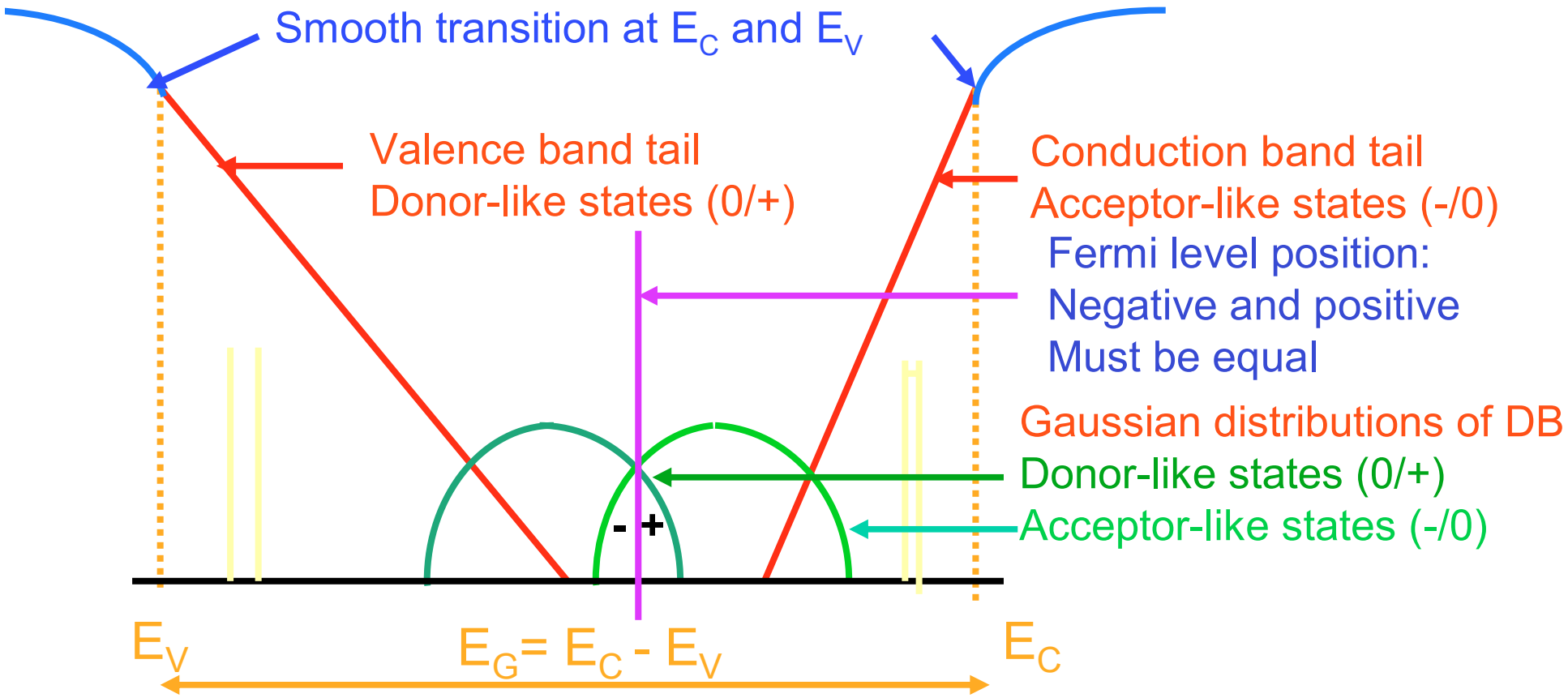

- Density of extended states is assumed parabolic like in c-Si
- Mobility edges at conduction and valence bands E_C and E_V
- Doping impurities: shallow donor and acceptor localized levels
- Spatial disorder: conduction and valence band tails.
- Structural defects: levels near mid-gap → DB

Transport mechanisms

Conventional Scattering

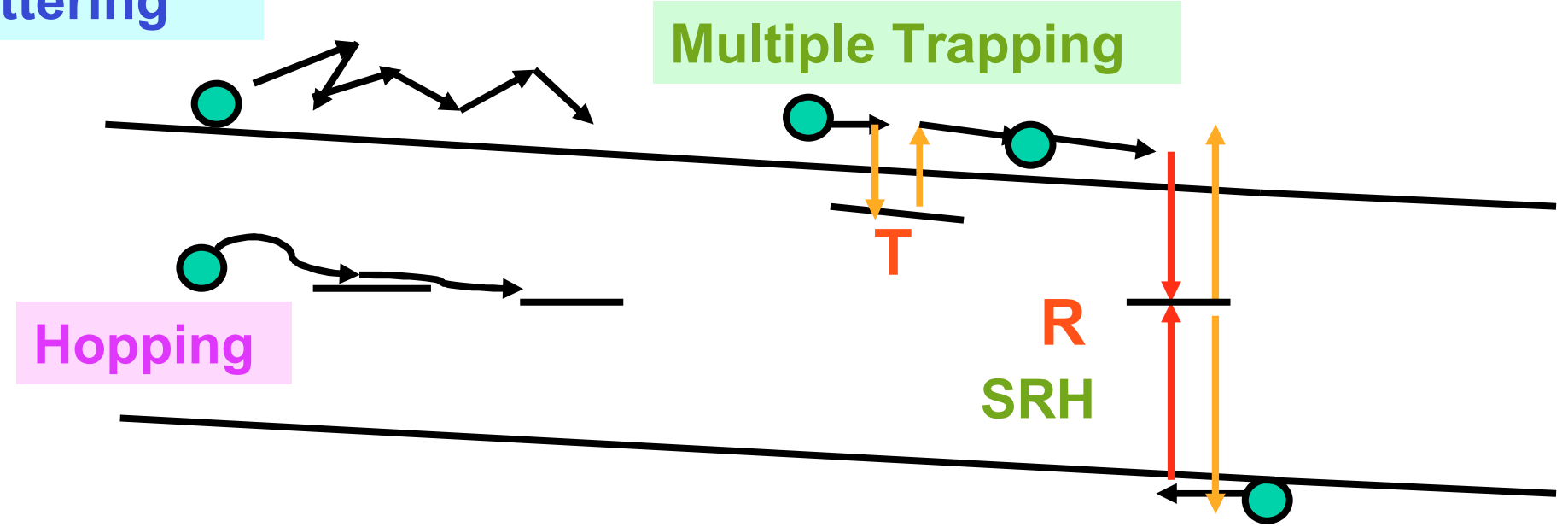

- **Conventional scattering:** extended state transport
→described by carrier concentrations and mobilities
- **Multiple trapping:** electrons and holes in extended states move by drift-diffusion, they are captured by tail states, remain immobile for some time, and are re-emitted back into extended states.
→ described also by concentration of carriers and mobilities
- **Hopping:** involves tunnel between localized states inside the mobility gap
Thermally activated and negligible at room temperature

POISSON'S EQUATION:

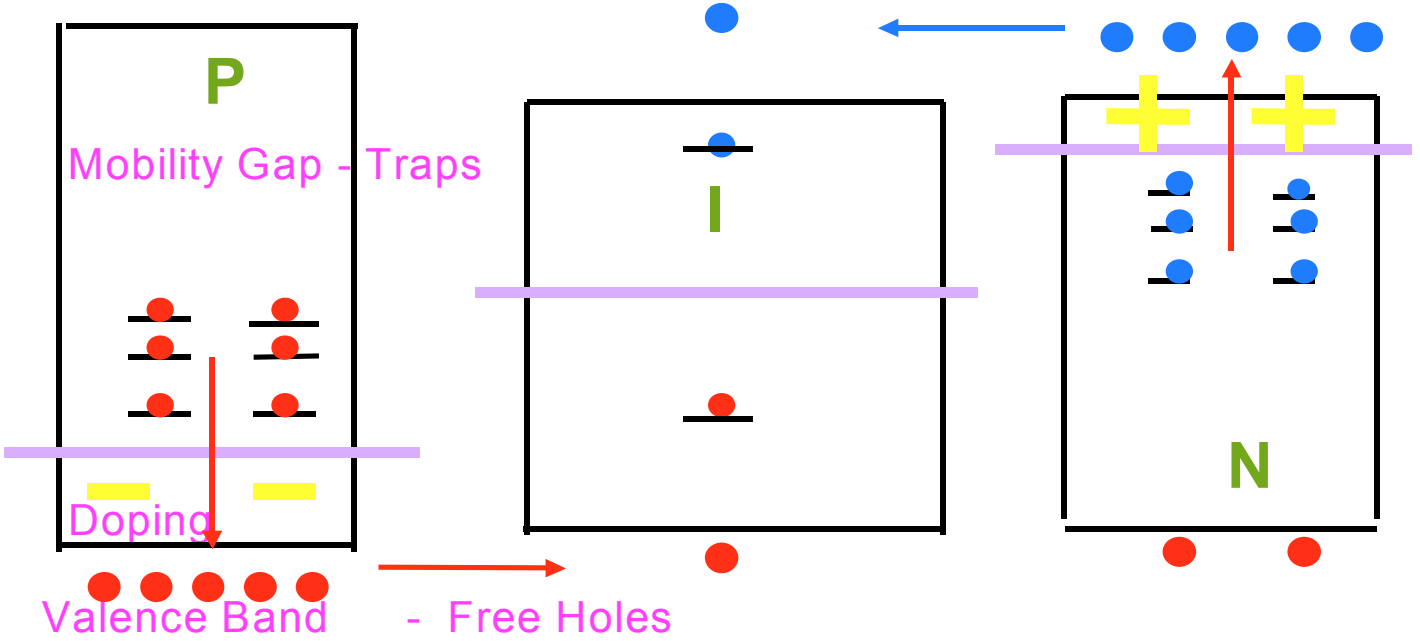

Poisson's Equation Equilibrium

$$\frac{d}{dx}\left(\varepsilon(x)\frac{d\Psi(x)}{dx}\right)=\rho(x)$$

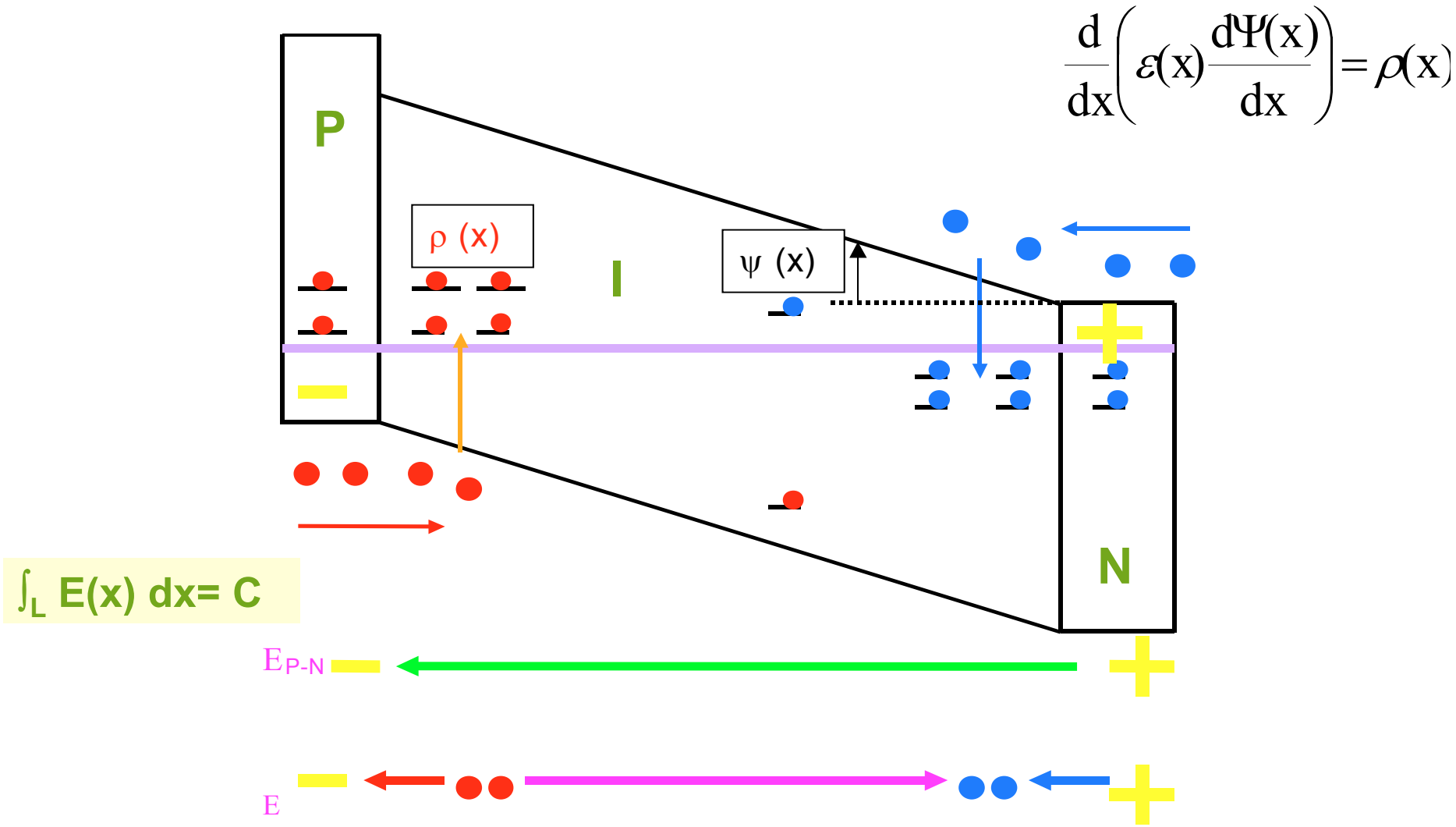

Poisson's Equation
Under illumination

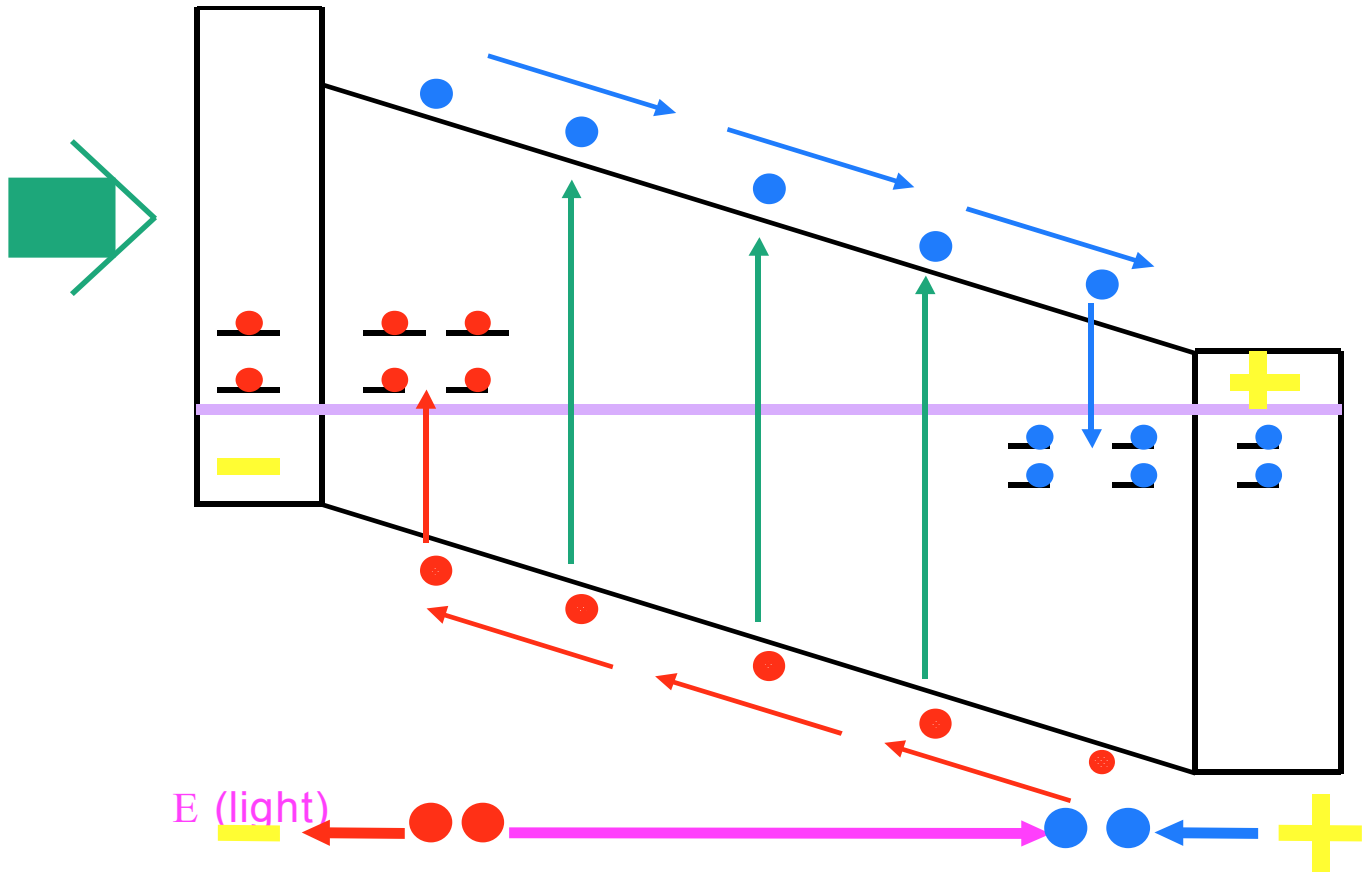

Continuity Equations

Electrical Currents:

(a) - Drift (Holes)

(b) – Diffusion (Holes)

(c) - Effective field: gap, electron affinity, (Electrons)

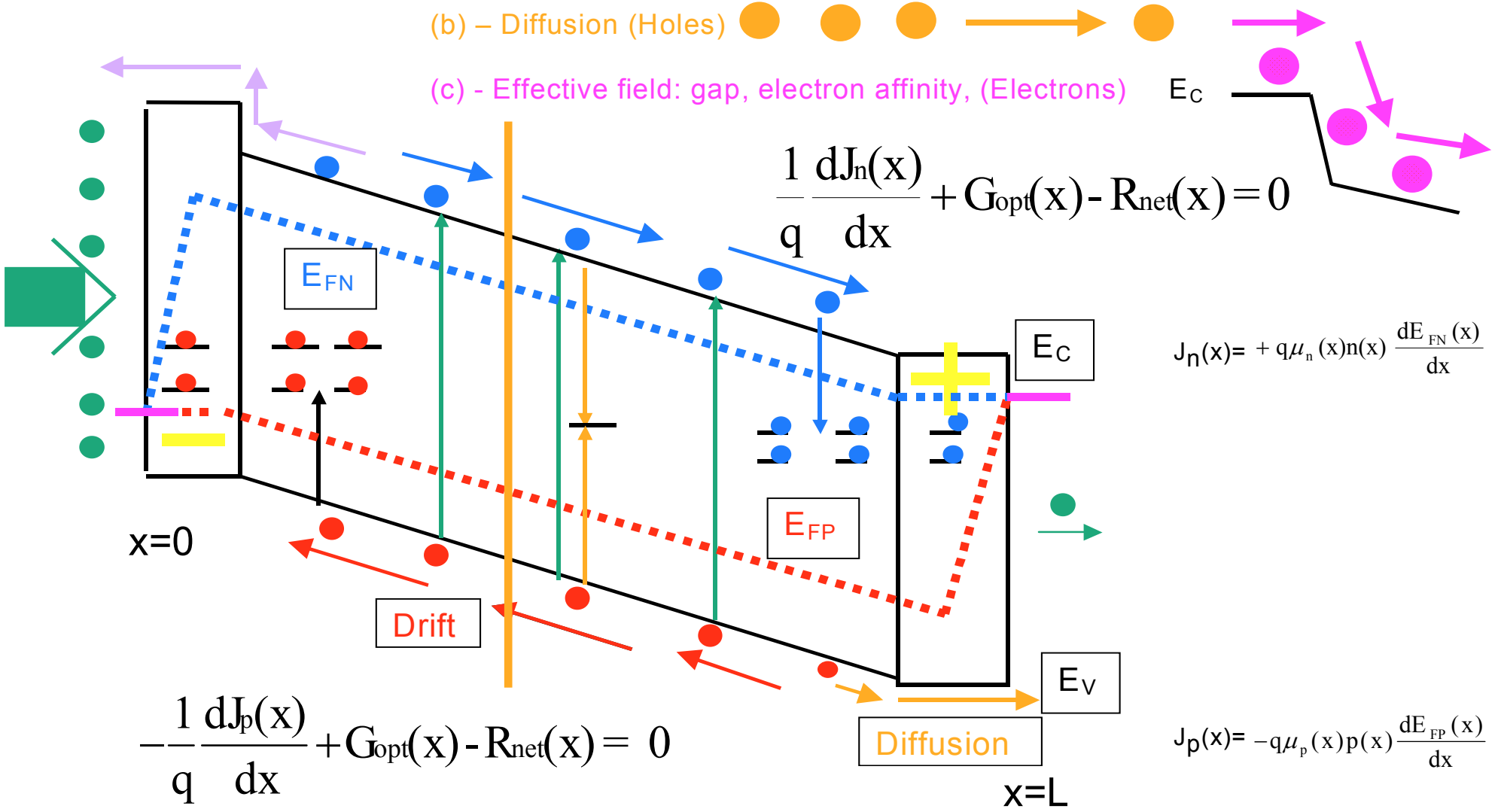

$$\frac{1}{q}\frac{dJ_n(x)}{dx} + G_{opt}(x) - R_{net}(x) = 0$$

$$J_n(x) = +q\mu_n(x)n(x)\frac{dE_{FN}(x)}{dx}$$

$$-\frac{1}{q}\frac{dJ_p(x)}{dx} + G_{opt}(x) - R_{net}(x) = 0$$

$$J_p(x) = -q\mu_p(x)p(x)\frac{dE_{FP}(x)}{dx}$$

Total current

$$\frac{1}{q}\frac{dJ_n(x)}{dx} + G_{opt}(x) - R_{net}(x) = 0$$

$$J = J_N + J_P$$

$$J = J_{n0} + J_{pL} + e\cdot\int_0^L Rnet(x)\cdot dx - e\cdot\int_0^L Gopt(x)\cdot dx$$

Total Current

Electron back diffusion

Hole back diffusion

Recombination losses

Optical current

Pin + optical layers

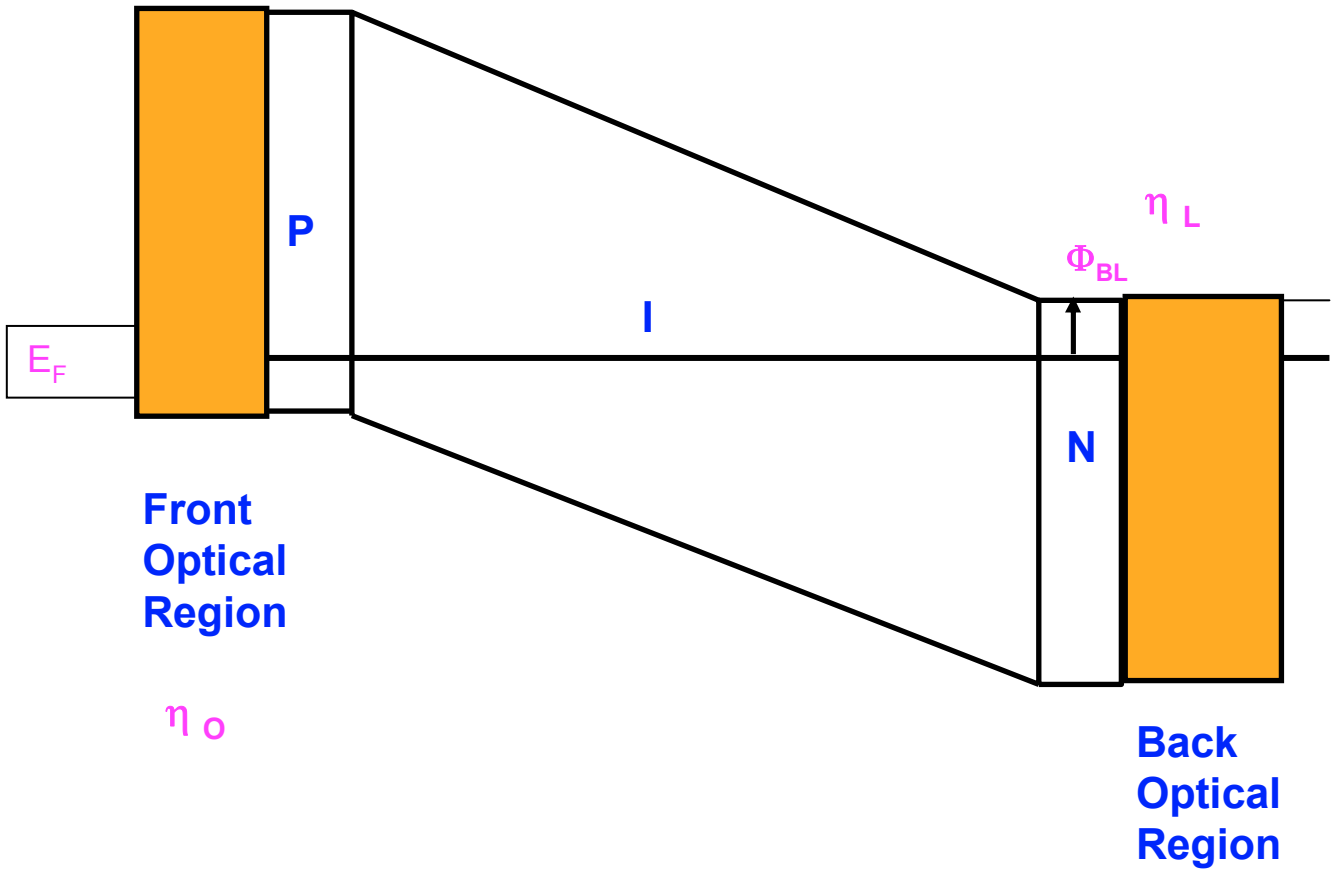

Charge, f, and R (equations)

$$\rho = q \cdot \int_{E_v}^{E_c} N(E) \cdot [1 - f(E)] \cdot dE$$ donor

$$\rho = -q \cdot \int_{E_v}^{E_c} N(E) \cdot f(E) \cdot dE$$ acceptor

$$f = \frac{1}{1 + e^{\frac{E_T - E_F}{k \cdot T}}}$$ FD

$$f = \frac{(n + p')\sigma_n}{(n + n')\sigma_n + (p + p')\sigma_p}$$ SRH

$$n' = N_c \cdot e^{\frac{E_T - E_c}{k \cdot T}}$$

$$p' = N_v \cdot e^{\frac{E_v - E_T}{k \cdot T}}$$

$$R = N_T \cdot v_{th} \cdot \sigma_n \cdot \sigma_p \cdot \frac{n \cdot p - n_i^2}{(n + n')\sigma_n + (p + p')\sigma_p}$$

$v_{TH} \sim 10^7 cm/s$

Boundary Conditions

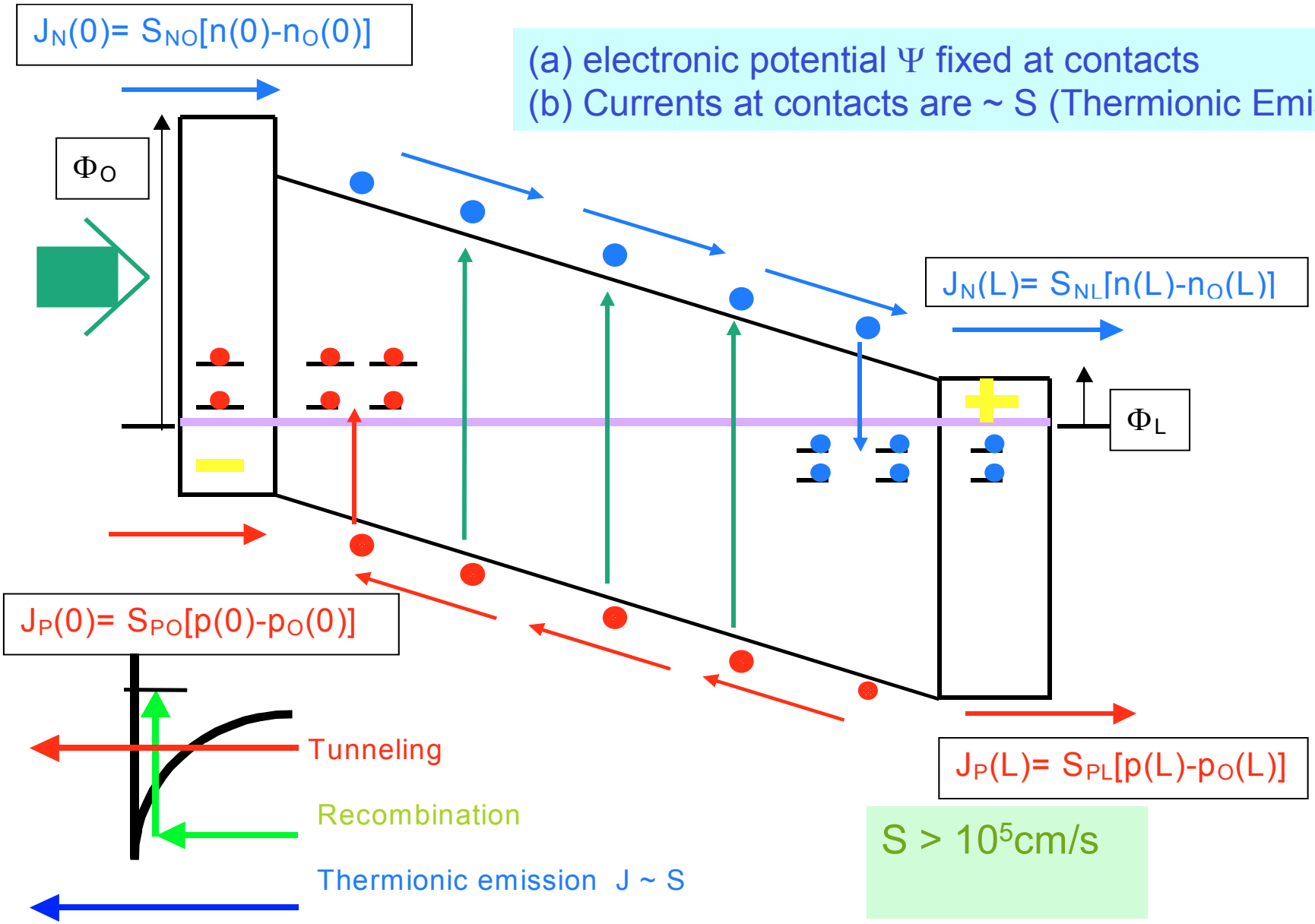

Working Strategy
Material Characterization

1- Dark conductivity

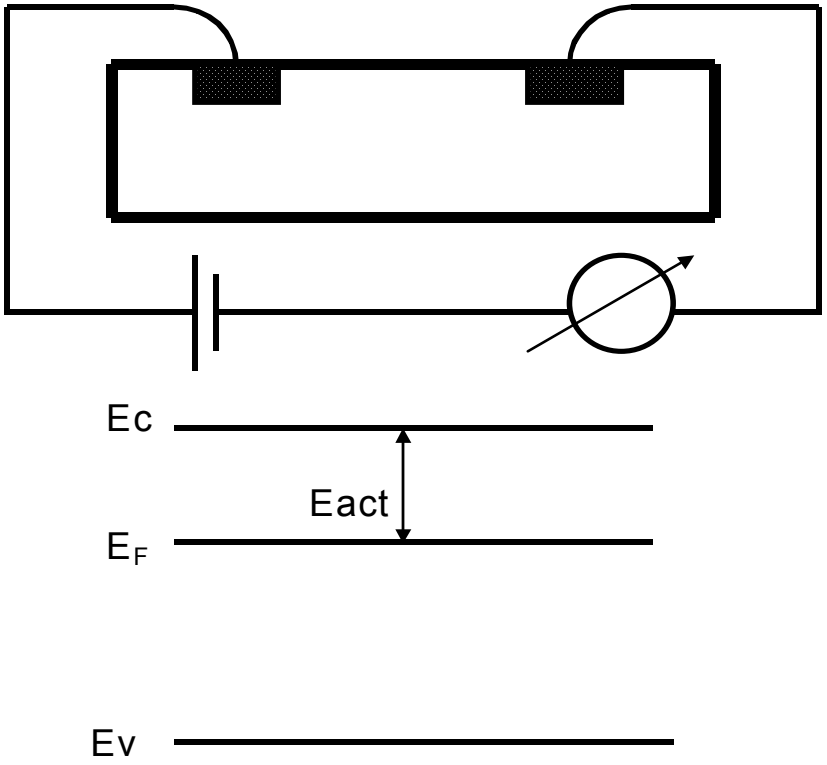

Mobility x Free carrier concentration (μ_nn or μ_pp)

Dark Conductivity vs. temperature ===> **Eact**

2- Photoconductivity

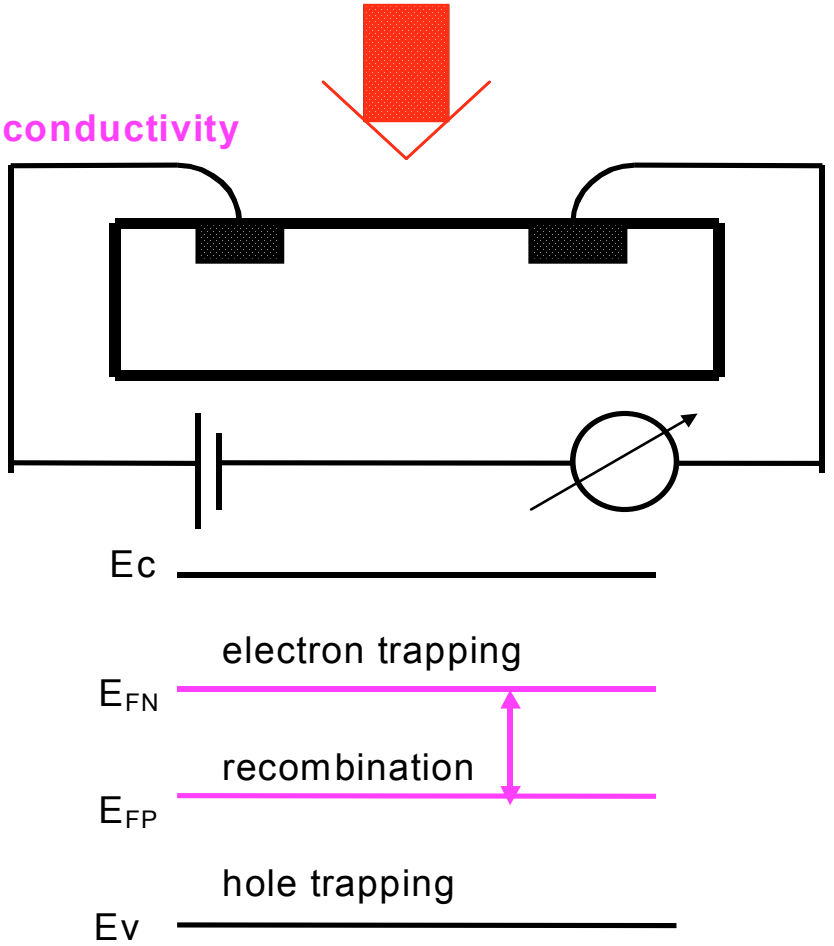

Light: AM1.5 or Red Light
Free carrier concentration lifetime
Density of dangling bonds (D^o)

Material Characterization

Subgap Absorption

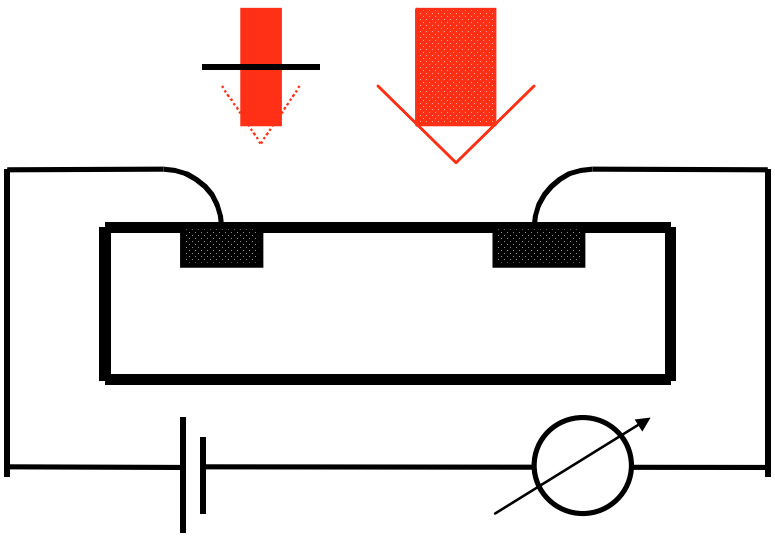

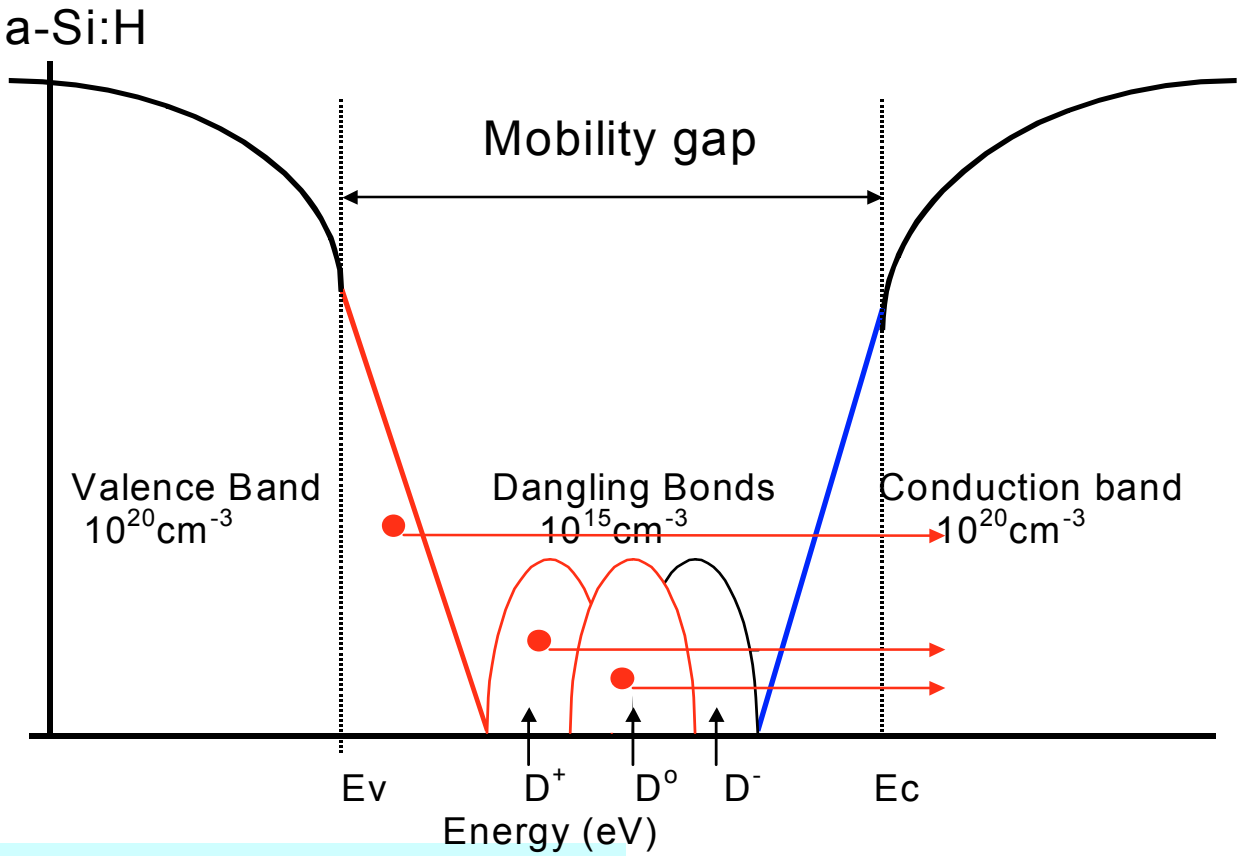

CPM: Constant Photocurrent Method
DBP: Dual Beam Photoconductivity, Others (PDS)
Valence Band Tail Slope and Dangling Bond Density (D^- and D^o)

Optical characterization of materials

4 - Reflection and Transmission:

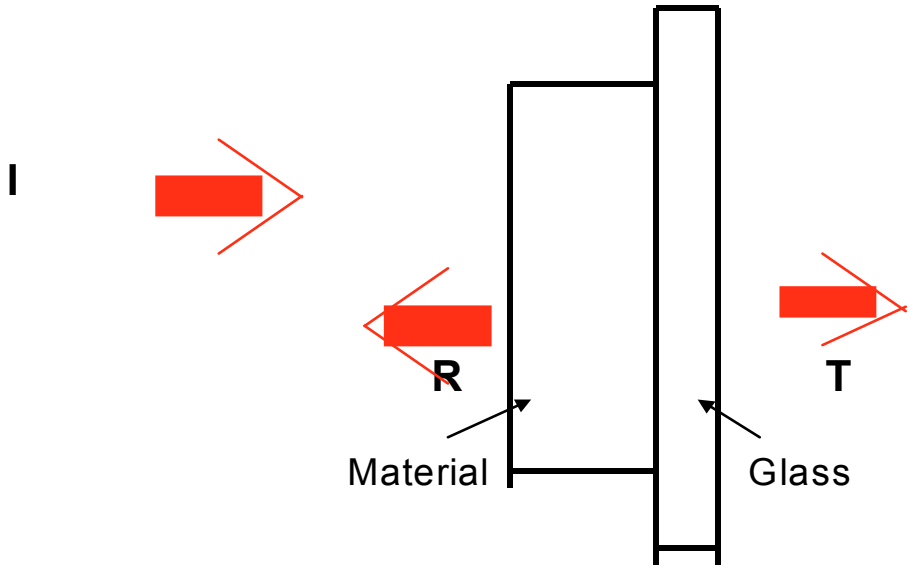

Absorption coefficients (α)
and Refractive Indexes (n)
Optical Gap (Tauc Gap)
$\alpha(h\nu)n(h\nu) \sim (h\nu - E_{OPT})^{1/2}$
Cutoff Wavelength or Photon Energy

E_{OPT} (a-Si:H) = 1.72eV
E_{OPT} (c-Si) = 1.12eV
E_{OPT} (μc-Si:H) = 1.1ev (I) –2.00eV (D)

Other techniques

5 - Electron Spin Resonance:

Dangling Bond concentration --> D^o

6 - Internal Photoemission:

Mobility Gap

SSPG
Modulated conductivity
Minority carrier diffusion length
Conduction Band Tail (**Time of Flight**)

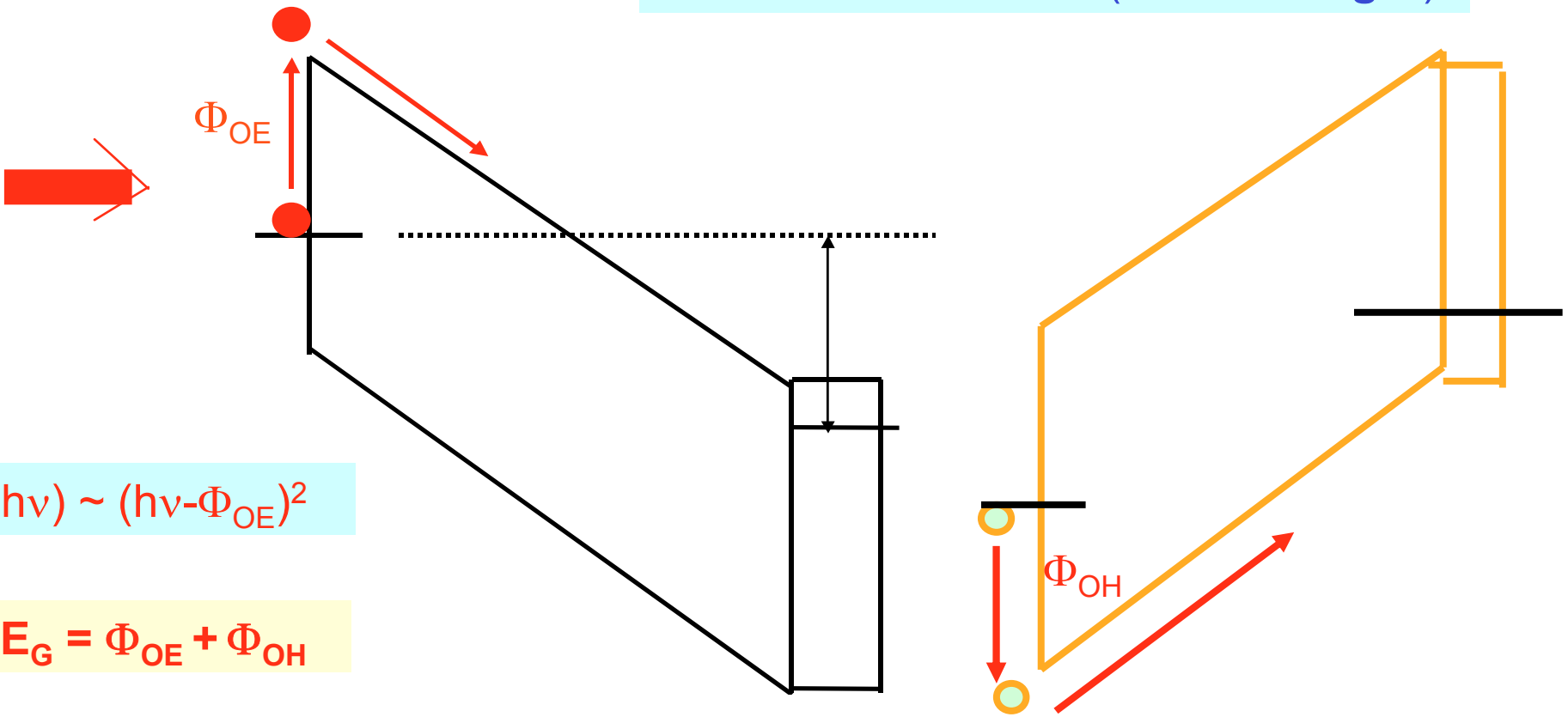

$Y(h\nu) \sim (h\nu - \Phi_{OE})^2$

$E_G = \Phi_{OE} + \Phi_{OH}$

Inputs – Equilibrium
Poisson's Equation – n,p

$$\frac{d}{dx}\left(\varepsilon(x)\frac{d\Psi(x)}{dx}\right)=\rho(x)$$

Dielectric permittivity ε → books

$$\rho(x)= q[p(x)-n(x) + p_T(x) - n_T(x) + N_D{+}(x) - N_A{-}(x)\ ]$$

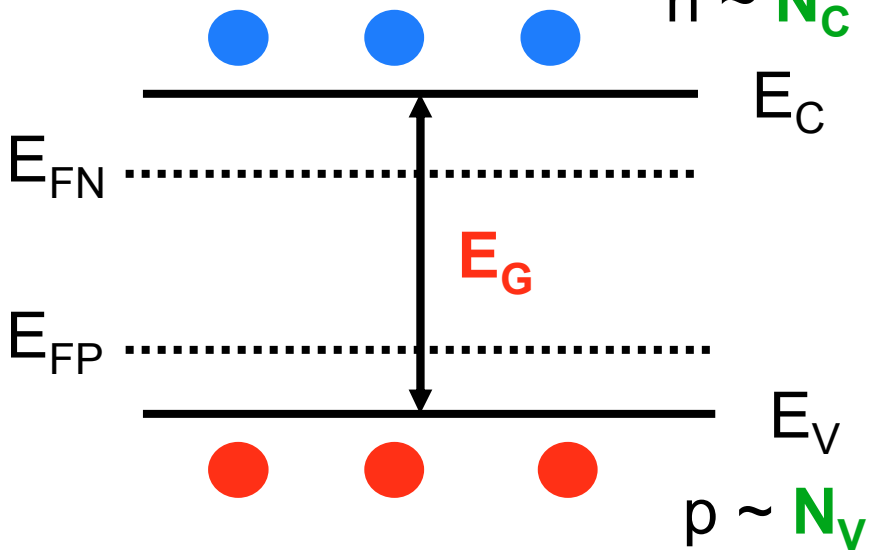

$n \sim N_C \exp(E_{FN} - E_C)$

$p \sim N_V \exp(E_V - E_{FP})$

$E_G = E_C - E_V$

N_C :effective conduction density of states
→ input (literature, fitting) (cm-3)
N_V :effective valence density of states
→input (literature, fitting) (cm-3)
Usually $N_C = N_V$ → (1) (1-3x10^{20})

E_G: mobility gap (eV), (1)
→ input (experiment)

Inputs – Equilibrium
Poisson's Equation - DOS

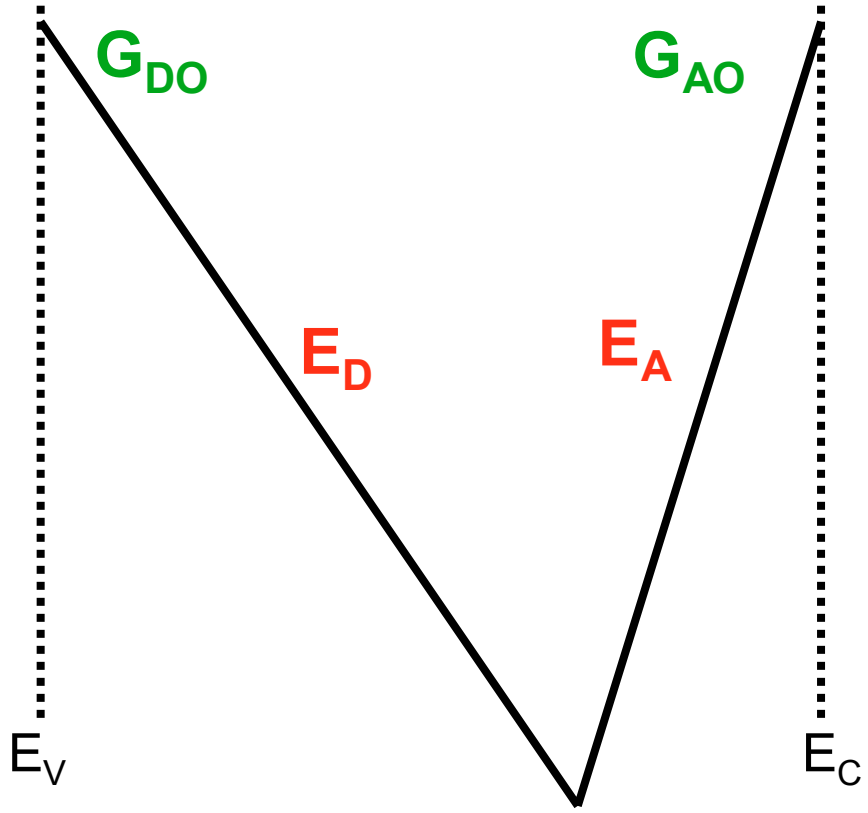

Conduction band tail (acceptor-like)

$g_D(E)=G_{DO}\exp(-E/E_D)$ $G_{DO}kT\sim N_V$

Valence band tail VBT (donor-like)

$g_A(E)=G_{AO}\exp(-E/E_A)$ $G_{AO}kT\sim N_C$

G_{DO} density of localized states at Ec ($cm^{-3}eV^{-1}$) → **input (literature)**

G_{AO} density of localized states at Ev ($cm^{-3}eV^{-1}$) → **input (literature)**

Usually $G_{DO}= G_{AO}$ **(2)**

E_D: donor tail characteristic energy (eV) → **input (experiment) (2)**

E_A: acceptor tail characteristic energy (eV) → **input (literature, fitting) (3)**

Inputs – Equilibrium
Poisson's Equation - DOS

E_V

Usually
- $N_{AG1} = N_{DG1}$
- $N_{AG2} = N_{DG2}$
- $N_{AG3} = N_{DG3}$
- $N_{DG1} = N_{DG3} = 2xN_{DG2}$

$N_{DB} = 5xN_{DG2}$

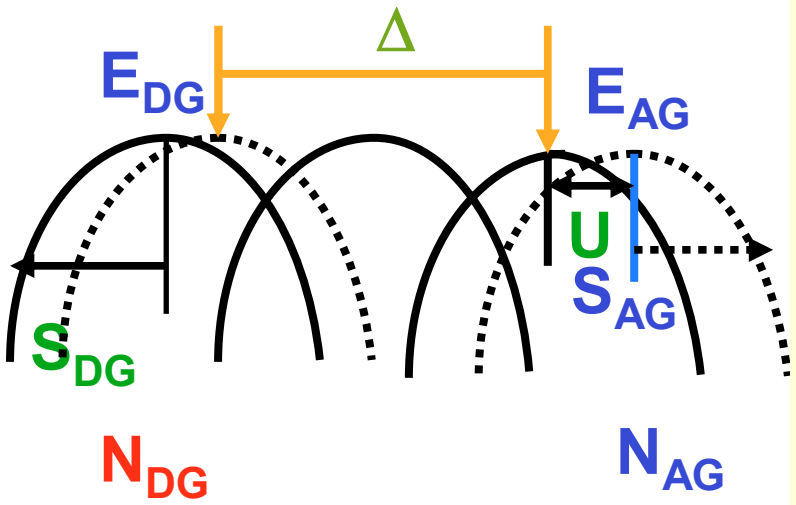

E_C

$$g_{AG}(E) = \frac{N_{AG}}{\sqrt{2\pi}S_{AG}} \exp\left[-\frac{(E-E_{AG})^2}{2S_{AG}^2}\right]$$

$$g_{DG}(E) = \frac{N_{DG}}{\sqrt{2\pi}S_{DG}} \exp\left[-\frac{(E-E_{DG})^2}{2S_{DG}^2}\right]$$

N_{DG}, N_{AG} total number of states enclosed in Gaussians (cm-3) → inputs (4) $N_{DG} = N_{AG}$

E_{DG}, E_{AG}, peak energies (eV)

→input We have to reproduce the experimental i-layer activation energy

$E_{AG} = E_{DG} + U$

U: correlation energy (literature)

S_{DG}, S_{AG}: standard deviations (eV)

→ inputs (4) Usually $S_{AG} = S_{DG}$

Inputs – Equilibrium
Poisson's Equation - DOS

p-layer → N_A- (fully ionized, fix DOS)
We have to reproduce the p-layer activation energy $E_{ACT(P)}$ **(experiment)**

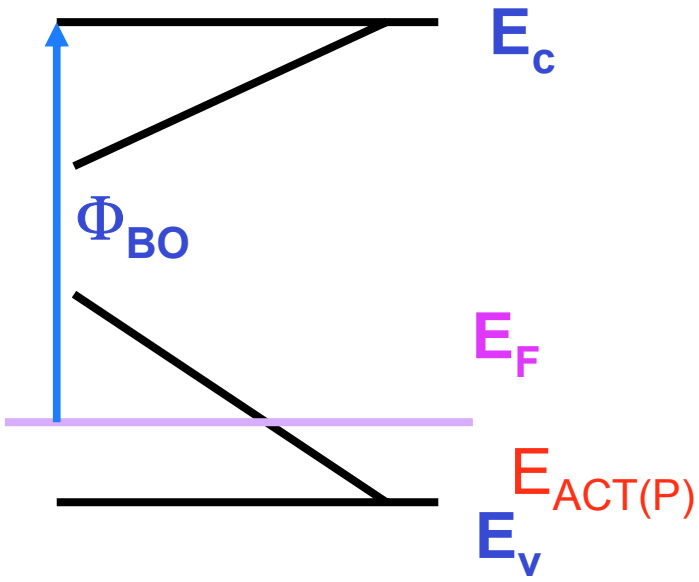

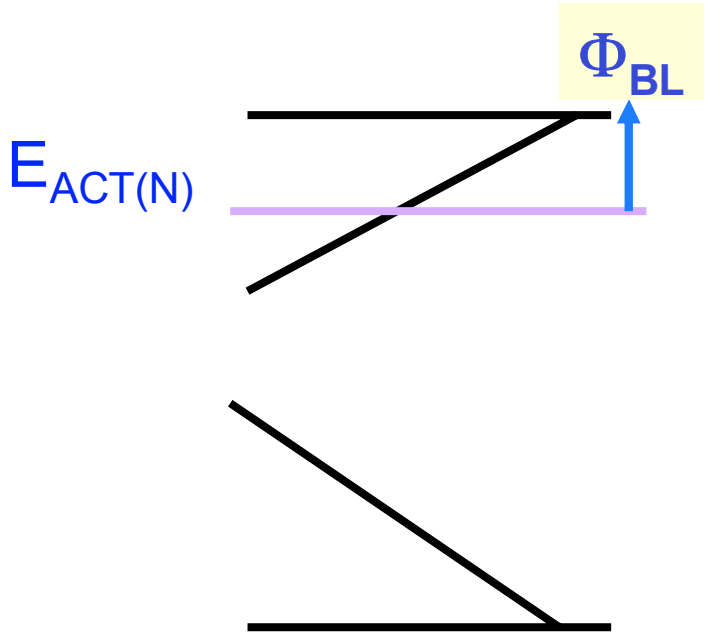

$\Phi_{BO} = E_{G(P)} - E_{ACT(P)}$
$\Phi_{BL} = E_{ACT(N)}$
Flat band conditions

n-layer → N_D+ (fully ionized, fix DOS)
We have to reproduce the n-layer activation energy $E_{ACT(N)}$ **(experiment)**

Non – Equilibrium
Poisson's + Continuity Equations

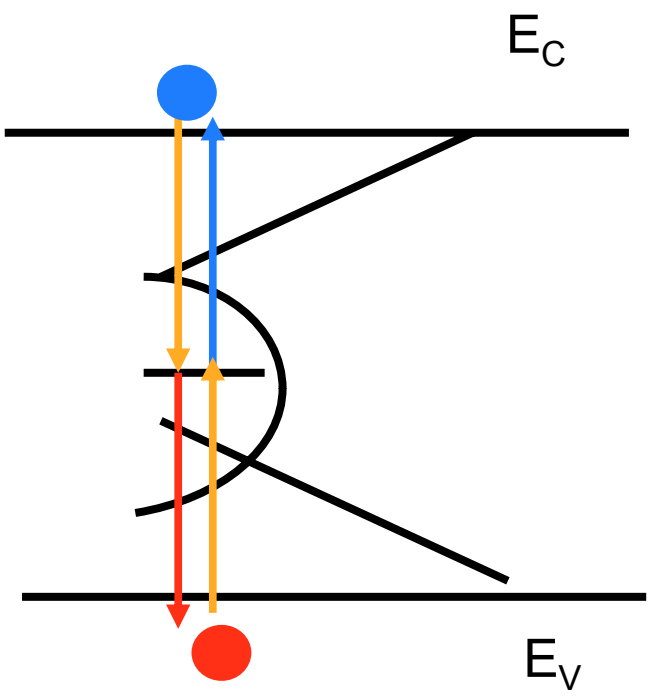

Tail cross sections → σ_{NA}, σ_{PA}, σ_{ND}, σ_{PD}

→ inputs (literature, fitting)

$\sigma_{NA} << \sigma_{PA}$, and $\sigma_{PD} << \sigma_{ND}$ (6) (6)

Often but not always

$\sigma_{PA} = \sigma_{ND}$ and $\sigma_{NA} = \sigma_{PD}$

Mid-gap cross sections → σ_{NA}, σ_{PA}, σ_{ND}, σ_{PD}

→ inputs (literature, fitting)

$\sigma_{NA} << \sigma_{PA}$, and $\sigma_{PD} << \sigma_{ND}$ (8) (8)

Often but not always

$\sigma_{PA} = \sigma_{ND}$ and $\sigma_{NA} = \sigma_{PD}$

Recombination (**R**) and occupation functions (**f**) ($\mathbf{n_T}$ **and** $\mathbf{p_T}$) are functions of the cross sections.

Non – Equilibrium Continuity Equations

Scattering Electron Mobility μ_N
→ inputs (literature, fitting) (9)

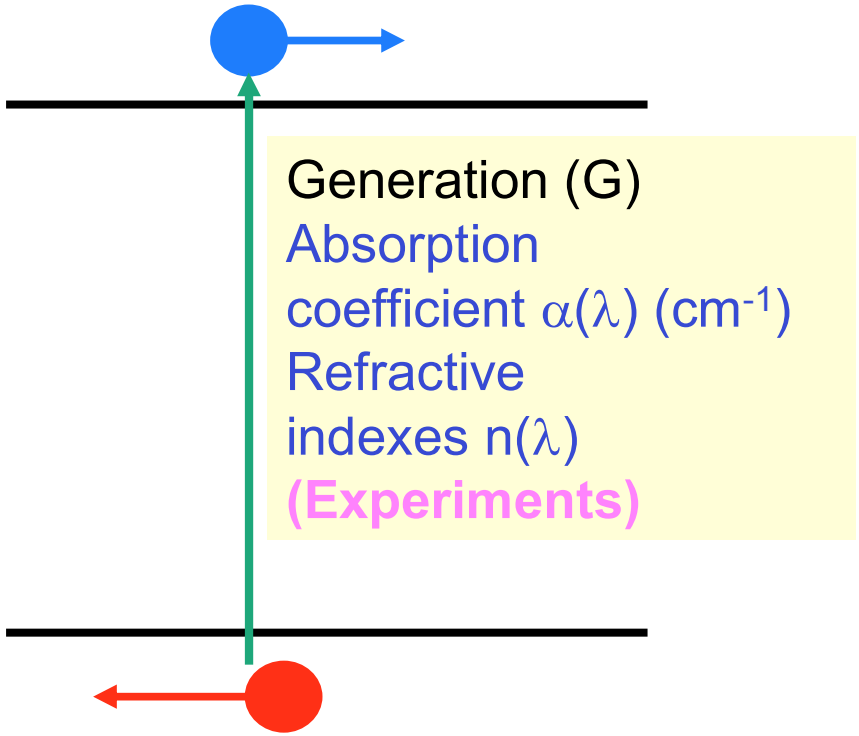

Generation (G)
Absorption coefficient $\alpha(\lambda)$ (cm^{-1})
Refractive indexes $n(\lambda)$
(Experiments)

Scattering Hole Mobility μ_P
→ inputs (literature, fitting) (10)

Measured Drift Mobilities μ_N and μ_P:
$\mu_{ND} = \mu_N [n/(n+n_t)]$ and $\mu_{PD} = \mu_P [p/(p+p_t)]$
$\mu_N \sim 0$ and $\mu_P \sim 0$ in localized states

Light source described by:
- wavelengths (λ_i) (nm)
- fluxes Φ_{Oi}. (photons/cm^2/sec)

Incoming flux $\Phi_O = \Phi(x=0)$

One electron-hole pair/photon

$J_N(x=0) = S_{NO}[n(x=0)-n_{EQ}(x=0)]$, etc
Surface recombination velocities:
S_{NO}, S_{NL}, S_{PO}, S_{PL} → inputs → (literature)
High enough to avoid contact limitations

Critical parameters: How many?

- **a-Si (~1.8eV)**

E_D and N_{DG} can be carefully measured (DBP, PDS).

E_G can be also measured (IPE).

E_A only impacts on the high forward dark J-V.

$\sigma_{PA,}$ in tails has much less impact on device outputs that $\sigma_{ND.}$

We have five critical parameters per layer:

μ_N, μ_P, σ_{PA} (DB), σ_{ND} (DB). and σ_{ND} (T).

and 13 non-critical inputs.

- **μc-Si (~1.2-1.6eV)**

In low gap materials tails do not play a significant role!

We end up with four critical parameters per layer:

μ_N, μ_P, $\sigma_{PA,}$ (DB) and σ_{ND} (DB)

and seven non-critical inputs

Device characterization

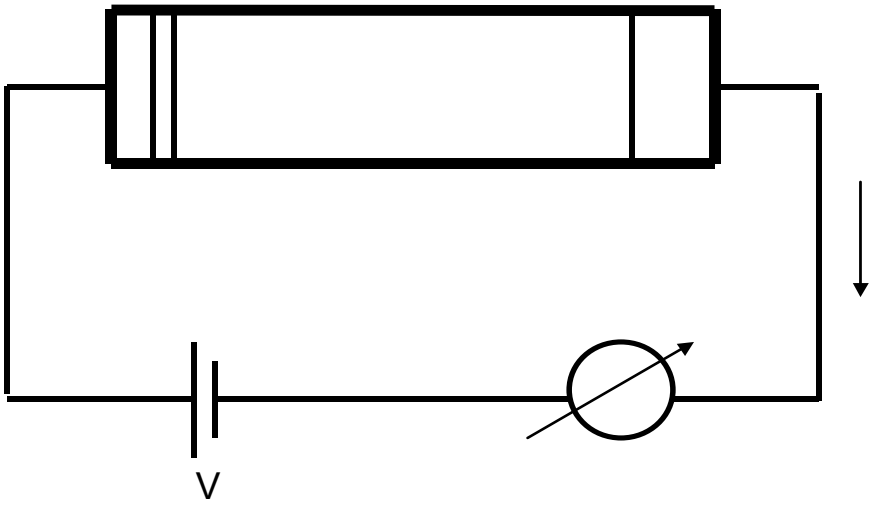

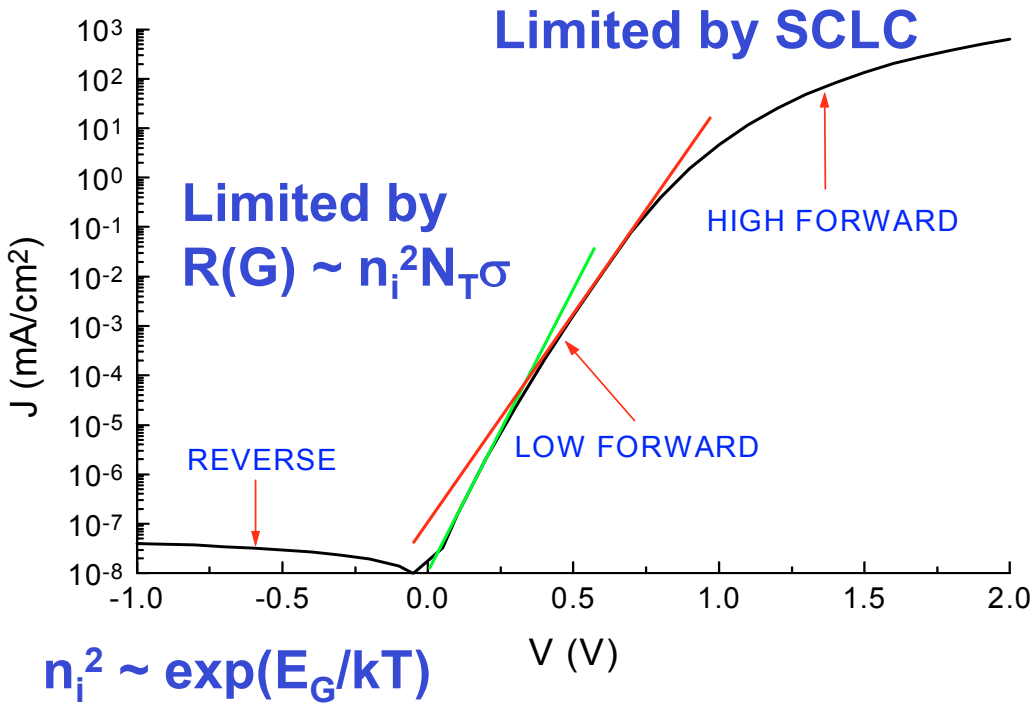

$n_i^2 \sim \exp(E_G/kT)$

Dark Current - Voltage Curve

Low – forward current mechanisms

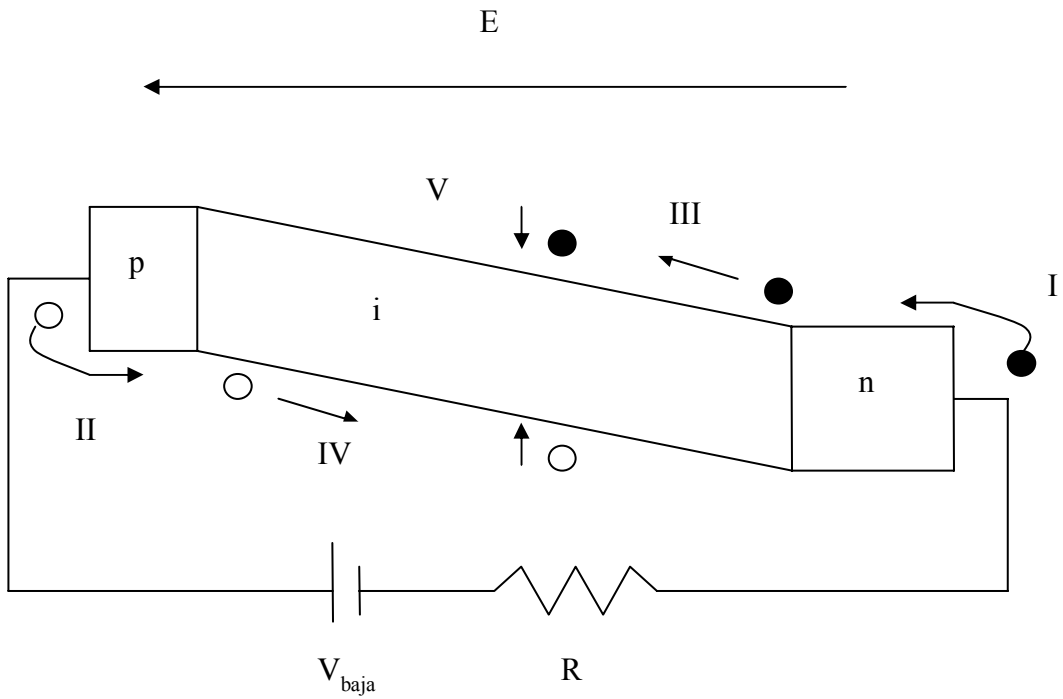

High – forward current mechanisms

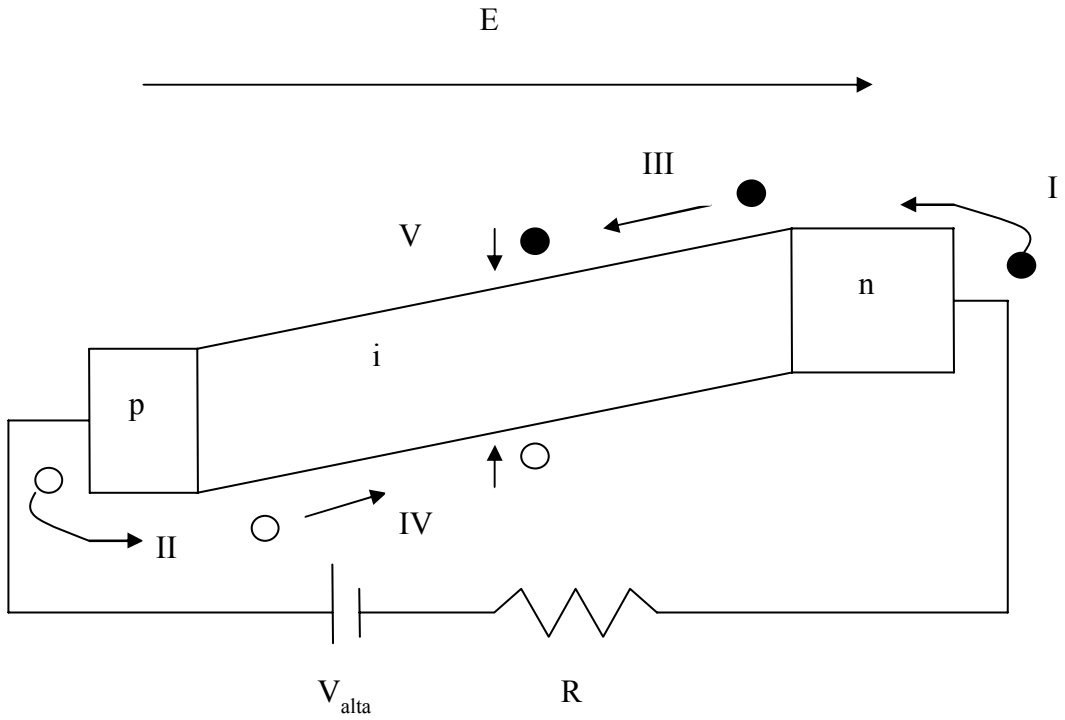

Device characterization

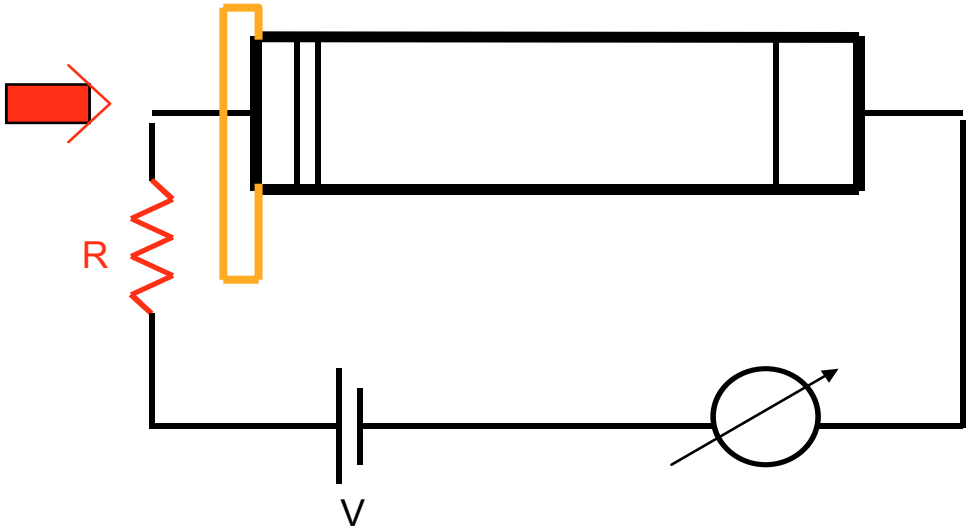

J

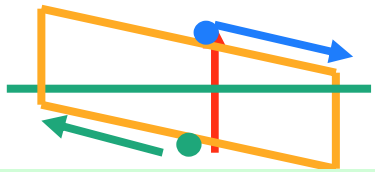

Jsc ~ 17 - 18 mA/cm^2
V_{OC} ~0.85-0.9 V, FF~0.7

Light Current - Voltage Curve

J_{PHOTON} (sub-gap) ~ 0.3 mA/cm^2
J_{PHOTON} (TCO) ~ 0.5 - 4 mA/cm^2

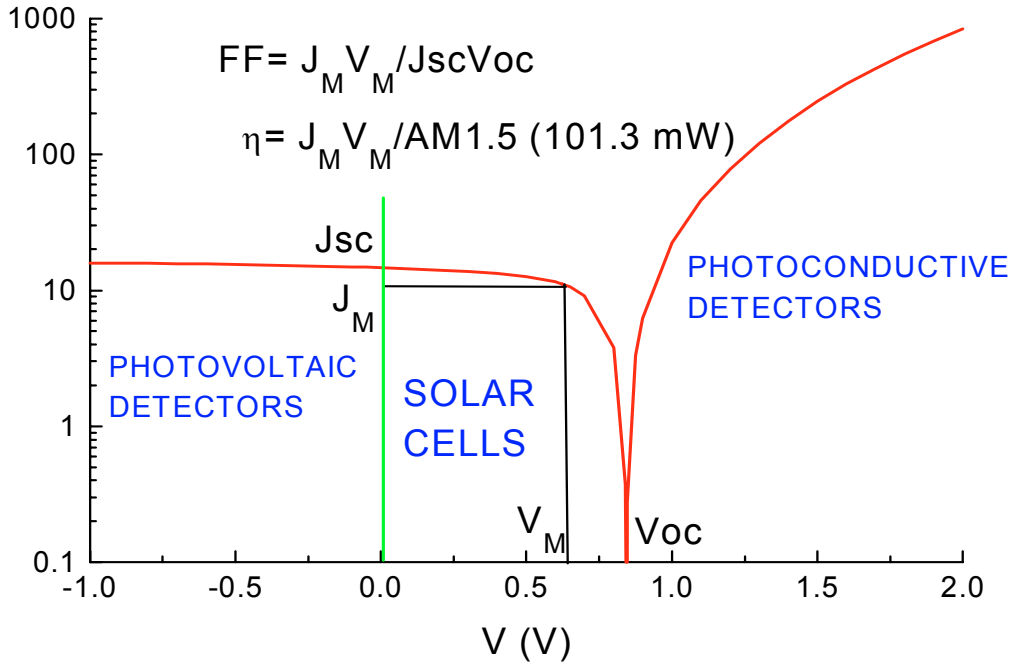

DEGRADATION EXPERIMENTS:
Materials and Solar Cells can be degraded by exposure to Optical irradiation –
•AM1.5 Spectrum (100 mW/cm^2)
(Short circuit conditions, Voc conditions)
* Voltage stressing and Current Injection

Solar Spectrum

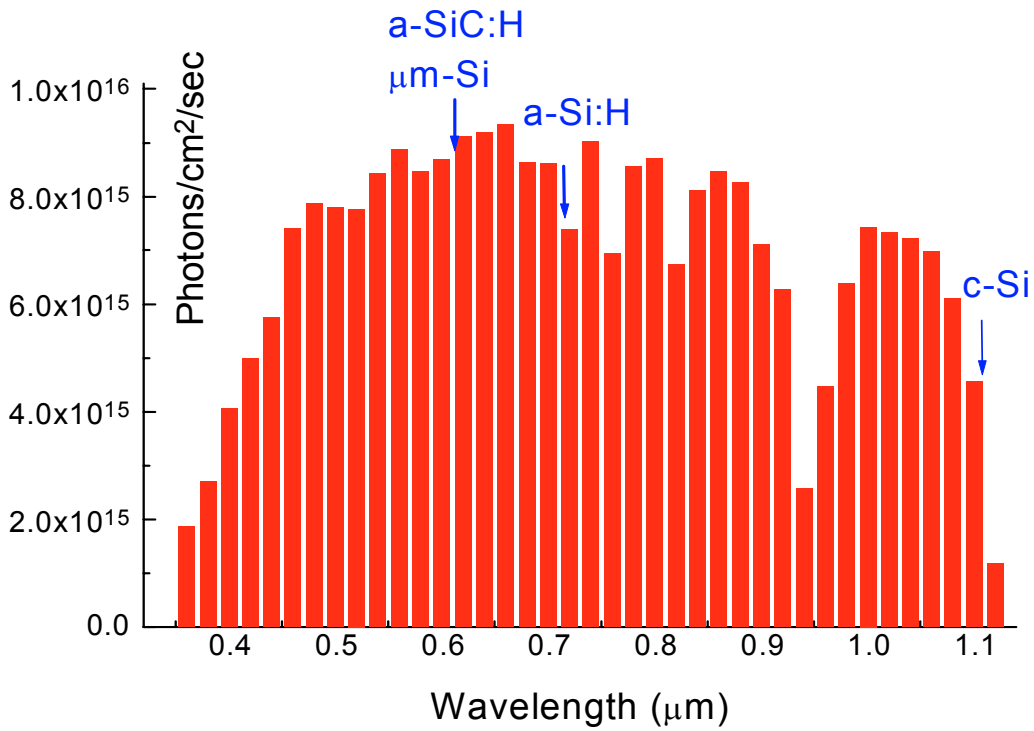

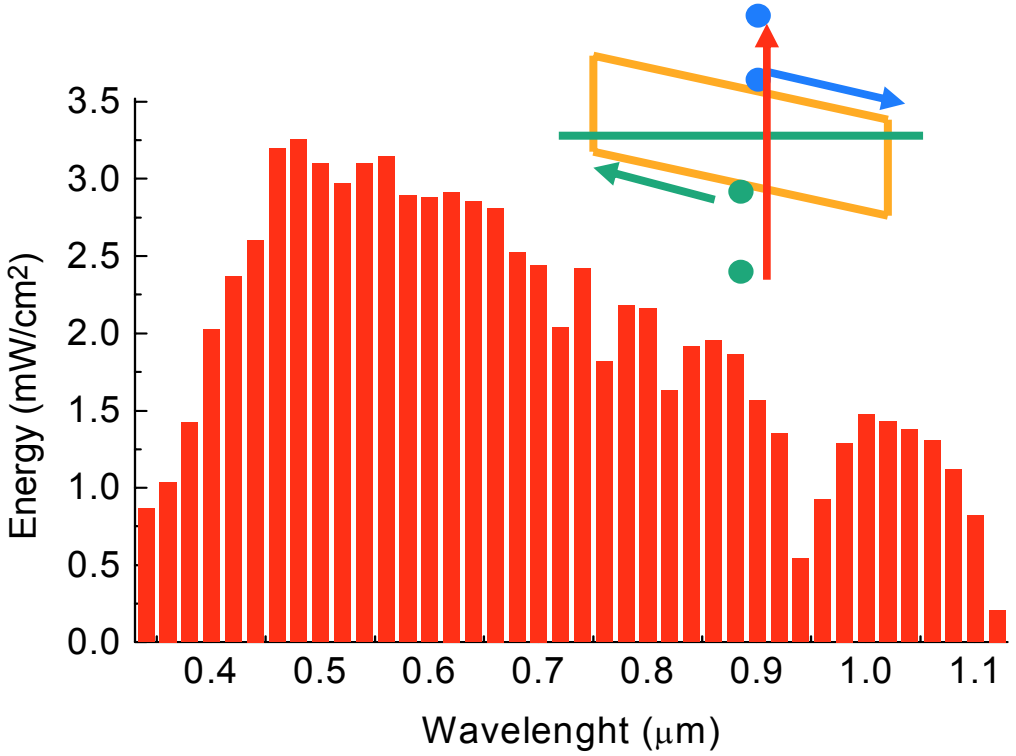

$\eta(\%) = J_M V_M / q\Phi < 100\%$

Maximum Currents:

J_{PHOTON}= 43.25 mA/cm² (c-Si)

J_{PHOTON}= 15.28 mA/cm² (a-SiC:H)

J_{PHOTON}= 22.20 mA/cm (**a-Si:H**)

Experimental Jsc ~ 17 - 18 mA/cm²

Maximum efficiencies:

$\eta(\%)$ = 79.7 (c-Si) - 50.5 (a-Si:H) absorbed energy

$\eta(\%)$ = 48.4 (c-Si) - 38.2 (a-Si:H) optical gap

$\eta(\%)$ = 45.6 (c-Si) – 23.6 (**a-Si:H**) activation energy

Highest experimetal efficiencies ~ 15%

Device characterization

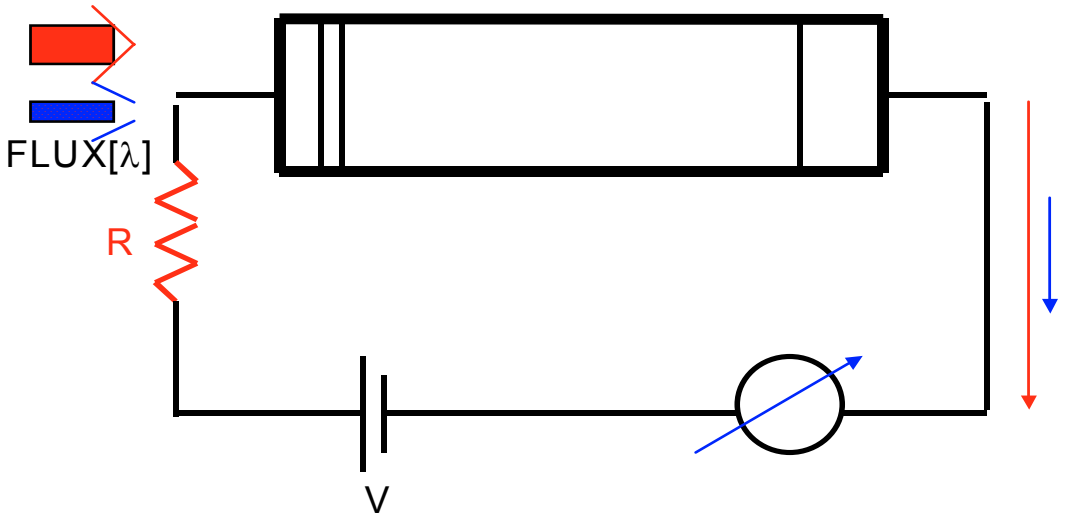

SPECTRAL RESPONSE

$QE = J(\lambda)/[q\Phi(\lambda)]$

$\Phi(\lambda) = FLUX(\lambda)$

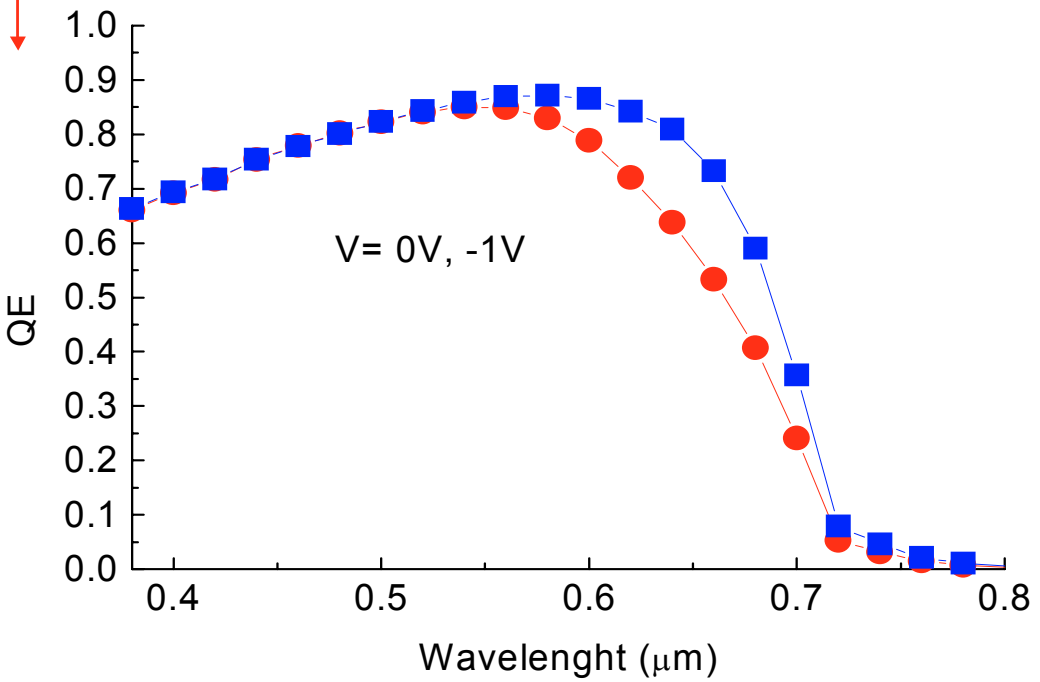

QE is function of:

- i-layer absorption coefficient and length
- absorption losses in p- and TCO
- reflection losses at the front surface
- effectiveness of light-trapping by textured substrates and TCO

* recombination and e.b.d. losses

Working strategy and getting started (1991)

- (a) - Collection of experimental data.
- (b) - Understanding of the transport mechanisms.
- (b) - Fitting of experimental solar cell J-V and SR.
- (c) - Moving from simple to complex device structures.
- (d) - Gaining confidence in the input parameters.
- (e) – Using the computer code as prediction tool.

  ==> Solar Cell Design.

- 1991 - a-Si:H Schottky barriers (Wronski, PSU).
- Characterization of the intrinsic layer: DBP, Photoconductivity.
- Solar Cell characterization: dark J-V and QE.
- three different i-layer thicknesses (0.9, 1.3, 2μm).
- 5 T (25, 50, 75, 90, 110 C).
- Fitting all these experiments ==> lower uncertainty.

Reality

- Dark J-V of Schottky barriers were successfully fitted for:
  (a) different i-layer thicknesses at a fixed temperature.
  (b) at different temperatures for a fixed i-layer thickness.

- The i-layer was grown at different deposition conditions.
  J-V and SR curves were changing on and on.

- Lesson 1: Fitting data with numerical modelling is much more difficult than with analytical modelling where many parameters are ignored.

- Fittings of dark J-V Schottky barriers were possible for different i-layer thicknesses using an uniform density of ionized donors (6×10^{14} cm^{-3}) inside the i-layer (DB~ 5×10^{15} cm^{-3}) .

Reality

Lesson 2: elaborated modelling does not necessarily helps (DOS).

- To fit dark J-V of a-Si p-i-n at different thicknesses we did not need to ionized donors in the i-layer.

- Lesson 3: what is learned in simple devices does not necessarily apply directly to more complex devices.
- Lesson 4: Better quality materials does not imply better solar cells (defect pool model).
- Lesson 5: Physics has to be constantly updated.

• **Inverse modelling:** fitting of experiments could be automatically achieved by running the computer code commanded by an auxiliary program that minimizes the mean square deviation between data and simulations.

Some important results (1992-1998)

- **Basic Device Physics:**

  Why the high forward dark J-V in p-i-n a-Si homojunctions is higher than in m-i-n a-Si Schottky barriers?

- **SR > 1 in a-Si based devices:**

  In a-Si based sensors BLUE bias light could give rise to

  SR >1. The QE peak is function of: bias and monochromatic light intensities, device length, DOS, forward bias voltage..

- **a-SiC/c-Si Hybrid Cells - Evidence of Tunneling:**

  Light J-V with good FF can not be explained without invoking tunneling currents flowing through the VB.

  spike present at the a-SiC/c-Si interface.

1

Fitting experimental dark and light J-V in Schottky barriers and in p-i-n a-Si devices

Red light source with intensities of 9×10^{15} #/cm^2/sec 7×10^{16} #/cm^2/sec (S)

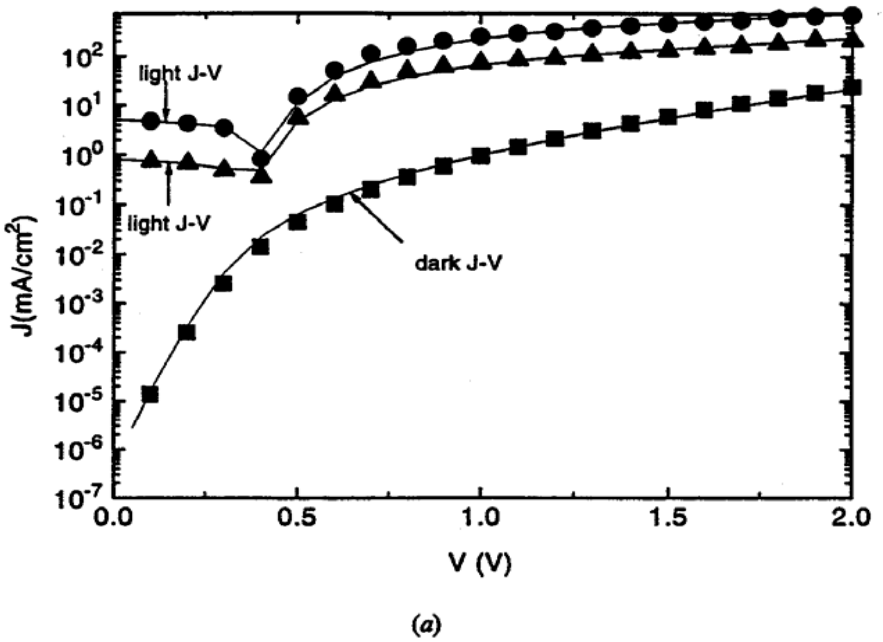

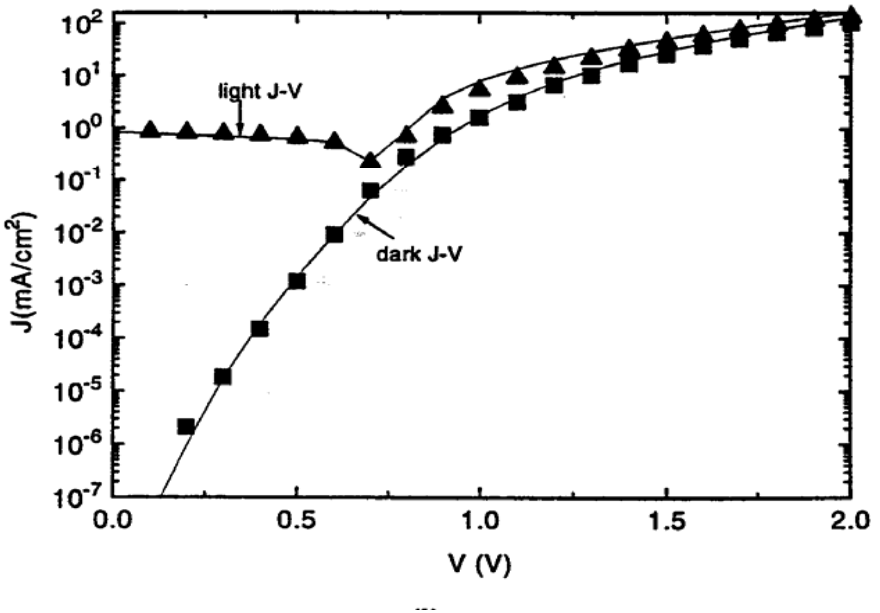

Transport mechanisms in the dark

1

p-i-n vs. Schottky

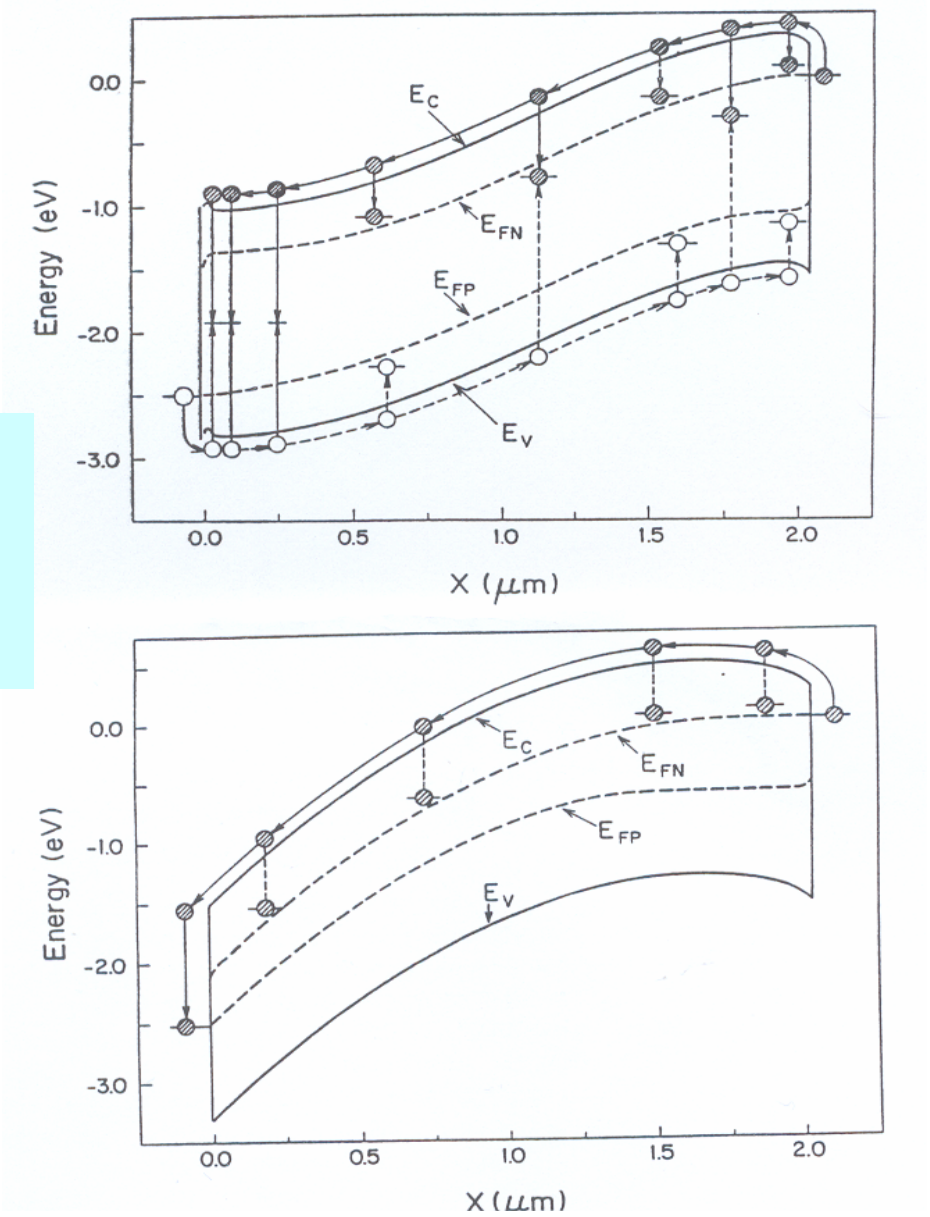

2

Measured QE characteristics of a Ni/(i)-a-Si/(n)-a-Si Schottky barrier for three different applied voltages: -3, 0, and 0.2V under

(a) Dark conditions

(b) Red bias light illumination

(c) Blue bias light illumination

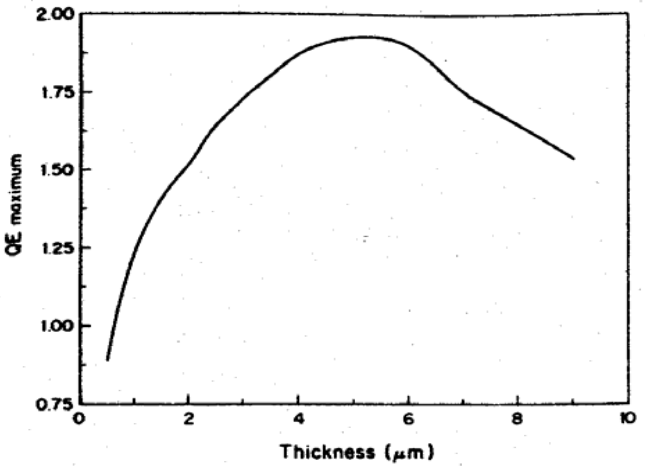

Predicted QE peak for different (i)-layer thicknesses

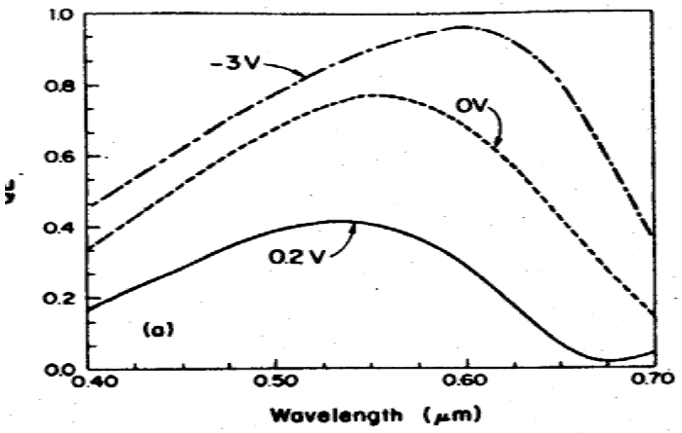

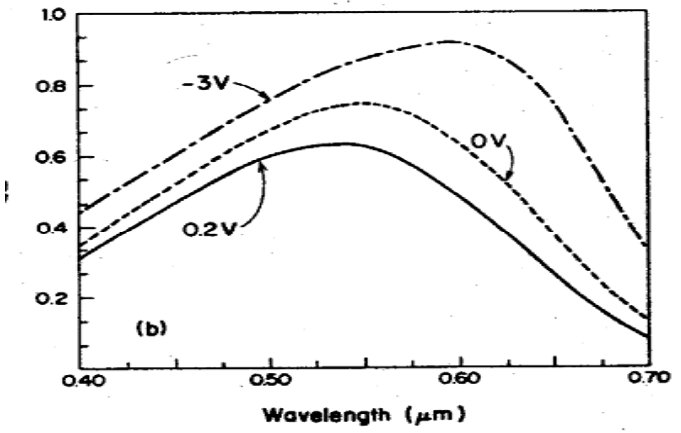

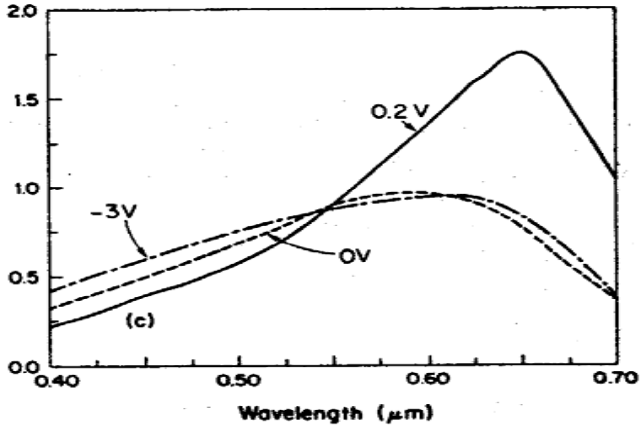

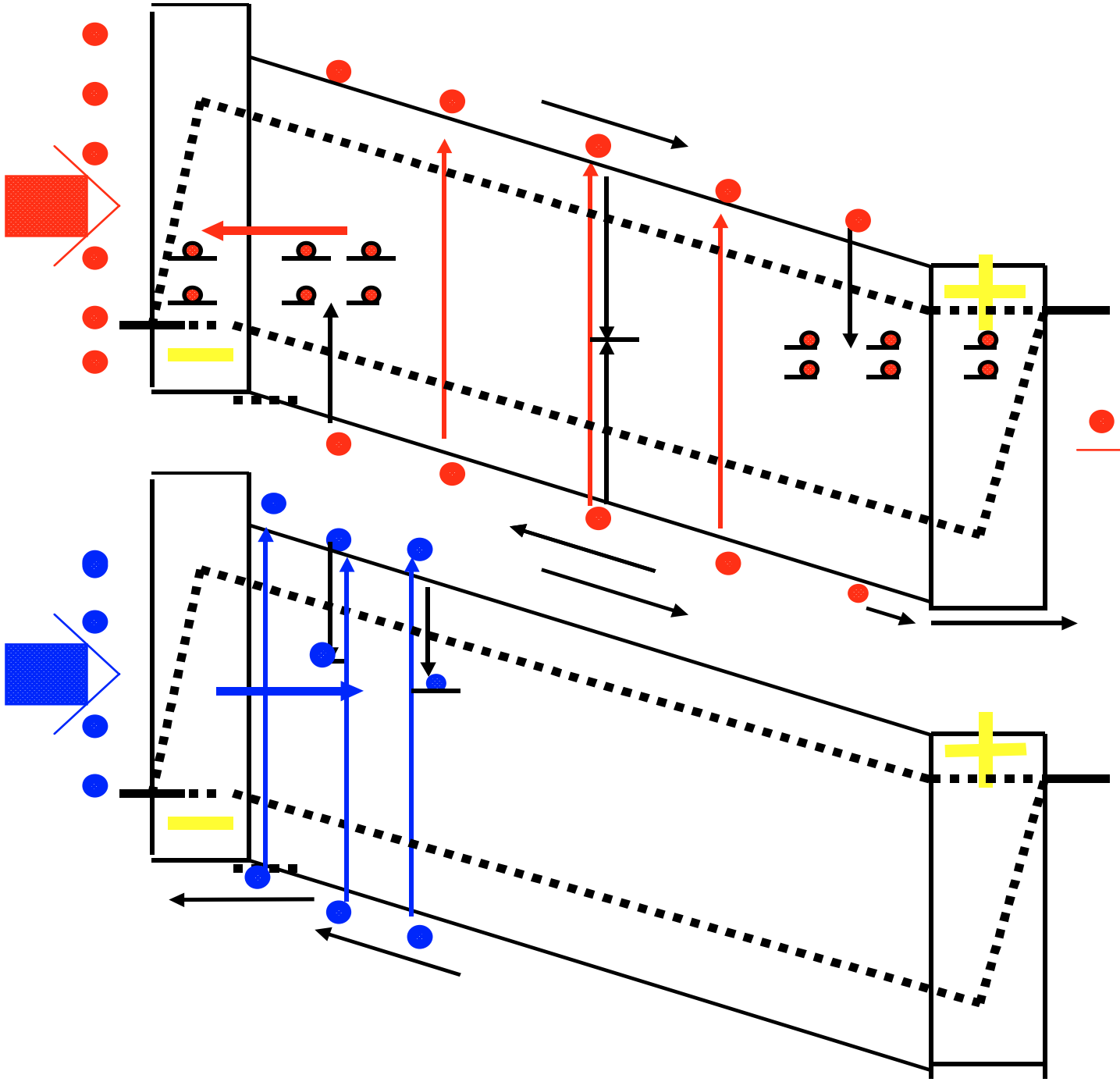

Red and blue bias light generate modifications in the electric field with opposite directions at the front region of the i-layer

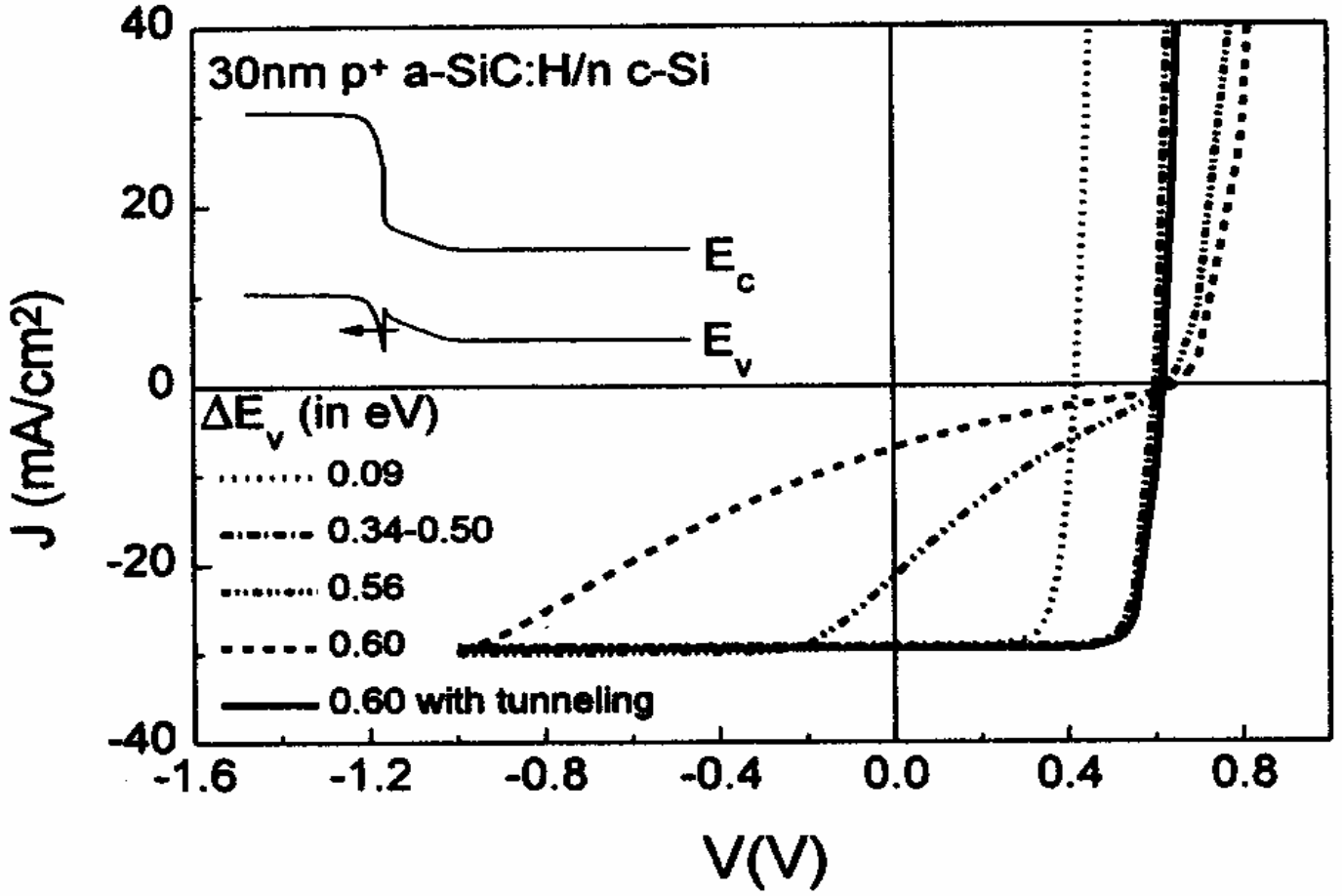

The spike at the a-SiC/c-Si interfaces was measured with internal photoemission and it was found to be ΔE_V= 0.6eV

Only by including the tunneling path at that VB spike it becomes possible to reproduce high experimental FF with our simulations

Modeling refinements: DB are really amphoteric

DB behave as donors and acceptor-like states → they are amphoteric
DB can be represented by two energy levels separated by U
D^+ (0 electrons), D^0 (1 electron) and D^- (2 electrons)

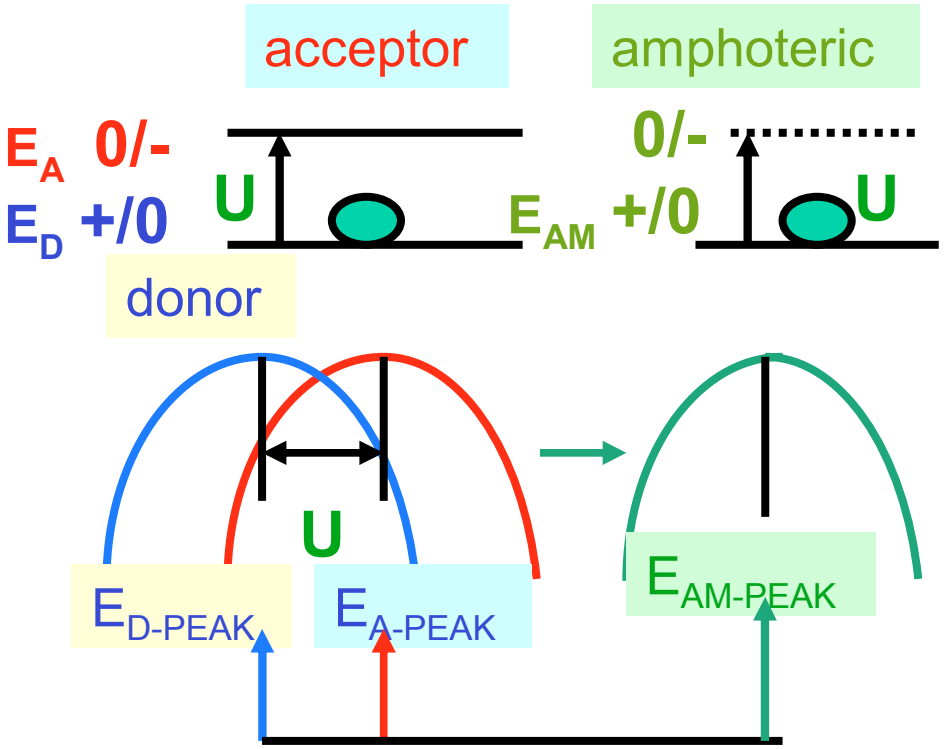

Amphoteric states with energy E_{AM} can be approximated by donor – acceptor pairs with energies E_D and E_A

σ_{ND} (σ_N^+) >> σ_{NA} (σ_N^0) (charged >> neutral)
σ_{PA} (σ_P^-) >> σ_{PD} (σ_P^0) (charged >> neutral)
U > 0 (positive correlation energy)

- $E_{AM\text{-}PEAK} = E_{D\text{-}PEAK}$
- $E_{A\text{-}PEAK} = E_{D\text{-}PEAK} + U$

DB approximated by donor-acceptor pairs

- U > 0
- $\sigma_{CH} >> \sigma_0$ CH= Charged 0= Neutral

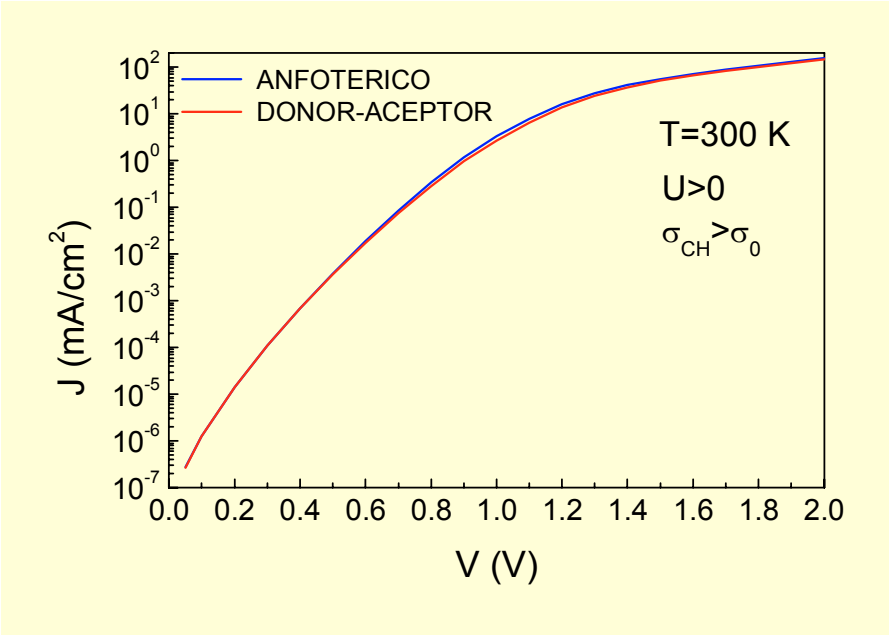

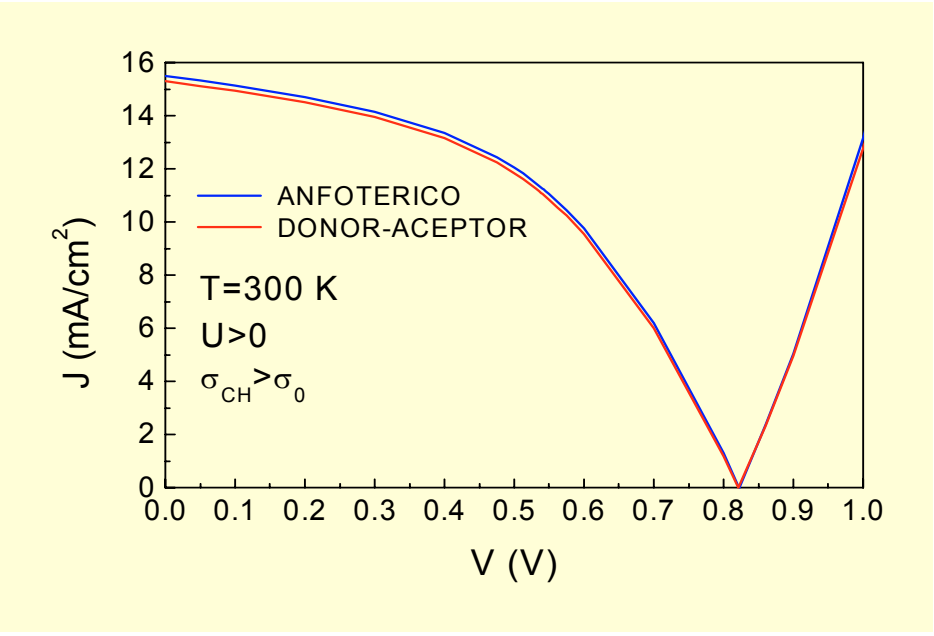

Approximation fails when U>0 and $\sigma_{CH} \leq \sigma_0$, or when U<0.

Trap density U>0
Acceptor-Donor or Amphoteric

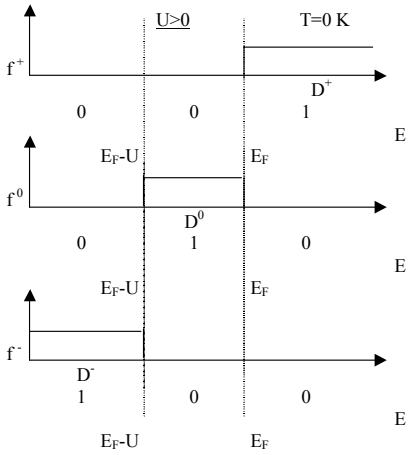

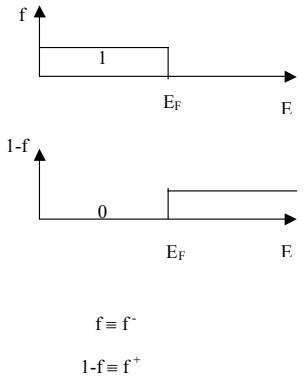

U>0

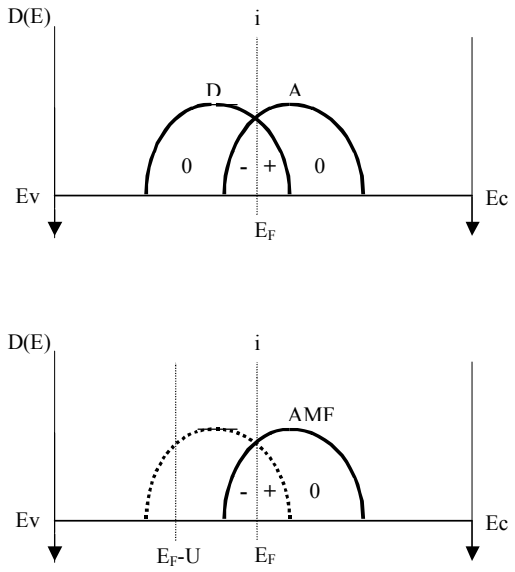

$$\rho = q \cdot \int_{E_v}^{E_c} N(E) \cdot \left[1 - f(E)\right] \cdot dE \quad \text{DONOR}$$

$$\rho = -q \cdot \int_{E_v}^{E_c} N(E) \cdot f(E) \cdot dE \quad \text{ACCEPTOR}$$

$$\rho = q \cdot \int_{E_v}^{E_c} N(E) \cdot \left[f^{+}(E) - f^{-}(E)\right] \cdot dE \quad \text{AMPHOTERIC}$$

Double occupied states move U to the left
The approximation keeps unaltered the charge distribution

U>0 and $\sigma_p^- = \sigma_p^0$ ($\sigma_n^+ = \sigma_n^0$,)
amphoteric state (-) → only can trap holes

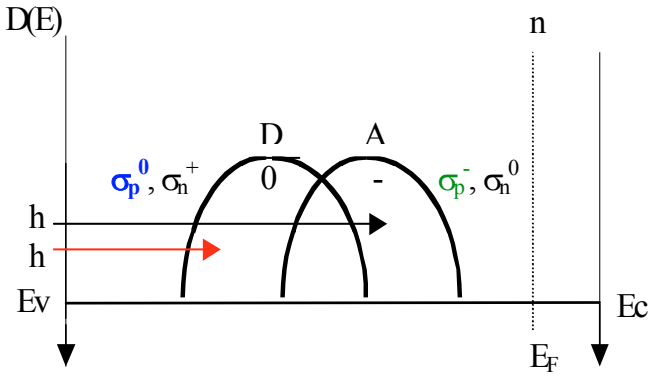

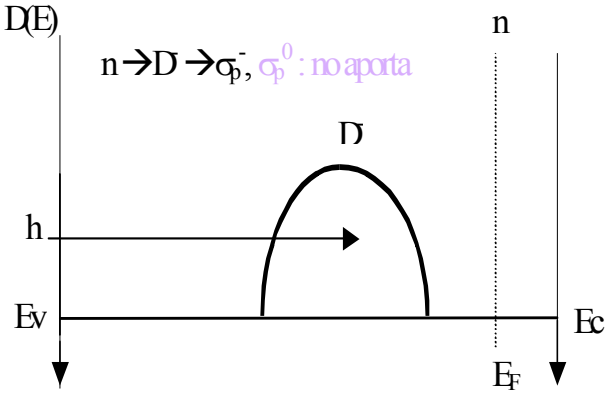

Defect Pool Model

Successful in describing the defect density in doped and un-doped a-Si

Accounts for the origin of DB
WB ↔ DB conversion
H mediates in the reaction

WB ↔ 2DB (i=0)
Si – H + WB ↔ (DB + Si-H) + DB (i=1)
2(Si – H) + WB ↔ (Si-H-H-Si) + 2DB (2)

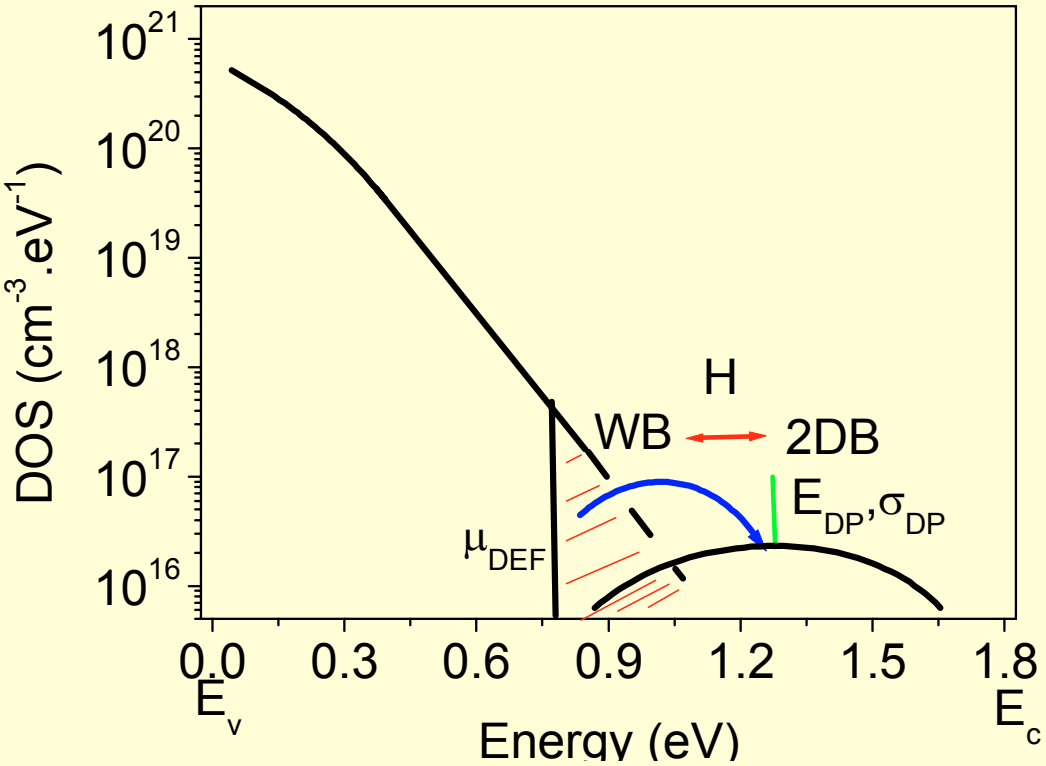

- Energy distribution of WB → VB tail state distribution $g_D(E)=G_{DO}\exp(-E/E_D)$
- P(E): distribution of available defect sites: Gaussian distribution
  E_{DP}: peak position or defect pool center σ_{DP}: defect pool standard deviation

$$P(E) \equiv \left[\frac{1}{\sigma_{DP}\sqrt{2\pi}}\right] \exp\left[\frac{-(E-E_{DP})^2}{2\sigma_{DP}^{\ 2}}\right]$$

Defect Pool

DB density results from minimizing the free energy G of the system WB + DB + Si-H + H

Chemical Defect Potential

$\mu_D = \langle e \rangle - kTs_e$ (+ H term)

~ E_F ($D^+ \rightarrow$ p-a-Si)

~ E ($D^0 \rightarrow$ i-a-Si)

~ $2E - E_F + U$ ($D^- \rightarrow$ n-a-Si)

Two (one) algorithms of Powell and Deane (Schuum) No evidences of defect pool in μc-Si

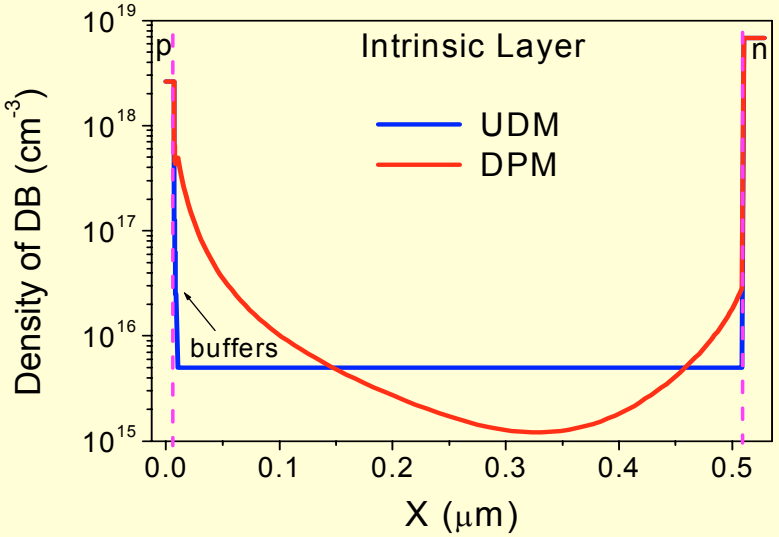

DB density becomes function of the E_F position

T_{EQ}: freezing or equilibration temperature

D(E) at $T < T_{EQ}$ = D(E) at T_{EQ} (frozen at T_{EQ})

E_{DP} coincides with D^+ peak = $E_F + \Delta/2$

$\sigma_{DP} \leftarrow \Delta = 2\rho\sigma_{DP}{}^2/E_D - U \sim 0.44$eV

Out	New	Same
N_{G1}, N_{G2}, N_{G3}	T_{EQ}	E_D
E_{G1}, E_{G2} , E_{G3}	E_{DP}	G_{DO}
$S_{G1} = S_{G2} = S_{G3}$	H	$\sigma_N{}^0$, $\sigma_P{}^-$, $\sigma_N{}^+$, $\sigma_P{}^0$

a-Si solar cell characteristics

- The electric field inside the i-layer of a p-i-n cell becomes less uniform.
- There are more defects near the p/i and i/n interfaces.
- Stronger F near interfaces and weaker F in the bulk.
- *At equilibrium* we have *F ~ 10^5 V/cm (interfaces) F ~ 10^4 V/cm (bulk).*
- *At maximum power we have F ~ 10^2 V/cm in the bulk.*

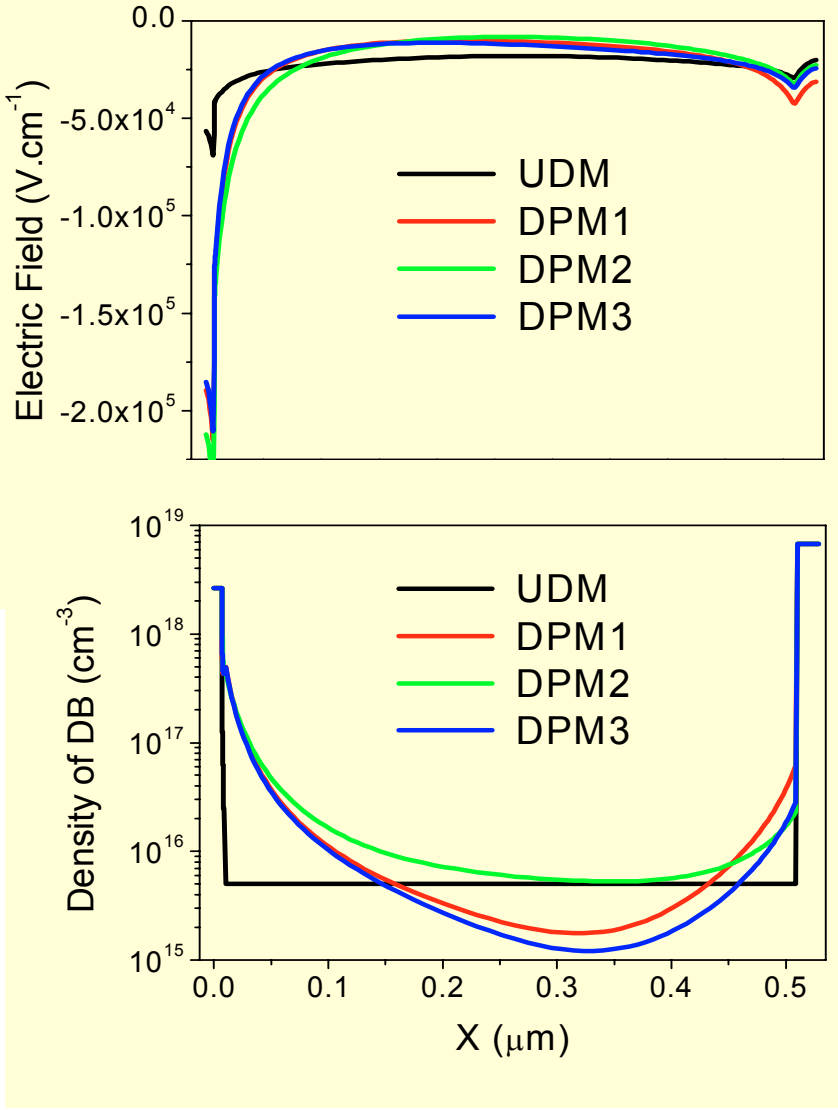

Design to increase the efficiency: Gap Grading

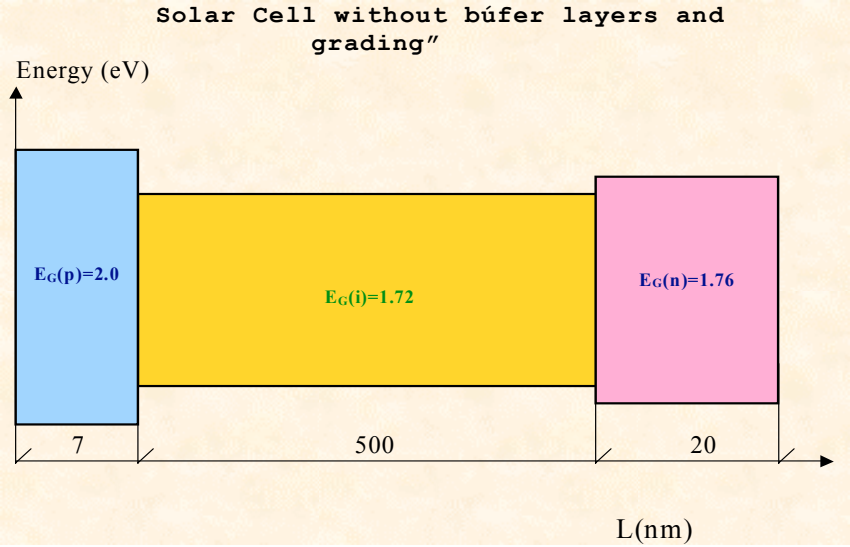

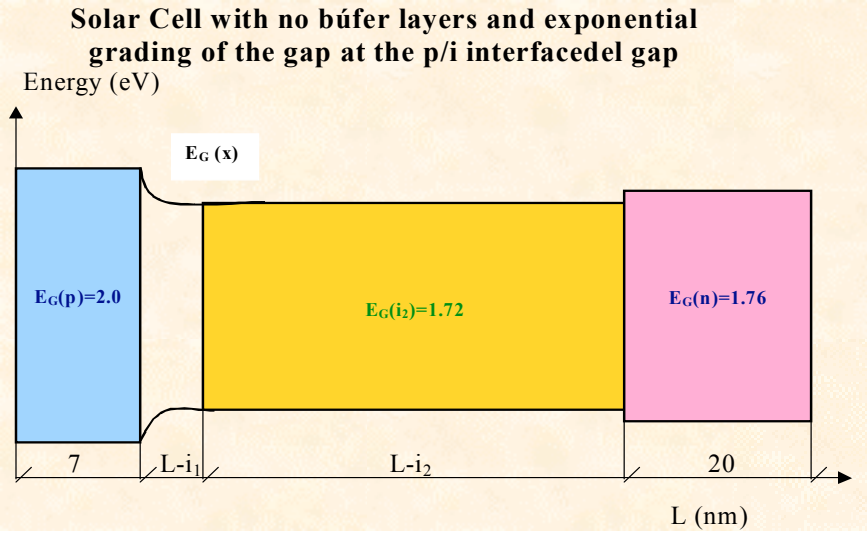

- Band-gap profiling of the intrinsic layer assisting transport of holes in the low field region

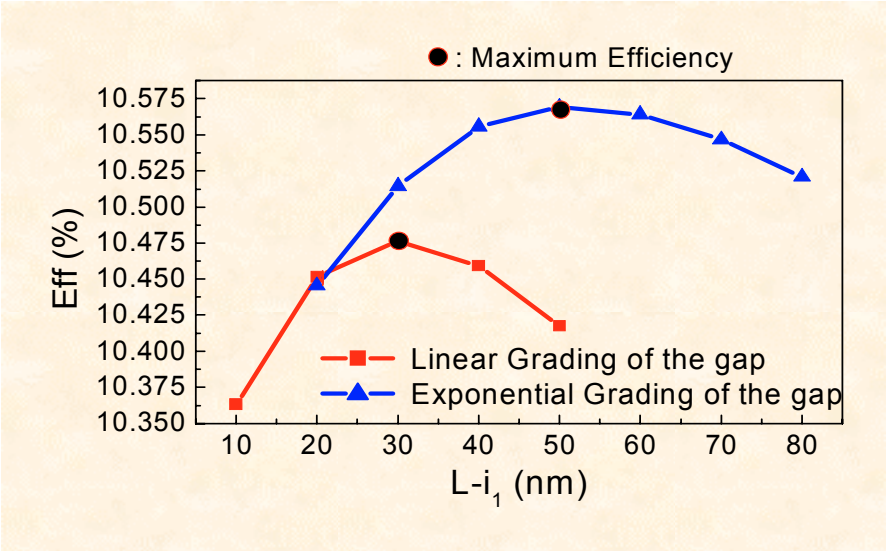

Doping and Gap Grading

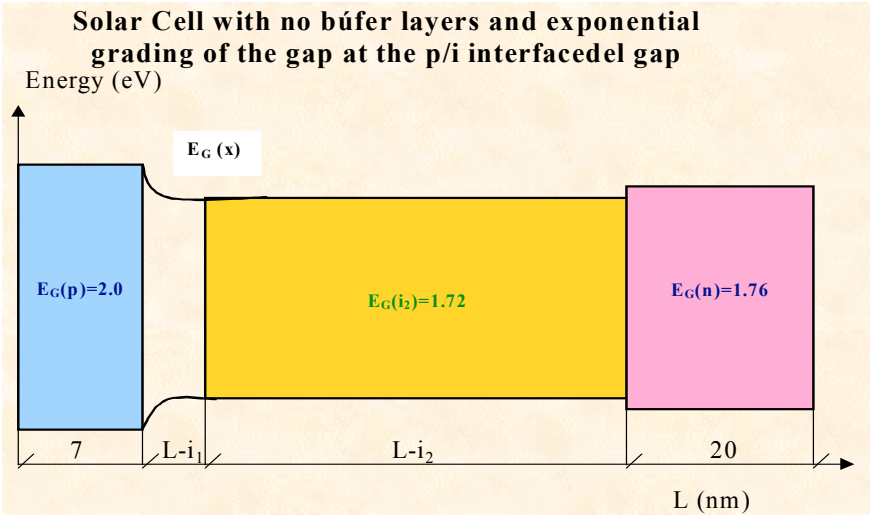

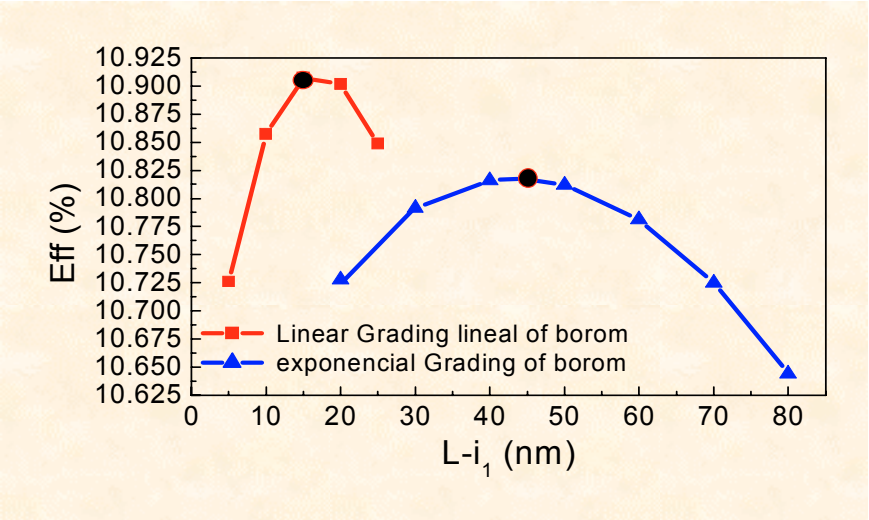

- Field redistribution using low-level of impurity doping
- They will also introduce more defects

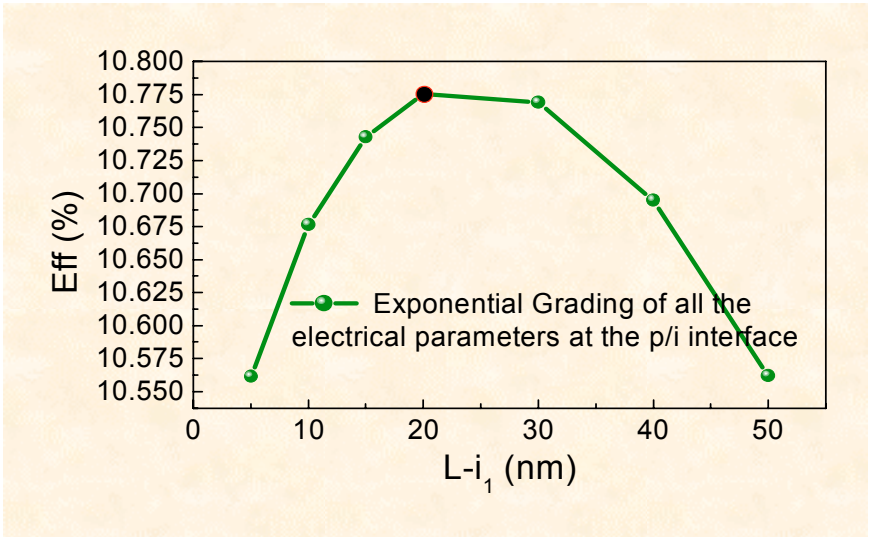

Exponential Grading of all electrical parameters

- E_G, χ, E_{DP}, σ_{DP}, N_A, E_D, E_A, μ_n, μ_p, N_c, N_v, $\sigma_{CH,0}$.
- $Eff_{máx}$=10.77%.
- Highest impact: E_D.

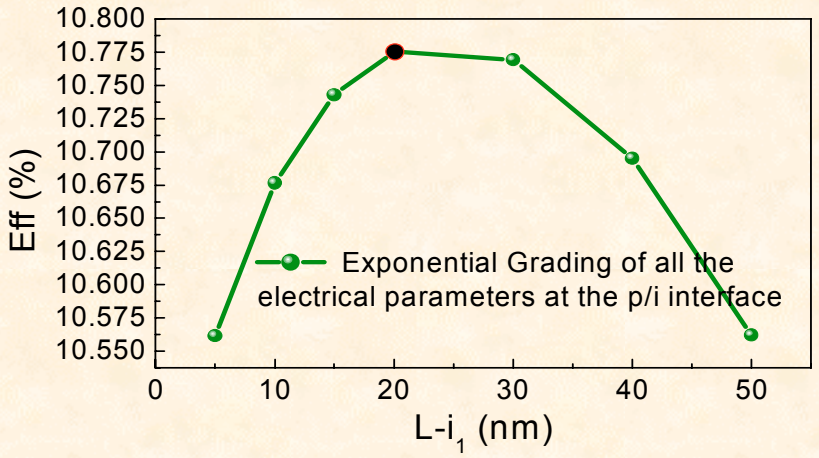

UDM: p/i interface

- Grading N_{DB} → decrese of Eff.
- Recommend removal of buffer layers to increase the Eff → contradicts experimental findings.

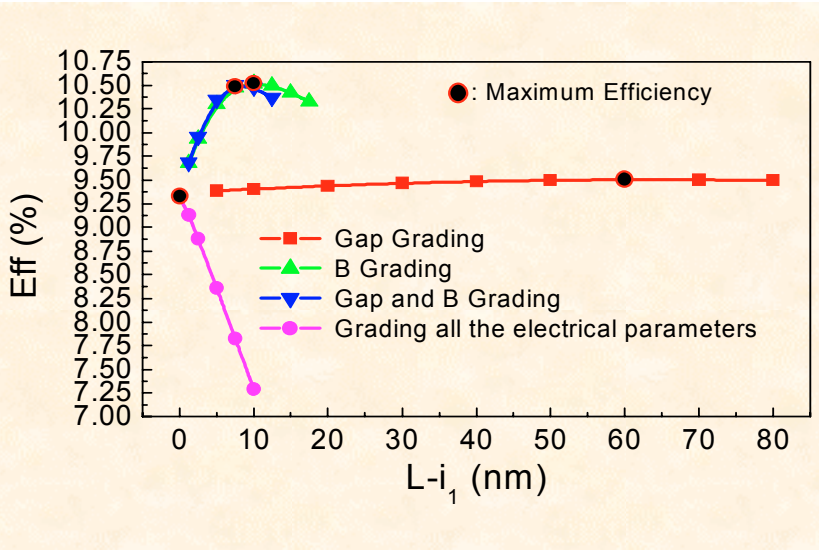

i/n interface

- Gap grading increases Eff.
- P grading decreases Eff.

Metastability in a-Si

- Discovered by Steabler and Wronski (SWE) (1977)
- After illumination in a-Si:

  (a) E_F shifts towards mid-gap

  (b) Dark and Photo conductivity decrease

  SWE *is a bulk* effect (??)
- Evidence of increasing density of neutral Si DB
- Metastable DB can be removed by annealing *1-3 hours above 150C*

- SWE is caused by ?? (more than 15 models were proposed) →

  Recombination of excess free carriers generated by light or by contact injection
- *Saturated defect density ~ 10^{17} cm^{-3} (initial defect density ~5-810^{15} $cm^{-3)}$*
- Light induced DB (LDB) are intrinsic to a-Si:H

Metastability in a-Si Solar Cells

- (a) - Largest changes occur in FF.
- (b) - Changes in J_{SC} and and V_{OC} are small.
- (c) – Thicker cells degrade deeper.
- (d) – Cells with high impurity concentration (> $10^{18}cm^{-3}$) in the intrinsic layer degrade deeper than cells with highly pure intrinsic layers.
- (e) – Cells operating at high T (60-90C) stabilize at higher efficiencies than cells operating a 300K.
- (f) – Exposure to high (low) intensity illumination causes deeper (reduced) degradation.
- (g)– Cells with intrinsic layers made with highly hydrogen-diluted silane stabilize at a higher η.
- (h) No correlation between films and cell stability. Defect pool model influences results on cells. Fermi level change with position in cells.

Metastability in a-Si Solar Cells

- *Rate of degradation under 1 sun is*
  (a) – high during first tens of hours
  (b) – decreases over time
  (c) – stabilizes after hundreds of hs
  (d) – initial efficiency can be recovered by annealing
  (150C for several hours)
- *Degradation not caused by*
  (1) – diffusion of ions or dopants
  (2) – electrical migration
- *LDB introduce extra recombination and trapping*
- *SWE modifies the electric field inside the device*

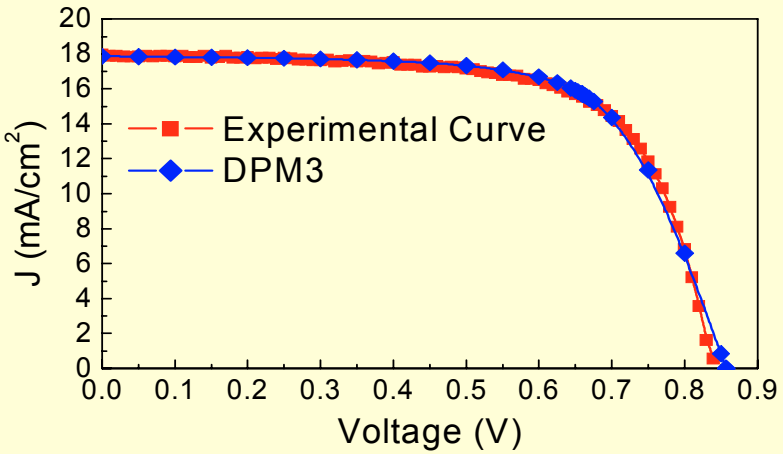

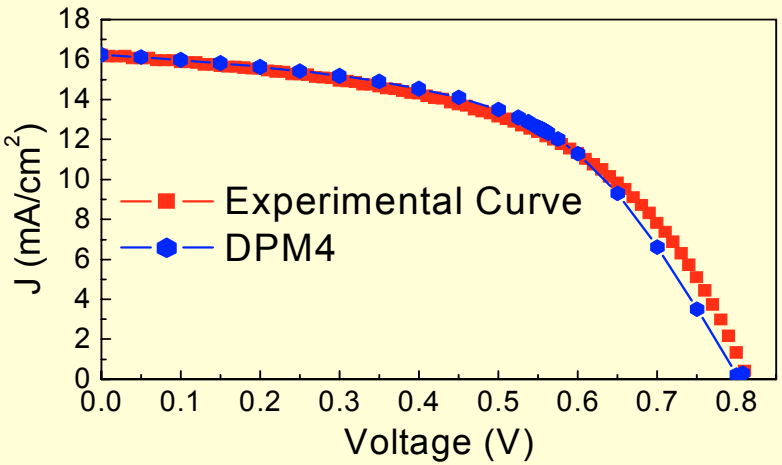

Comparing the DB densities

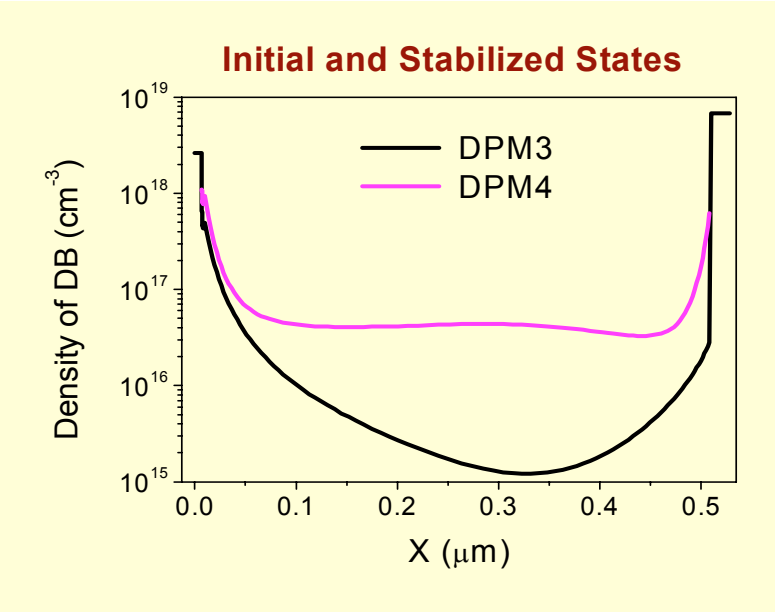

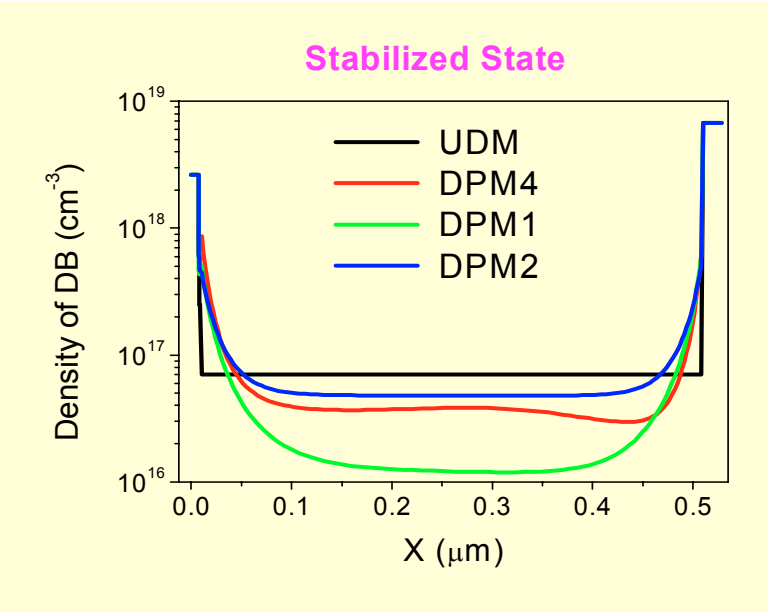

- Schuum's model → :reasonable fittings at different i-layr thicknesses for the initial and stabilized state
- Cross sections are slightly different in each case .

μc – Si

- **Poly Si:**
- Large grains ≥ 100nm
- no amorphous phase
- crystalline grains and boundaries
- Columnar structure → 2D
- **μc – Si** :
- Small grains ~ 20-30nm
- Mixture of crystalline grains, grain boundaries, amorphous phase and voids
- contain amorphous tissue
- crystalline grains and grains boundaries
- **1D or 2D?**

Polycrystalline Si: Grain Size of 0.1μm - 100μm

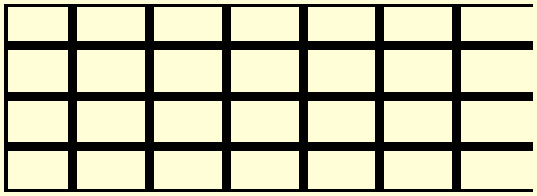

Microcrystalline Si: Grain Size of 30nm or less

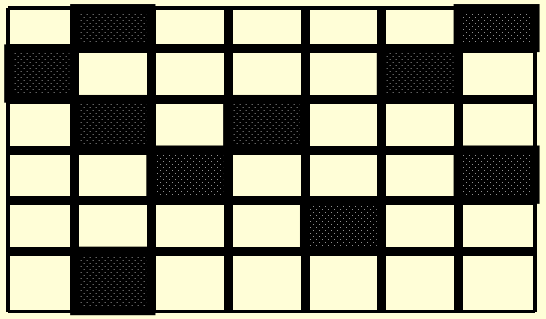

Best Material:
High Deposition Rate
Low Substrate Temperature
Small Fraction of Voids
Low content of Oxygen
Low or Lack of Degradation upon Light Soaking

Comparing a-Si and μc-Si

a-Si:H

- Frequency deposition:
  13.5 MHz - 200MHz
- Low temperature deposition T_S ~ 420 - 520K
- Deposition rate (PECVD) ~ 0.3 nm/sec at 13.5 MHz
  5 times higher at VHF-GD
- Staebler Wronski Effect
  Degradation of its electrical properties under illumination
  Dark conductivity increases
  Photoconductivity decreases

μc-Si:H

- Same frequency deposition: but prepared at higher H dilutions and RF power
- Low substrate temperature T_S < 500C (High T_S poly-Si)
- Advantages over a-Si:
- (a) - lower SWE
- (b) - higher light absorption in the infrared region
- Drawbacks:
- (a) - thick absorbing layers at low deposition rates
- (b) anomalous incorporation of impurities (mainly O)

Device Quality Material
Intrinsic a-Si and μc-Si

- Dark conductivity < 10^{-10} Ω^{-1} cm^{-1}
- AM1.5 conductivity > 10^{-8} Ω^{-1} cm^{-1}
- Activation Energy ~ 0.8eV
- Mobility Gap < 1.8eV (1.72eV)
- Density of Dangling Bonds
  $\leq 10^{16}$ cm^{-3} (opto-electrical)
  and 8×10^{15} cm^{-3} (ESR)
- $\mu\tau_{ELECTRONS}$ ~ 10^{-6} cm^2/V
- $\mu\tau_{HOLES}$ ~ 10^{-8} cm^2/V
- Minority L_D ~ 100-200nm
- Absorption Coefficient
  $\geq 3.5 \times 10^4$ cm^{-1} at 600nm and
  5×10^5 cm^{-1} at 400nm

- Dark conductivity < 10^{-7} Ω^{-1} cm^{-1}
- AM15 conductivity > 10^{-5} Ω^{-1} cm^{-1}
- Activation Energy ~ 0.53-0.57eV
- Mobility Gap: 1.2 –1 6 eV
- Density of Dangling Bonds
  $\leq 10^{16}$ cm^{-3} (ESR)
- $\mu\tau_{HOLES}$ ~ 10^{-7} cm^2/V
- Minority L_D > 500nm
- Crystalline volume fraction (Raman) > 90%
- Lower values are acceptable in μ c-Si cells.

Light absorption of a-Si and μc-Si

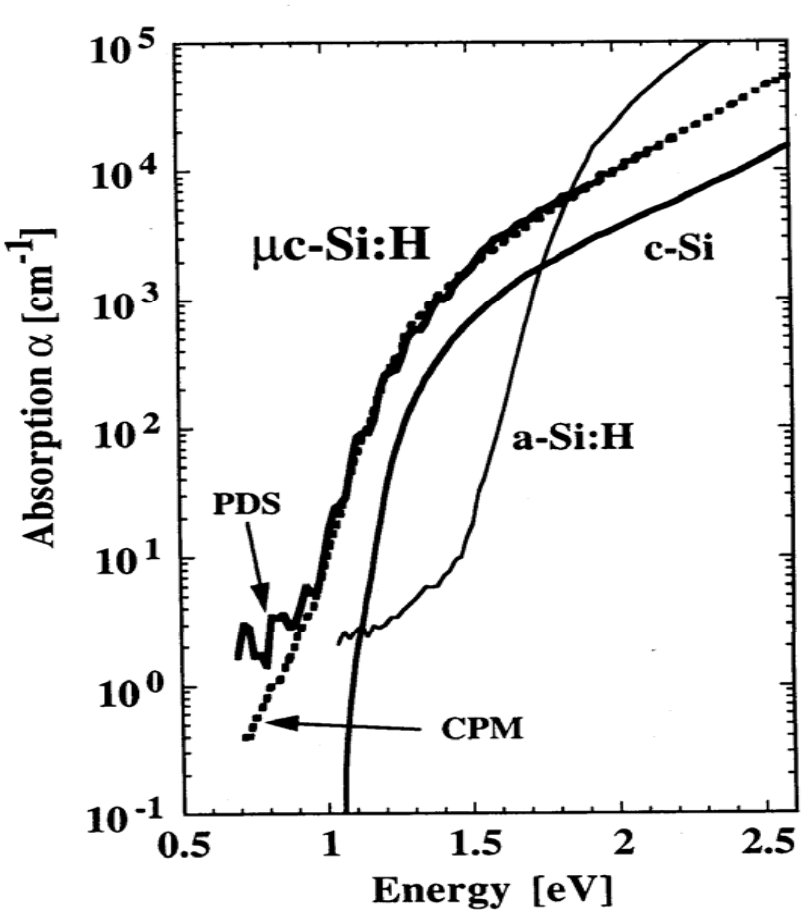

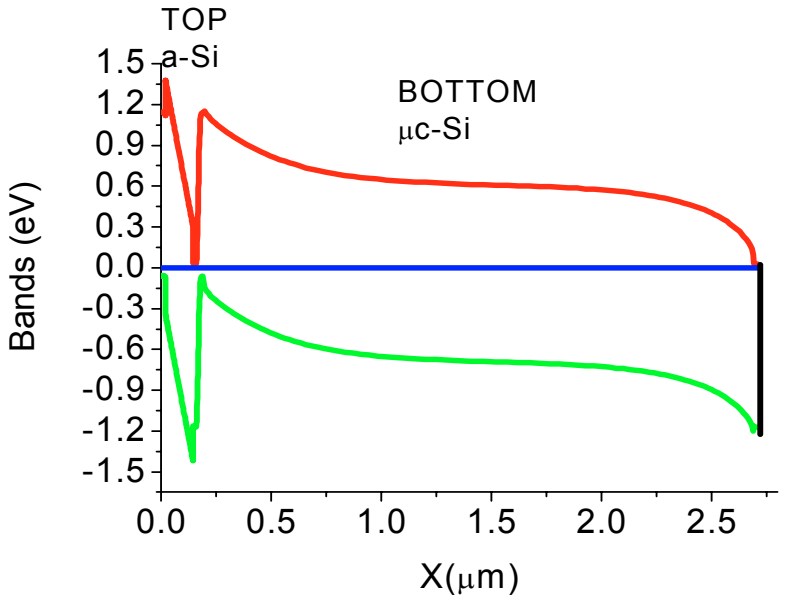

a-Si/μc-Si Tandem

Main breakthroughs in solar cells over the past 25 years (MRS –2004)

- (1) Textured transparent contacts for light trapping
- (2) a-Si deposited with hydrogen dilution for greater stability
- (3) a-SiC and μc-Si doped layers for higher Voc and better blue response
- (4) TCO/silver and TCO/aluminum rear contact for enhanced reflectivity
- (5) Multi-gap, multi-junction devices for optimum utilization of the solar spectrum
- (6) μc-Si intrinsic layers for improved red-response and stability
- (7) Band gap tailoring and engineering of device structure for optimum performance (a-SiGe and a-Si)

Front electrode
Textured contacts – Light trapping

- **TCO** (pin) SnO_2:F, ZnO:Al, relatively thick ~ 600nm and textured. (nip). ITO (In_2O_3:Sn) 70-80 nm
- Requirements: Highly transparent lo light and highly conductive
- Ability to scatter light → **Haze ratio** ($T_{DIFFUSE}/T_{TOTAL}$)

($T_{TOTAL} = T_{DIFFUSE} + T_{SPECULAR}$ usually taken in air)

- Optimum Haze Ratio ~ 6-15%.

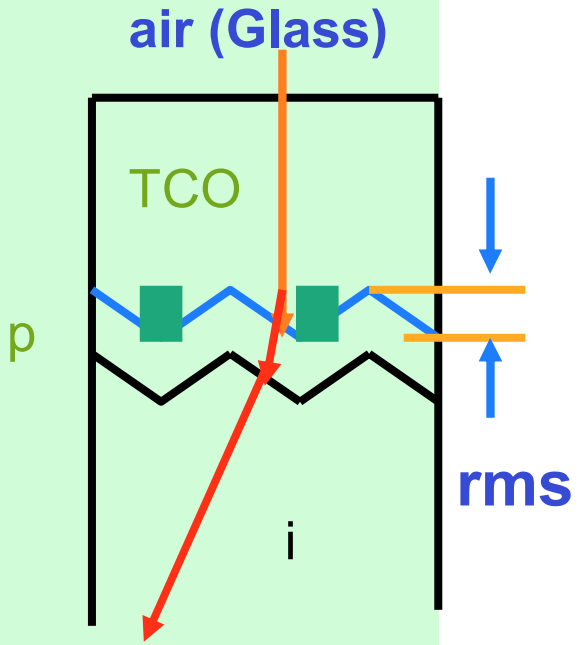

- Should provides an antireflection layer.
- Sheet resistance is high.

→ Metal grid to reduce series resistance.

→ And to keep FF reasonably high.

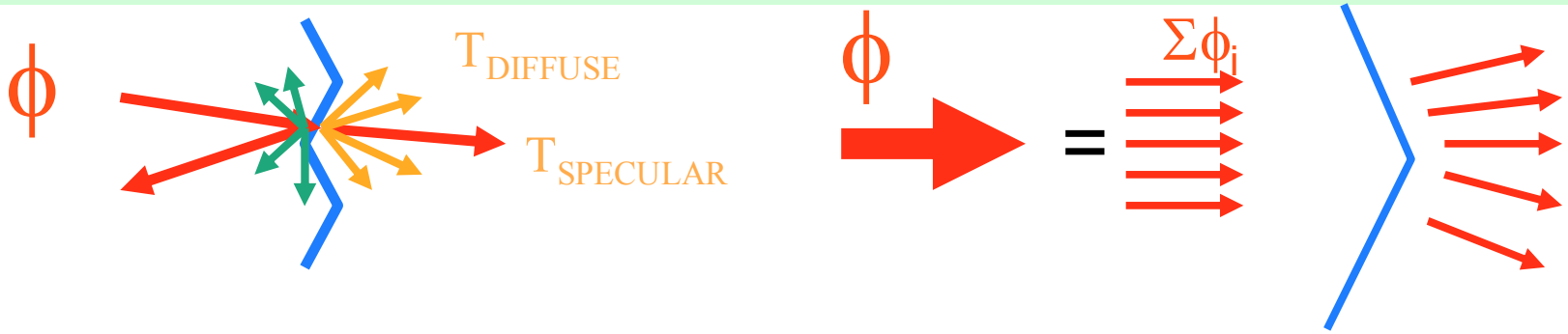

Rough and Flat TCO
Hydrogen diluted a-Si

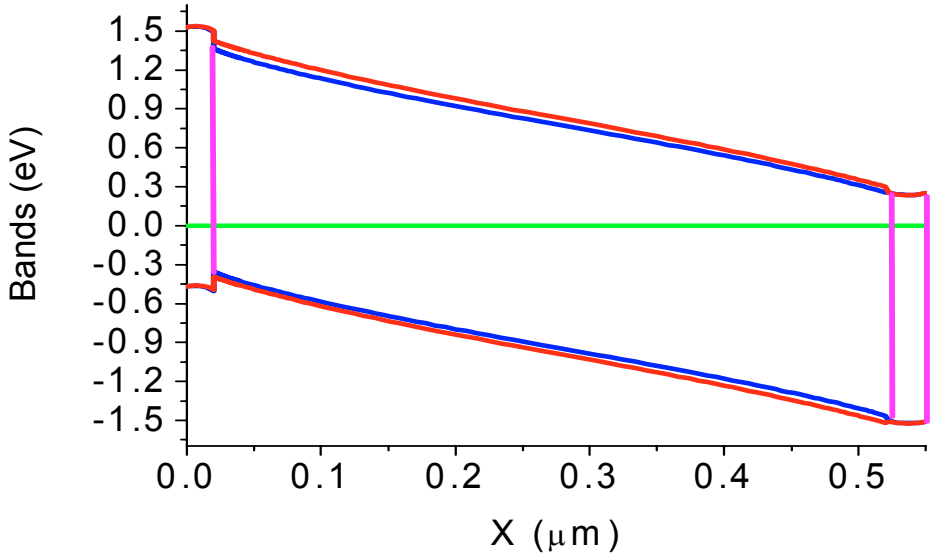

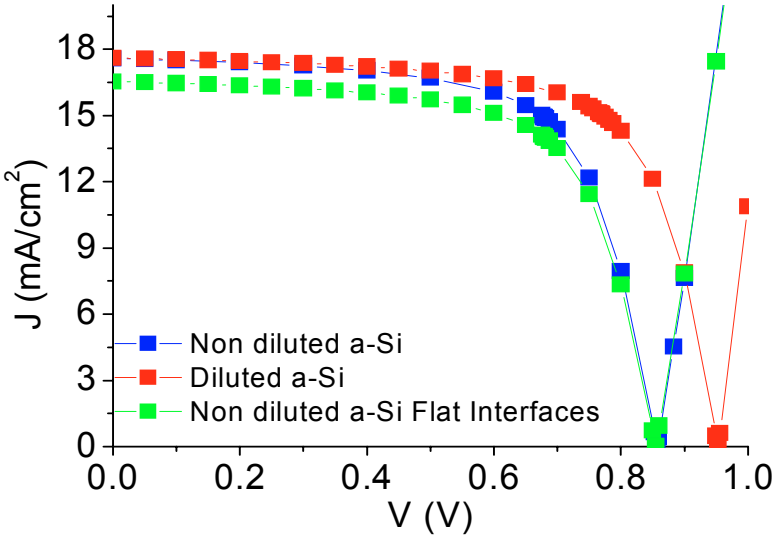

- Rough TCO increases Jsc by ~ 1mA/cm^2
- a-Si gap is increased from 1.72 to 1.82eV

→ Voc increases ~ 0.1V= ΔE_G

a-SiC and μc-Si doped layers

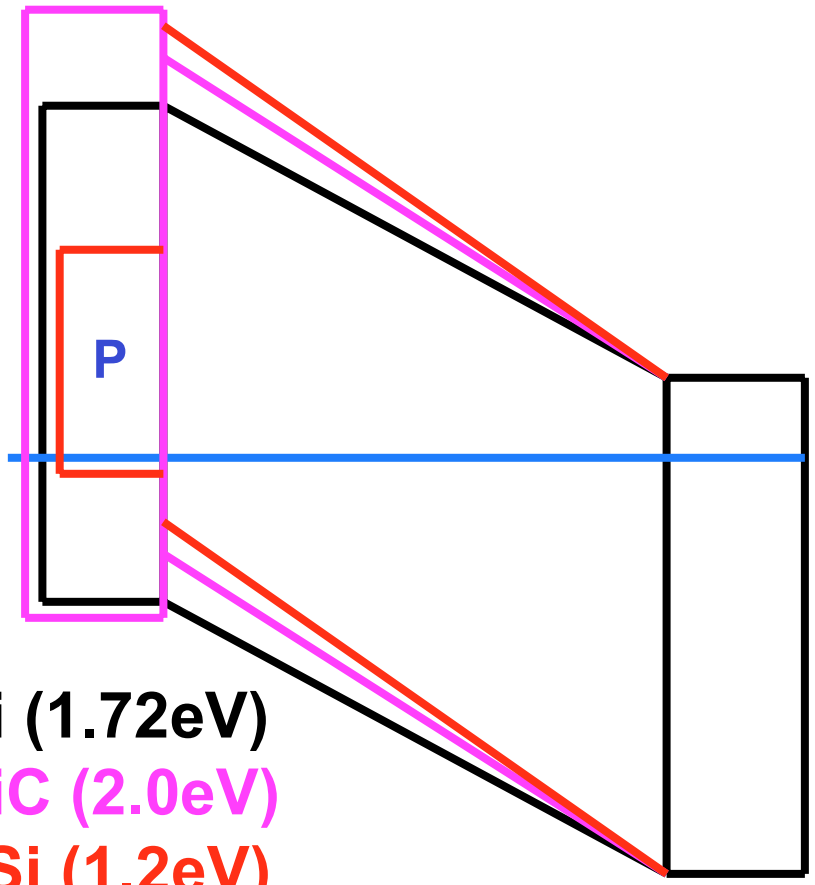

a-Si (1.72eV)

a-SiC (2.0eV)

μc-Si (1.2eV)

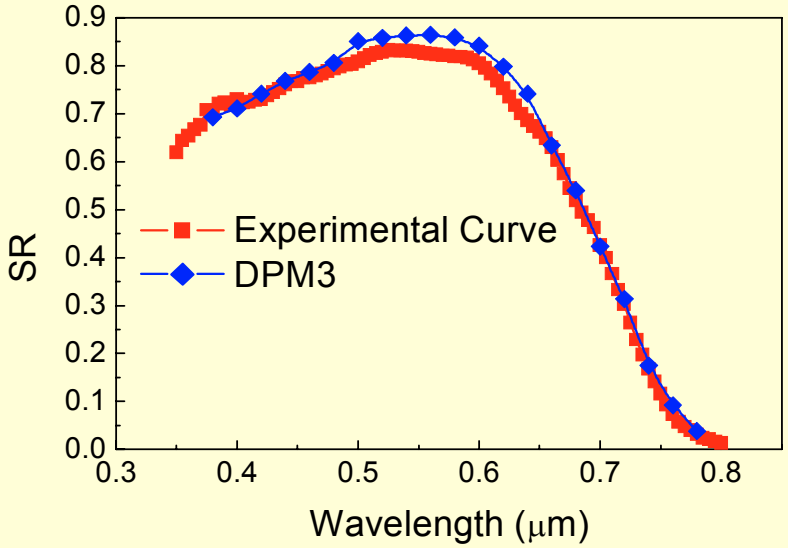

Device Quality Material
Doped a-Si and μc-Si

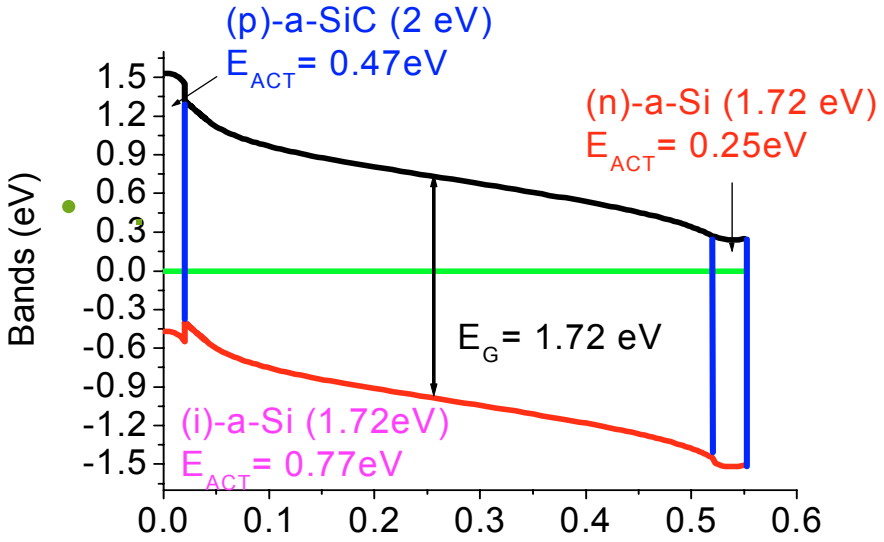

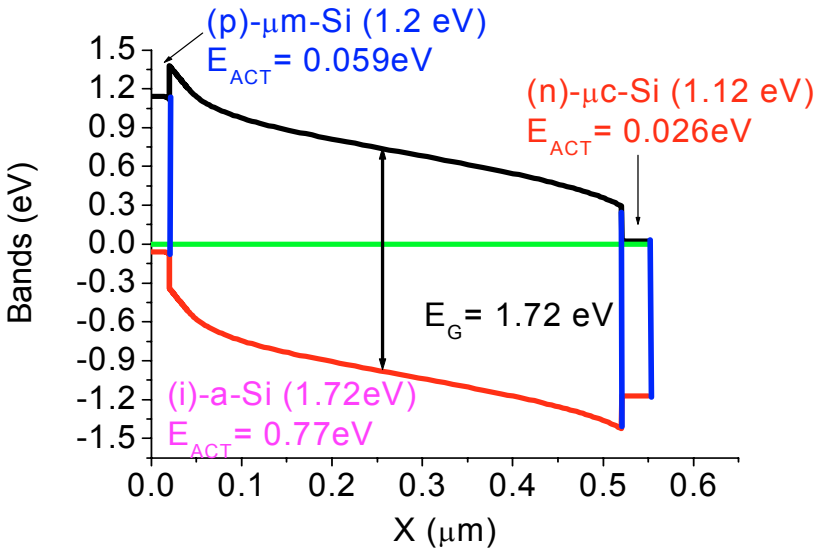

a-Si

- p-type (20nm thick)
- Conductivity > $10^{-7}\ \Omega^{-1}\ cm^{-1}$
- Activation Energy < 0.5 eV
- Band Gap (Tauc) > 2.0 eV
- Absorption Coefficient at 400nm < $3x10^{5}\ cm^{-1}$
- Absorption Coefficient at 600nm < $10^{4}\ cm^{-1}$
- n-type (15nm thick)
- Conductivity > $10^{-4}\ \Omega^{-1}\ cm^{-1}$
- Activation Energy < 0.3 eV
- Band Gap (Tauc) > 1.75 eV

μc-Si

- p-type (20nm thick)
- Conductivity $2.6X10^{-2}\ \Omega^{-1}\ cm^{-1}$
- Activation Energy ~ 0.059eV
- n-type (15nm thick)
- Conductivity $2.5\ \Omega^{-1}\ cm^{-1}$
- Activation Energy ~ 0.026eV

(i)layer built-in potentials
μc-Si vs. non μc-Si doped layers

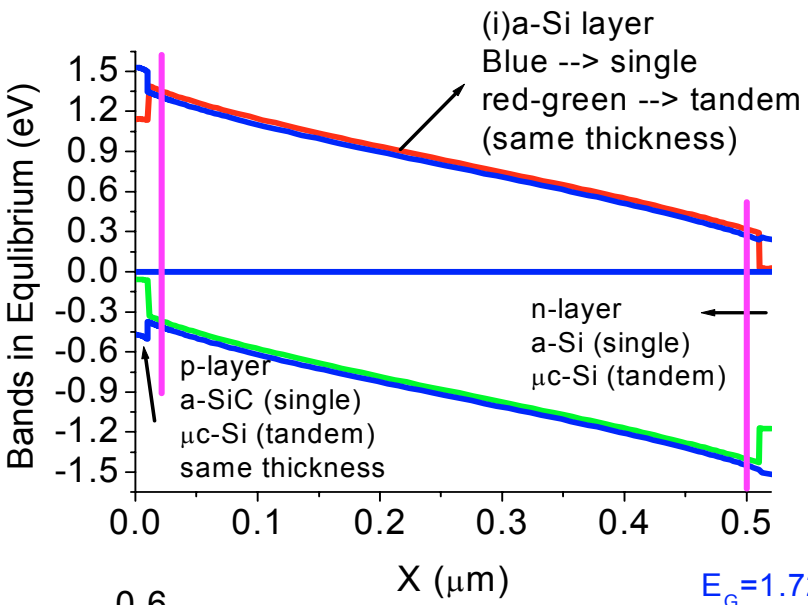

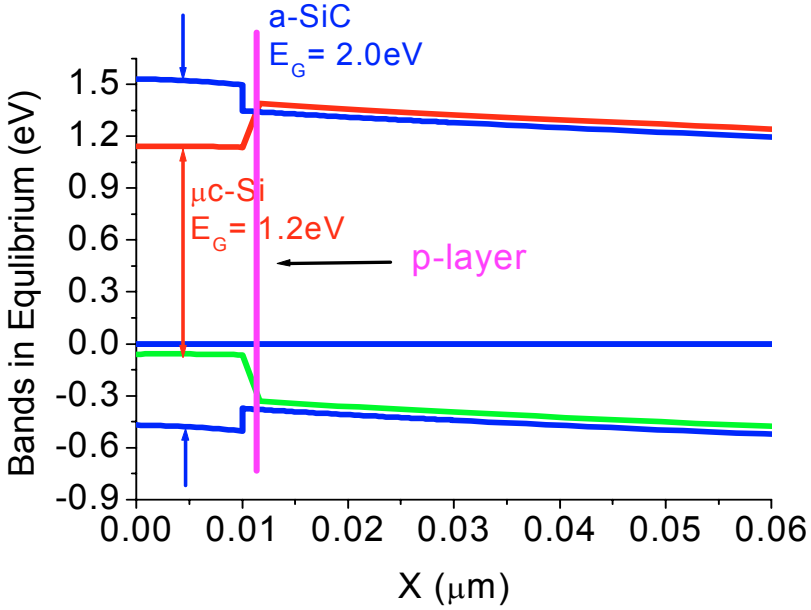

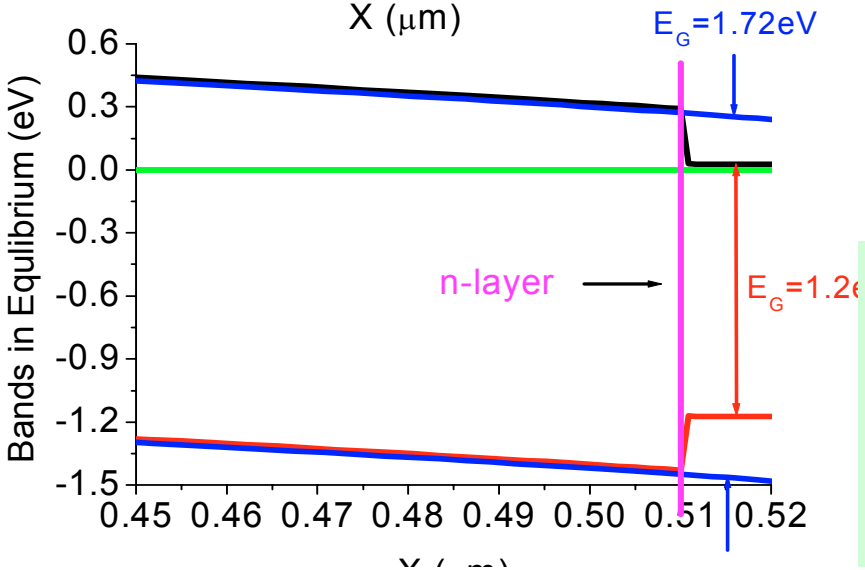

μc-Si doped layers provide high built-in potentials

Similar built-in potentials can be obtained in the (absorbing) i-layers with μc-Si or with a-Si based doped layers

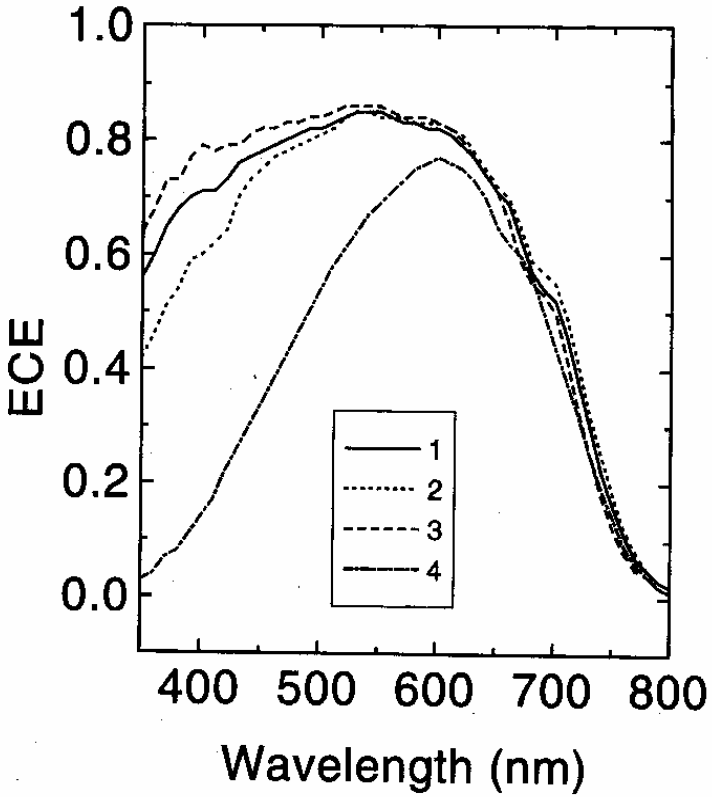

Fig. 1. Spectral response (ECE) of the p-μc-Si:H/i-a-Si:H/n-a-Si:H cell with different buffer layers at p/i interface. Cell 2: 1.5 nm a-SiC:H buffer, Cell 3: 1.5 nm a-Si:H (WB) buffer, Cell 4: 3.0 nm a-Si:H (WB) buffer. Cell 1 is a reference cell (p-a-SiC:H/i-a-Si:H/n-a-Si:H) for comparison.

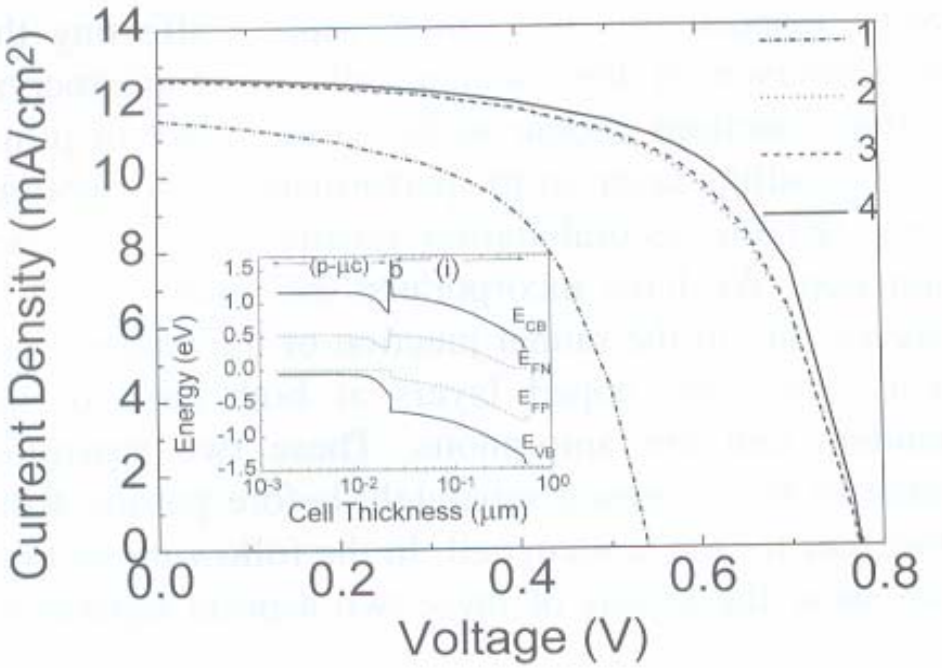

Fig. 2. $I-V$ characteristics from the computer simulations by AMPS for p-μc-Si:H/i-a-Si:H/n-a-Si:H cell with different buffer layers at p/i interface. (1) Without buffer, (2) 1.5 nm a-SiC:H buffer, (3) 3 nm a-Si:H (WB) buffer, (4) 1.5 nm a-Si:H (WB) buffer. Inset is the computer generated band diagram at J_{sc} condition of the cell with 1.5 nm a-Si:H (WB) buffer layer.

p(μc-Si)/(i)a-Si/(n)a-Si

TCO/silver and TCO/aluminum rear contact for enhanced reflectivity

- Silane/ hydrogen dilution: 0.95 (5%)
- Substrate configuration:

SS: cells were deposited onto SS

- **n-type μc-Si:** doped with P, 0.05μm, PECVD.
- **intrinsic μc-Si:H**: 3μm, HWCVD technique
- **p-type μc-Si**: doped with B, 0.025μm, PECVD
- **ITO**: Indium Tin Oxide,
- **Au (gridlines)**.

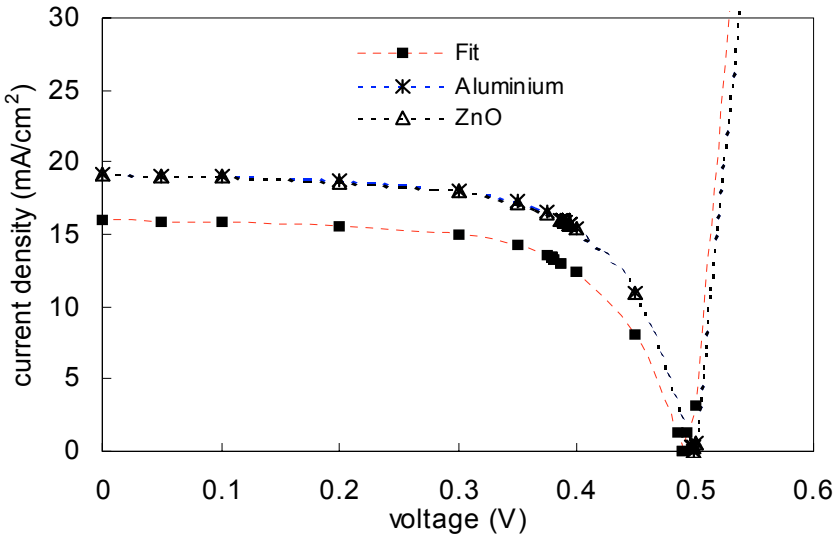

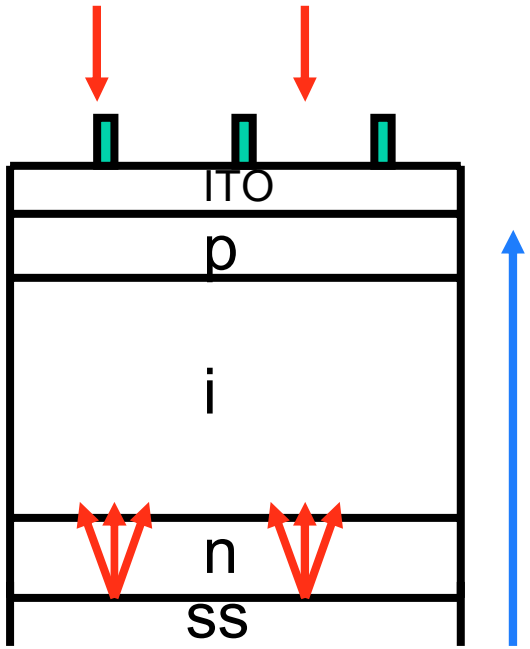

- Al or/and zinc oxide (ZnO) at the back contact
- Back reflector is included in simulations
- J_{sc} increases ~4mA/cm^2, resulting in an efficiency enhancement from 5.1% to 6.2%
- Extra light absorbed at back region of the i-layer reflected off the back contact
- The enhancement of Jsc is more significant in solar cells with thinner i-layers

μc-Si (i)-layers
Single p-i-n solar cells

AM1.5 illumination a-Si alloy top cell on SS (4 different hydrogen dilutions)

	Jsc (mA/cm^2)	Voc (V)	FF	Pmax(mW/cm^2)
Near optimum	10.04	1.018	0.732	7.48
Optimum	9.88	1.028	0.761	7.73
On-the-edge	9.82	0.624	0.426	2.61
Over-the-edge	8.95	0.459	0.562	2.31

(MRS 2004, (R. S.Guha))

Order improves in the growth direction at any given dilution
Problems in solar cells with intrinsic layers in excess to 1μm

Thickness (nm)	Jsc (mA/cm^2)	Voc (V)	FF	Pmax(mW/cm^2)
335	9.45	0.47	0.651	2.89
470	10.98	0.466	0.672	3.44
720	12.99	0.439	0.640	3.65
1040	14.8	0.434	0.621	3.99
1395	16.51	0.414	0.578	3.95
1980	17.87	0.393	0.510	3.58

(MRS 2004, (R. S.Guha))

FF decays with thickness → deterioration of the material quality with increasing thickness; Voc decays with thickness → grain size is increasing

μc-Si (i)-layers
Single p-i-n solar cells

Beginning with a very high H dilution to reduce the incubation layer
Decreasing the hydrogen dilution with time
deposition conditions are kept near the edge
Small and uniform grain size throughout the whole film thickness
1D Modeling is applicable !! (we are lucky)

Thickness (nm)	Jsc (mA/cm^2)	Voc (V)	FF	Eff (%)
Baseline	22.58	0.495	0.603	6.74
20% ticker No profiling	21.48	0.482	0.632	6.54
20% ticker with profiling	25.15	0.502	0.663	8.37

(MRS 2004, (R. S.Guha))

Multi-junction devices for optimum utilization of the solar spectrum

Total fluxes (#/cm^2/sec)	Flat Band Voltage (V_{FB})	Jsc Voc
1.328 x 10^{17} 21.2 mA/cm^2	1.72-0.33- 0.25= 1.14V	17 mA/cm^2 0.9V
0.996 x 10^{17} 37.1 mA/cm^2	1.2-0.059-0.026= 1.11V	25 mA/cm^2 0.53V
0.339 x 10^{17} 58.3 mA/cm^2	1.12-0.08-0.09= 0.95V	35 mA/cm^2 0.52V

Single a-Si (17x0.9) → 15.3mW
Single μc-Si: (25x0.53) → 13.2mW
Single c-Si: (35x0.52) → 18.2 mW
a-Si/ μc-Si Tandem:
[(25/2)x(0.9+0.53)= 17.9mW
a-Si/ μc-Si/c-Si Triple:
[(35/3)x(0.9+0.53+0.52)= 22.7mW

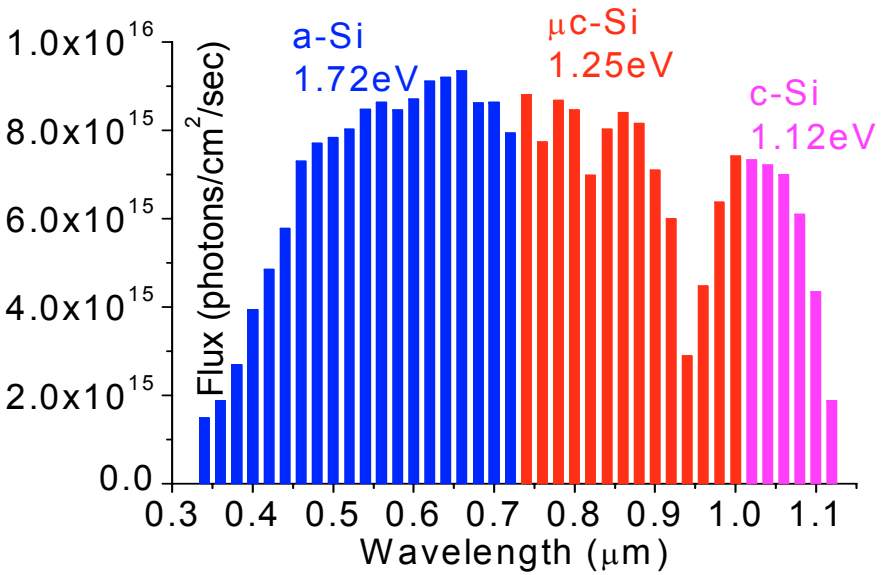

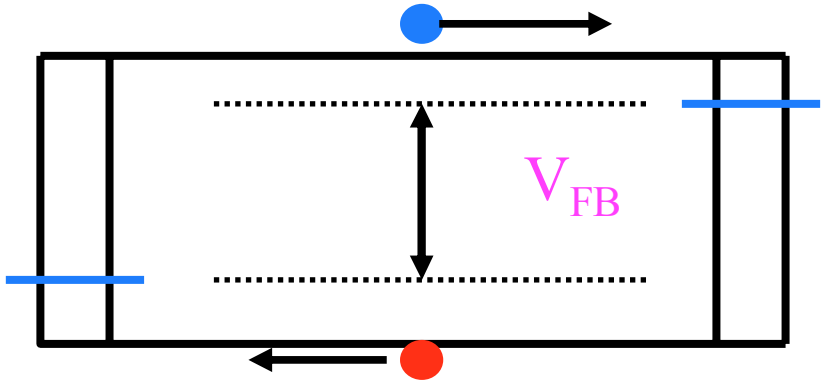

Micromorph concept
a-Si/μc-Si Tandem

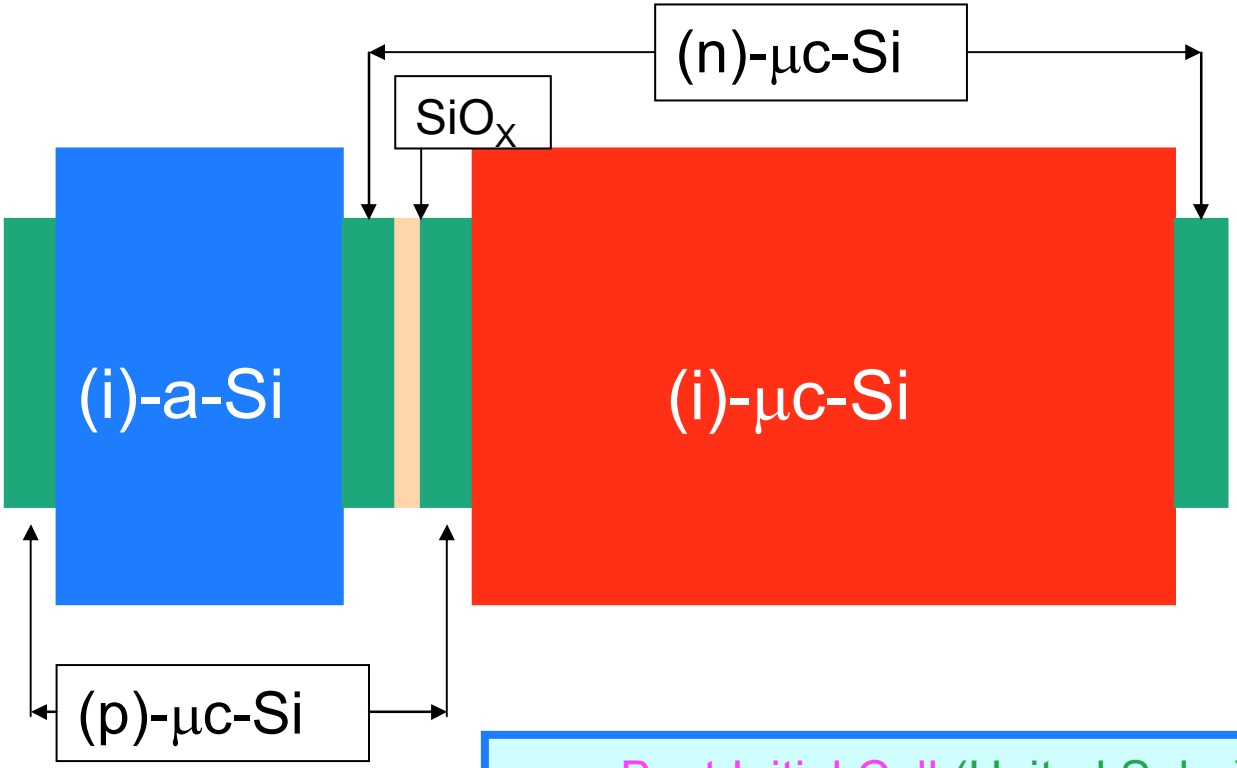

- a-Si (1.7-1.8eV) and μc-Si (1.12-1.25eV) are combined
- Advantages:
  (a) Optimal combination for terrestrial solar spectrum
  (b) a-SiGe is replaced by μc-Si
  (c) μc-Si is stable

- Best Initial Cell (United Solar)
  Jsc= 13.14 mA/cm2, Voc= 1.359V, FF= 0.733, **η= 13.1%** (1998)
- Best Stable Cell → near **11%** in the lab. (United Solar)
  Jsc= 11.55 mA/cm2, Voc= 1.40V, FF= 0.666, **η= 10.82%**

Tandem and TRJ Bands

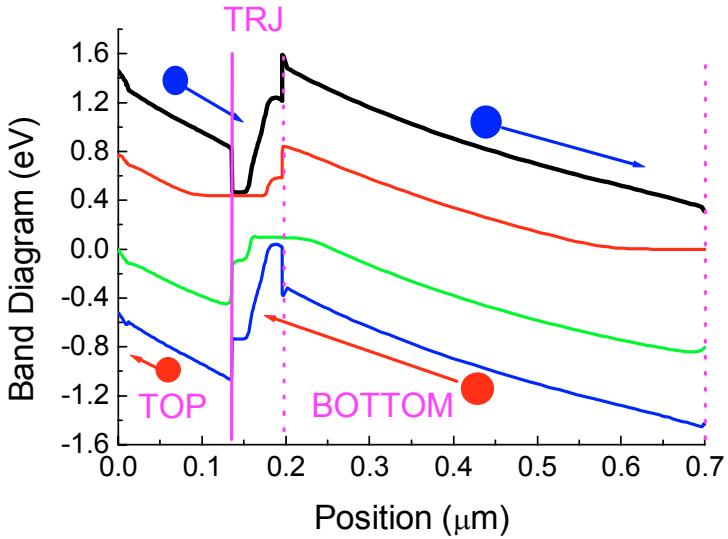

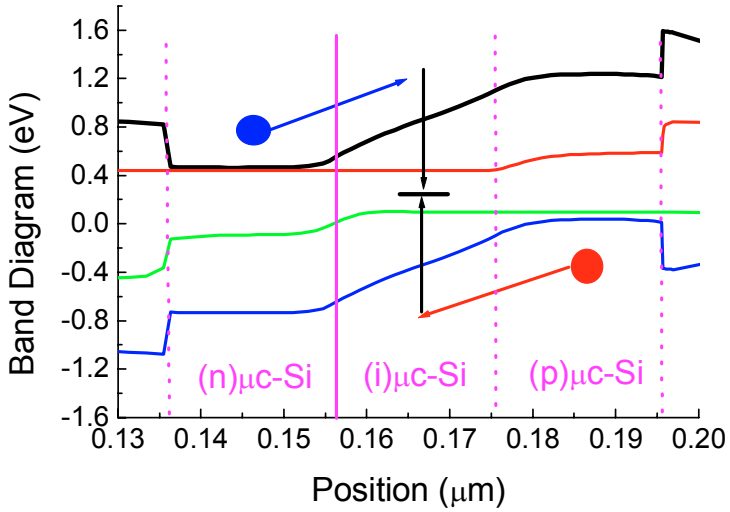

TRJ → μc-Si doped layers provide efficient recombination junctions for photo-carriers

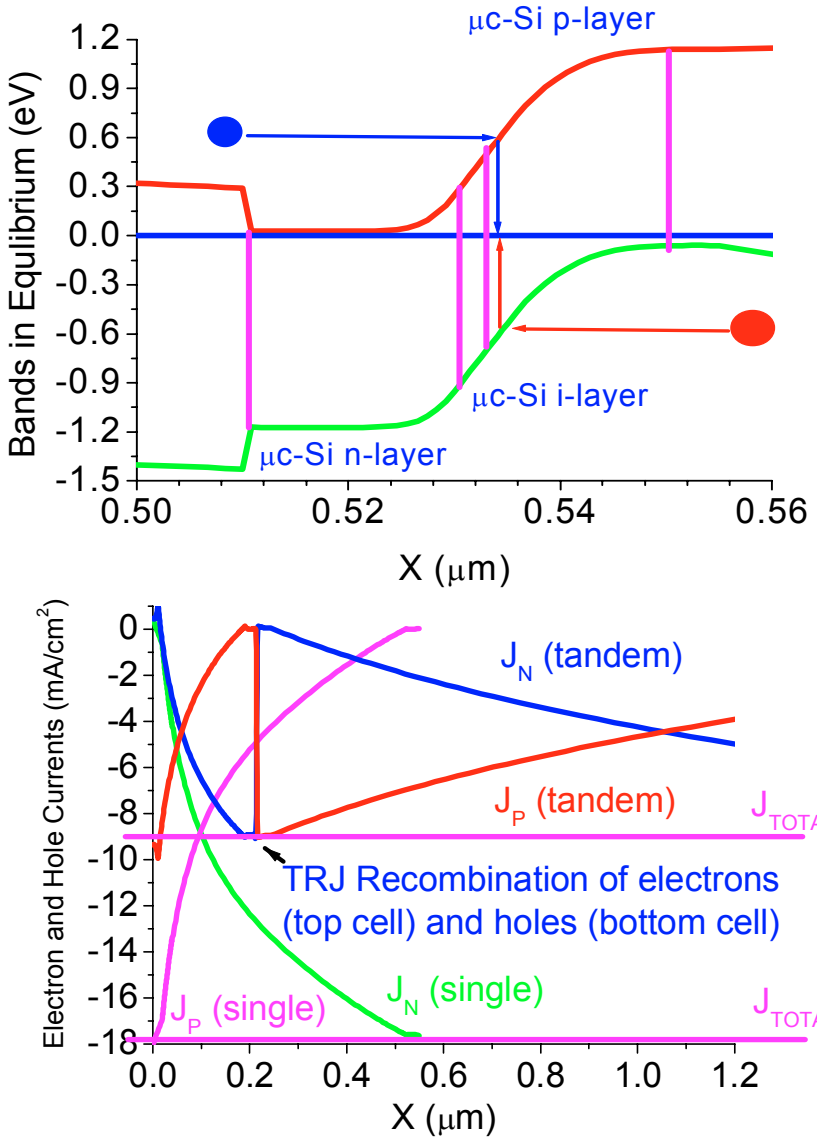

a-Si p-i-n vs. a-Si/μc-Si tandem

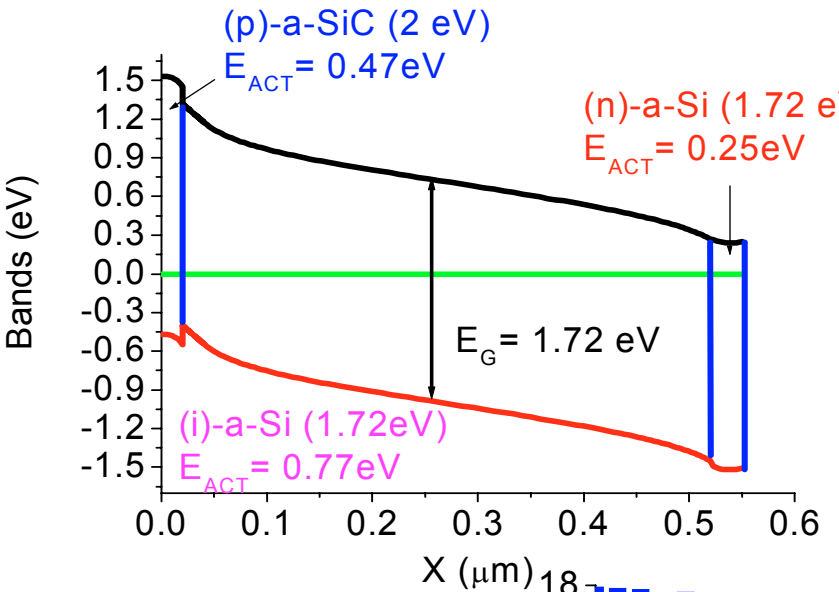

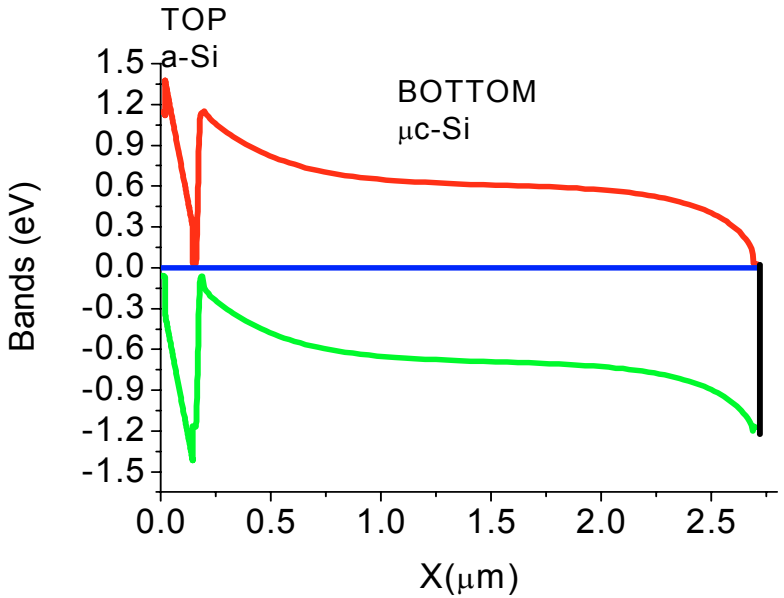

a-Si Single

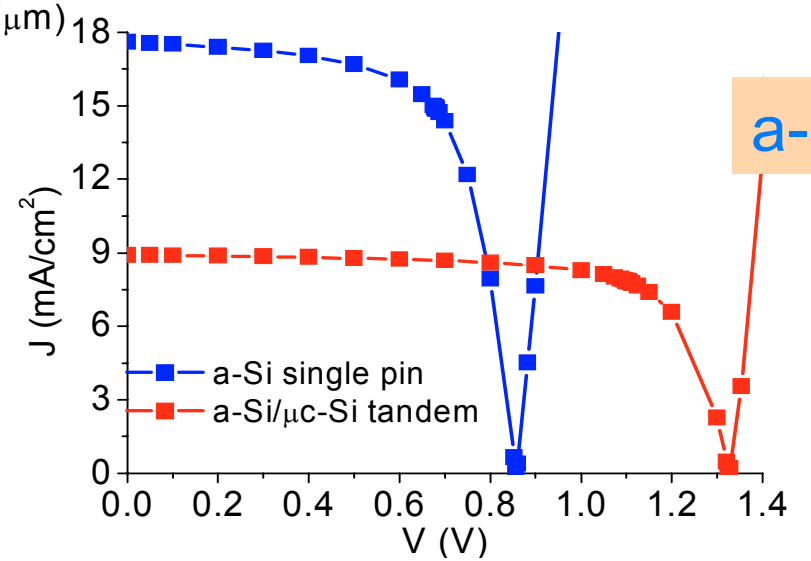

a-Si/μc-Si Tandem

μc-Si intrinsic layers for improved red-response and stability

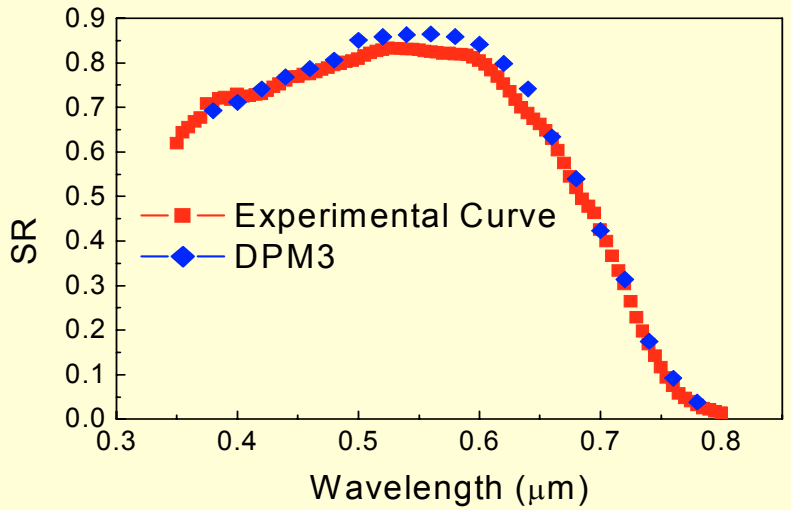

a-Si pin SR

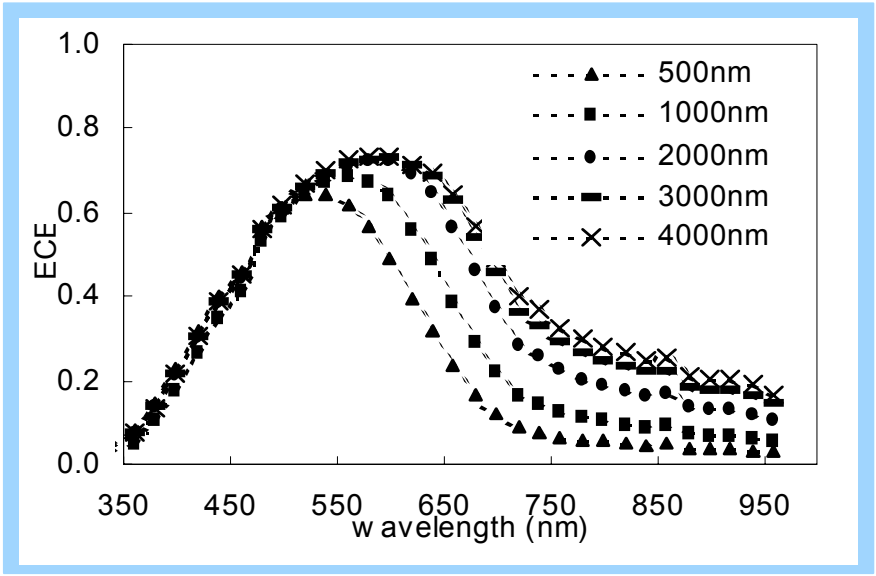

μc-Si nip SR

a-Si/ μc-Si tandem SR

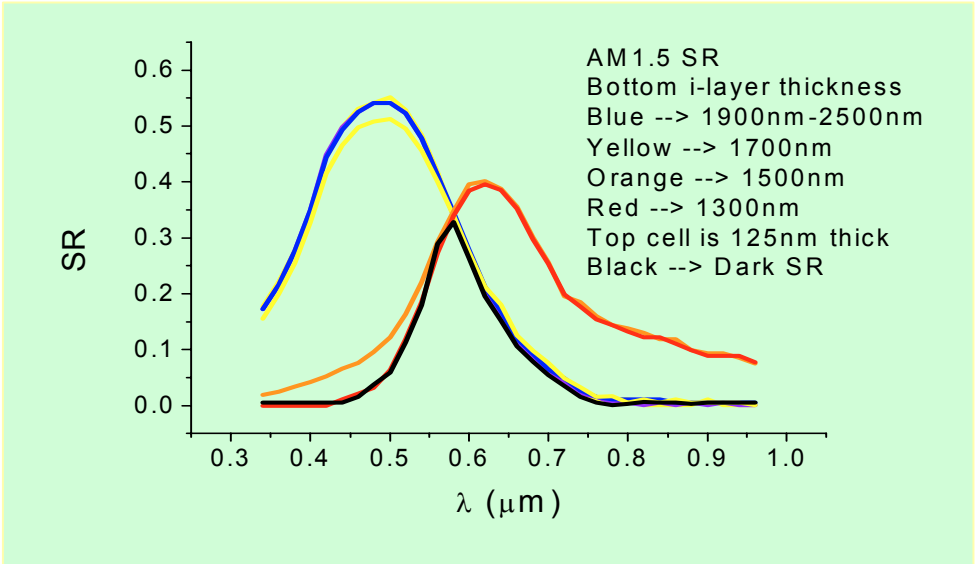

Generation profiles in a-Si p-i-n and a-Si/μc-Si tandem

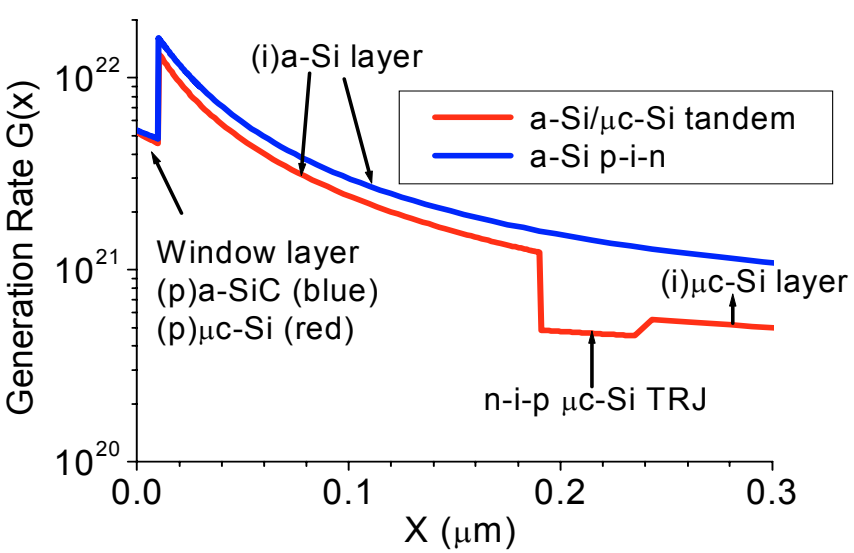

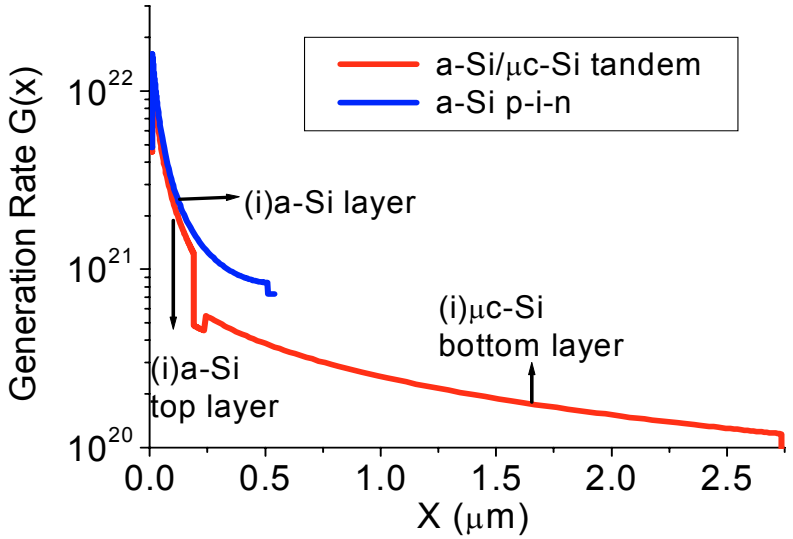

Generation profile in the second junction is much more uniform than in the first junction

μc-Si doped layers provide low optical losses

Multi-junction technology

- More efficient utilization of absorbed photon energy.
- Smaller thickness of each component.
- Less sensitive to light-induced degradation.
- Strong electric field even after degradation.
- Reduced photo-current density in bottom cell.

Differences with single junction.

- Current density in all component cells has to be equal.
- μc-Si doped layers provide high built-in potentials, low optical losses and efficient recombination in TRJ for photo-carriers.
- Generation profile in the second and third junction is much more uniform than in the first junction.
- Band-gap engineering is needed in a-SiGe components.

Device quality a-SiGe

- Dark conductivity < $5X10^{-8}$ Ω^{-1} cm^{-1}
- AM1.5 photoconductivity > $1x10^{-5}$ Ω^{-1} cm^{-1}
- Urbach Tail < 60 meV
- Activation Energy ~ 0.7eV
- Gaps ~ 1.45 - 1.7eV
- Density of Dangling Bonds $\leq 10^{17}$ cm^{-3} (CPM, PDS)
- Photo-electronic properties of a-SiGe deteriorate with Ge content.
- Urbach tail slope does not change for decreasing gaps (> 1.25eV)
- Transport properties of a-SiGe are not as good as in a-Si
- Band gap engineering scheme: decreasing gap from the top and from the bottom towards the inner bulk
- The best valence between absorption profile and internal electric field has to be designed (transport and recombination)

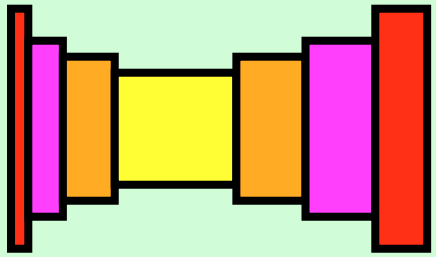

a-SiGe Band Gap Engineering

$\int_L \xi(x)\,dx = C = \Psi(L) - \Psi(0) - V$

- FB-BB: front- back buffer
- FGL: front graded layers
- BGL- back graded layers
- LGL: low band-gap layer

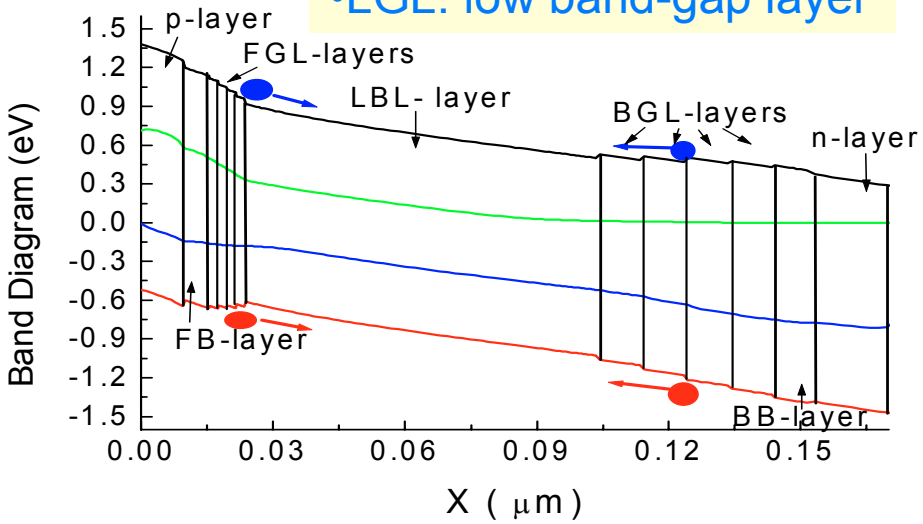

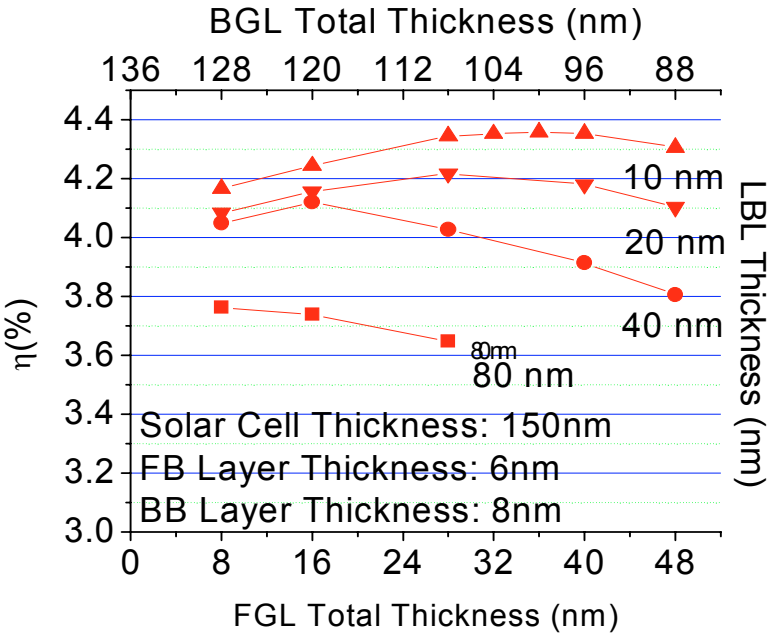

- Profiling in the (i)a-SiGe E_G has strong influence Voc and FF.
- Minimum E_G is placed closer to the p/i interface than to the i/n interface
- U-, V-, W- shape profiles has been proposed → Exponential Grading
- In practice several thin layers with different E_G are deposited

Some conclusions

- Computer modeling allow us to explain the physics behind of some characteristic signatures present in the J-V and SR curves of different cell structures.
- The code calibration made by relying in simple cell structures have to be re-adapted to be used in more complex devices.
- More elaborate physical models do not necessarily lead us to a better fitting and interpretation of experimental results.
- Lack of agreement between computer predictions and experiments could teach us what is missing in our modeling.
- Cell structures to be modeled are becoming more complex.
- Numerical modeling is a very time consuming task.
- Computer modeling can be used as prediction tool.
- The most fruitful effort is to reproduce the experimental trends rather than accurate fittings.

Modeling Tandem Solar Cells

Anybody interested?